

MASTER

Open-Cycle OTEC System Performance Analysis

A. A. Lewandowski
D. A. Olson
D. H. Johnson



SERI

Solar Energy Research Institute

A Division of Midwest Research Institute

1617 Cole Boulevard
Golden, Colorado 80401

Operated for the
U.S. Department of Energy
under Contract No. EG-77-C-01-4042

DISCLAIMER

This report was prepared as an account of work sponsored by an agency of the United States Government. Neither the United States Government nor any agency Thereof, nor any of their employees, makes any warranty, express or implied, or assumes any legal liability or responsibility for the accuracy, completeness, or usefulness of any information, apparatus, product, or process disclosed, or represents that its use would not infringe privately owned rights. Reference herein to any specific commercial product, process, or service by trade name, trademark, manufacturer, or otherwise does not necessarily constitute or imply its endorsement, recommendation, or favoring by the United States Government or any agency thereof. The views and opinions of authors expressed herein do not necessarily state or reflect those of the United States Government or any agency thereof.

DISCLAIMER

Portions of this document may be illegible in electronic image products. Images are produced from the best available original document.

Printed in the United States of America
Available from:
National Technical Information Service
U.S. Department of Commerce
5285 Port Royal Road
Springfield, VA 22161
Price:

Microfiche \$3.00
Printed Copy \$ 6.50

NOTICE

This report was prepared as an account of work sponsored by the United States Government. Neither the United States nor the United States Department of Energy, nor any of their employees, nor any of their contractors, subcontractors, or their employees, makes any warranty, express or implied, or assumes any legal liability or responsibility for the accuracy, completeness or usefulness of any information, apparatus, product or process disclosed, or represents that its use would not infringe privately owned rights.

OPEN-CYCLE OTEC
SYSTEM PERFORMANCE ANALYSIS

A. A. LEWANDOWSKI
D. A. OLSON
D. H. JOHNSON

SEPTEMBER 1980

DISCLAIMER

This book was prepared as an account of work sponsored by an agency of the United States Government. Neither the United States Government nor any agency thereof, nor any of their employees, makes any warranty, express or implied, or assumes any legal liability or responsibility for the accuracy, completeness, or usefulness of any information, apparatus, product, or process disclosed, or represents that its use would not infringe privately owned rights. Reference herein to any specific commercial product, process, or service by trade name, trademark, manufacturer, or otherwise, does not necessarily constitute or imply its endorsement, recommendation, or favoring by the United States Government or any agency thereof. The views and opinions of authors expressed herein do not necessarily state or reflect those of the United States Government or any agency thereof.

PREPARED UNDER TASK NO. 3451.10

Solar Energy Research Institute

A Division of Midwest Research Institute

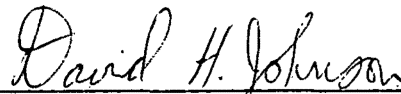
1617 Cole Boulevard
Golden, Colorado 80401

Prepared for the
U.S. Department of Energy
Contract No. EG-77-C-01-4042

THIS PAGE
WAS INTENTIONALLY
LEFT BLANK

PREFACE

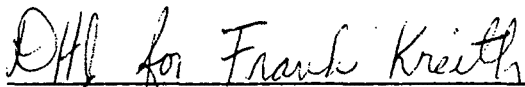
This report was prepared as part of Task 3451 (OTEC Research and Development) in the Thermal Conversion Research Branch of the Solar Energy Research Institute (SERI). The report describes an algorithm developed to calculate the performance of Claude-cycle OTEC systems and the results of using it to calculate the effect on performance of deaerating the warm and cold water streams before they enter the evaporator and condenser. We gratefully acknowledge the support of the Ocean Energy System Program Office at SERI and the Ocean Energy Systems Division of the U.S. Department of Energy.



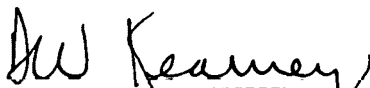
David H. Johnson, Task Leader
Solar Thermal Research Branch

Approved for

SOLAR ENERGY RESEARCH INSTITUTE



Frank Kreith, Branch Chief
Solar Thermal Research Branch



D. W. Kearney, Division Manager
Solar Thermal, Ocean, & Wind Division

THIS PAGE
WAS INTENTIONALLY
LEFT BLANK

SUMMARY

The objective of this report is to develop an algorithm to calculate the performance of Claude-cycle ocean thermal energy conversion systems and apply it to an analysis of the effect of warm and cold water deaeration on the performance of a system that uses a channel-flow evaporator and a horizontal jet condenser.

A Claude-cycle OTEC plant consists of an evaporator, a vapor turbine, a condenser (either surface or direct contact), a cold water pipe, warm and cold water pumps, a condenser exhaust pump, and, possibly, warm and cold water deaerators. The algorithm we developed to calculate system performance treats each of these components separately and then interfaces them to form the complete system, which allows a component to be changed without changing the rest of the algorithm. For this study we developed mathematical models of a channel-flow evaporator and both horizontal jet and spray direct-contact condensers. The algorithm was then programmed to run on SERI's CDC 7600 computer and used to calculate the effect on performance of deaerating the warm and cold water streams before they enter the evaporator and condenser, respectively.

Assumptions made in developing the algorithm invalidate its use in analyzing the off-design performance of a particular system. These assumptions also cause some of the penalties of inefficiency to influence cost rather than performance. The study of deaeration indicates that there is no advantage to removing air from the warm and cold water streams before they enter the evaporator and condenser, respectively, as compared to removing the air from the condenser.

Efforts should be made to improve this performance analysis algorithm so that the effects of inefficiency influence performance rather than cost or to develop an OC-OTEC cost analysis algorithm. Also, better data on OC-OTEC evaporator and condenser performance are needed to decide which of the various proposed concepts is best.

THIS PAGE
WAS INTENTIONALLY
LEFT BLANK

THIS PAGE
WAS INTENTIONALLY
LEFT BLANK

LIST OF FIGURES

	<u>Page</u>
1-1 Schematic of Claude Cycle.....	3
1-2 System Temperature Distribution.....	4
1-3 Westinghouse OC-OTEC Plant Configuration.....	6
2-1 Temperature/Entropy Diagram for Claude/OTEC Power Cycles.....	8
2-2 Main Program Flowchart, Open-Cycle Computer Model.....	10
2-3 Temperature Distribution for the Open-Cycle Model.....	11
2-4 Deaeration System Schematic.....	14
2-5 Deaeration Subroutine Flowchart.....	15
2-6 Turbine Velocity Diagram.....	21
2-7 Turbine Subroutine Flowchart.....	21
2-8 Proposed Westinghouse OC-OTEC Plant Configuration.....	25
2-9 Thermal Nonequilibrium for Open Channel Flow.....	26
2-10 Channel-Flow Flash Evaporator Subroutine Flowchart.....	27
2-11 Jet Condenser Subroutine Flowchart.....	29
2-12 Spray Condenser Subroutine Flowchart.....	32
2-13 Condenser Exhaust Schematic.....	34
2-14 Condenser Exhaust Subroutine Flowchart.....	34
3-1 Baseline Study Results.....	36
3-2 Baseline Simulation Flow Rates.....	37
3-3 Baseline Study Evaporator Length.....	39
3-4 Baseline Study Plant Outer Diameter.....	40
3-5 Comparison of Predeaeration and Baseline Studies.....	41
3-6 Comparison of Total Deaeration Power for Predeaeration and Baseline Studies.....	42

LIST OF FIGURES (concluded)

	<u>Page</u>
3-7 Comparison of Condenser Height for Predeaeration and Baseline Studies.....	44
3-8 Deaeration Stage Head Loss Effect on Total Deaeration Power.....	45
3-9 Deaeration Stage Head Loss Effect on Net Power.....	46
3-10 Steam Partial to Total Pressure Ratio Effect on Total Deaerator Power.....	47
3-11 Steam Partial to Total Pressure Ratio Effect on Net Power.....	48
3-12 Effect of Air Fraction Liberated on Total Deaerator Power.....	49
3-13 Effect of the Number of Deaeration Stages on Net Power.....	51
3-14 Effect of the Number of Deaeration Stages on Total Deaeration Power.....	52
3-15 Effect of Equilibrium Approach Fraction on Net Power.....	53
3-16 Effect of Turbine-Generator Efficiency on Net Power.....	55
A-1 Program OTEC.....	73

LIST OF TABLES

	<u>Page</u>
A-1 Input Parameters.....	64
A-2 Output Parameters.....	65

NOMENCLATURE

a	total surface area of condenser
A	cross-sectional area of turbine
A_c	cross-sectional area of condenser
B	$\frac{a}{m_c c_p}$ = jet condenser parameter
C	magnitude of vapor absolute velocity in turbine (subscript o: at stator inlet; subscript l: at stator exit, rotor inlet; subscript 2: at rotor exit; subscript u: tangential component)
c_p	specific heat of sea water
D	diameter of turbine (subscript m: mean; subscript o: outer; subscript h: hub)
d	depth of channel flow flash evaporator
e	$\frac{(0.0137)d}{d}$ = channel flow variable
f	fraction of steam condensed ($f = 0.99$)
f_g	$P_{vs}/P_{s,1}$ = deaerator first stage pressure parameter
f_l	nonequilibrium air release factor
f_r	surface roughness factor (0.014 for concrete)
g	gravitational constant
h_o	enthalpy of steam at turbine inlet
H_e	free fall head loss of channel-flow flash evaporator
H_g	sluice gate head loss of channel-flow flash evaporator ($H_g = 0.15$ m)
H_{te}	total head loss of channel flow flash evaporator
h_1	enthalpy of steam at exit of turbine
H_c	free fall head loss of condenser
H_d	distribution head loss of condenser
H_t	total head loss in a component

H_e	Henry number
h_l	enthalpy of saturated liquid
$h_{l,v}$	latent heat of vaporization
h_v	enthalpy of saturated vapor
H_{td}	total head loss in deaerator
H_{tc}	total head loss in condenser
H_p	head loss in cold water pipe
H_s	head loss in deaerator stage
Δh	change of enthalpy across turbine
k_c	channel-flow flash evaporator parameter
k	heat transfer coefficient
k_m	mass transfer coefficient
k_o	heat transfer coefficient at atmospheric pressure
L	blade length of turbine
l	length of channel-flow flash evaporator channel
$m_{a,i}$	nonequilibrium mass fraction of air dissolved in water at outlet of stage $i = \frac{\text{mass of air}}{\text{mass air} + \text{mass water}}$
m_{ea}	equilibrium mass fraction of air dissolved in water
$m_{ea,i}$	equilibrium mass fraction of air dissolved in water at outlet of stage i
M_a	molar weight of air
M_w	molar weight of water
\dot{m}_a	total mass flow rate of air released in evaporator and condenser
$\dot{m}_{a,i}$	mass flow rate of air leaving i^{th} deaerator stage
\dot{m}_c	cold water mass flow rate
\dot{m}	mass flow rate in a component of the system
\dot{m}_r	mass flow rate of air released in evaporator or condenser

m_s	steam mass flow rate
$m_{v,o}$	mass flow rate of uncondensed steam
$m_{t,i}$	total mass flow rate of gas through i^{th} deaerator (or condenser exhaust) compressor
$m_{v,i}$	mass flow rate of vapor through i^{th} deaerator compressor
m_w	warm water mass flow rate
N	number of deaeration stages
n	rotational speed of turbine
$P_{ac,in,i}$	i^{th} compressor inlet air partial pressure
$P_{as,i}$	air partial pressure in i^{th} deaerator stage
$P_{c,in,i}$	i^{th} compressor inlet pressure
$P_{c,out,i}$	i^{th} compressor outlet pressure
P_c	condenser pressure
P_o	outlet pressure of deaerator system (slightly above atmospheric)
$P_{s,i}$	total pressure in i^{th} stage of deaerator
$P_{vc,in}$	compressor inlet vapor partial pressure [$P_{vc,in} = P_{sat}(7^\circ\text{C})$]
P_{vs}	water vapor partial pressure in a deaerator stage [$P_{vs} = P_{sat}(T_{wwi}$ or $T_{cwi})$]
ΔP	vent condenser pressure drop ($\Delta P = 0.276$ kPa)
r	compression ratio
r_t	hub-to-tip ratio
R	$\frac{\Delta T_{\text{evap}}}{\Delta T_{\text{cond}}} = \frac{T_{wwi} - T_o}{T_1 - T_{cwi}}$
s_l	entropy of saturated liquid
s_v	entropy of saturated vapor
T_{cwi}	temperature of cold water at inlet of condenser
T_{cwo}	temperature of cold water at outlet of condenser
T_1	temperature of steam at inlet of condenser/outlet of turbine

T_o	temperature of steam at outlet of evaporator/inlet of turbine
T_{wwi}	temperature of warm water at inlet of evaporator
T_{wwo}	temperature of warm water at outlet of evaporator
U	peripheral wheel speed of turbine rotor
V	condenser volume
w	channel width
W	magnitude of vapor velocity relative to turbine rotor (subscript 1: at stator exit; subscript 2: at rotor exit; subscript a: axial component)
W_c	pumping power for a component of the system
\bar{W}	work per unit mass done by turbine
W_g	gross power output
$W_{s,i}$	i^{th} deaerator stage compressor power
W_d	total deaerator compressor power
x	quality of steam at exit of turbine
x_a	solubility of air in water = mole fraction of air dissolved in water
x_w	mole fraction of water in water plus air solution (III 1)
α	angle between the absolute vapor velocity and the horizontal (subscript 1: at stator exit, rotor inlet; subscript 2: at rotor exit)
β	angle between vapor velocity relative to the turbine rotor and the horizontal (subscript 1: at stator exit, rotor inlet; subscript 2: at rotor exit)
β_e	fraction of nonequilibrium = $1 - \eta_e$
ϵ_1	$v_1 (2 \cos \alpha_1 - v_1)$
ϵ_2	$v_2 (2 \cos \beta_2 - v_2)$
ζ	blade loss coefficient
η_{cp}	compressor efficiency
η_c	$\frac{T_{cwo} - T_{cwi}}{T_1 - T_{cwi}}$ = fraction of approach to equilibrium in condenser

η_e	$\frac{T_{wwi} - T_{wwo}}{T_{wwi} - T_o} =$ fraction of approach to equilibrium in evaporator
η_m	compressor motor efficiency
η_p	pump efficiency
η_{tg}	turbine-generator efficiency
η_g	generator efficiency
η_{TS}	total to static efficiency
θ	channel slope ($\theta = 2^\circ$)
ρ_w	density of warm water
σ_1	steam-to-air ratio at condenser inlet
σ_2	steam-to-air ratio at condenser outlet
v_1	ratio of tangential speed of rotor to absolute vapor velocity at rotor inlet
v_2	ratio of tangential speed of rotor to relative vapor velocity at rotor exit
Λ	specific volume (subscript 2: in the turbine at the rotor exit)

SECTION 1.0

INTRODUCTION

A vast amount of energy is stored as heat in the ocean. Some of this may be converted to useful work by adding heat to an engine from the warm surface water and rejecting heat from the engine to the cold deep water. This will be accomplished by ocean thermal energy conversion (OTEC) systems which are being developed by the Ocean Systems Branch of the U.S. Department of Energy (DOE). There are two types of OTEC systems, closed cycle (CC-OTEC) and open cycle (OC-OTEC). CC-OTEC systems use a working fluid isolated from sea water. The working fluid is evaporated by warm sea water and condensed by cold sea water through large heat exchangers. The fundamental operation of the CC-OTEC systems is well understood, and a full-scale pilot plant is being designed. However, it is anticipated that the large heat exchangers will corrode and biofoul in the ocean. The OC-OTEC systems use warm sea water as the working fluid, thus eliminating the warm water heat exchanger, and some versions exclude the cold water exchanger as well. Although OC-OTEC systems would eliminate the largest foreseeable problem with the CC-OTEC systems, their operation is not yet well enough understood to allow design of a full-scale plant.

OC-OTEC systems use either a vapor turbine (Claude cycle) or a hydraulic turbine (hydraulic cycle). The Claude cycle works by bringing warm sea water into an evacuated chamber where it is evaporated. The water vapor expands through the vapor turbine and is then condensed by cold sea water, either by direct contact or through a heat exchanger. Claude demonstrated that by using this cycle it is feasible to extract significant power from the ocean. However, it is not yet understood which of the various proposed schemes to evaporate and condense the warm sea water is most efficient. Also, a vapor turbine large enough to produce significant power has never been constructed. The efficiency of the evaporator and condenser and the required size of the vapor turbine strongly affect the cost of a Claude-cycle OTEC system. In the hydraulic-cycle systems warm sea water falls through a hydraulic turbine into an evacuated chamber. The various concepts that have been proposed differ in the method by which the water is then removed from the chamber. At present it is not understood whether it is feasible to extract significant power using any of these concepts. However, if one of them proves to be feasible, then the large vapor turbine of the Claude cycle could be replaced by a smaller hydraulic turbine, possibly resulting in a much cheaper plant per unit of energy converted.

DOE has asked the Ocean Energy Systems Program at the Solar Energy Research Institute (SERI) to develop the OC-OTEC concepts to the point that a full-scale pilot plant may be designed. The SERI program office recognizes that the two classes of OC-OTEC systems are in different stages of development. Data will be collected and analytical models developed to compare the performance of the Claude-cycle evaporator and condenser concepts. An evaporator and condenser concept will be chosen for full-scale subsystem test as a result of this comparison. The data from the full-scale subsystem testing will be used to compare the performance and economics of the chosen form of Claude-cycle OTEC system with that of the CC-OTEC pilot plant. As a

result of this comparison, a decision may be made to design a full-scale Claude-cycle OTEC pilot plant. Simultaneously with this effort, the various hydraulic-cycle concepts will be evaluated for feasibility. Specific problems with their fundamental operation will be identified and individually addressed through experimental and analytical studies. As a result of this work, one or more of these concepts may be shown to be feasible. Further development of these apparently feasible hydraulic-cycle concepts would then proceed as described for the Claude-cycle concepts. After sufficient data have been collected and models developed to predict performance, a decision will be made to proceed to full-scale subsystem testing of one concept. These test data will then be used to compare the performance and economics of a hydraulic-cycle OTEC system with a Claude-cycle OTEC and CC-OTEC system. Finally, the SERI Ocean Energy Systems Program may decide to design a full-scale hydraulic turbine OC-OTEC plant.

One factor in these decisions will be an analytical comparison of the performance and economics of each OC-OTEC system versus other OC- and CC-OTEC systems. This comparison will be based on OC- and CC-OTEC system analysis algorithms that incorporate common assumptions. The SERI in-house Ocean Energy Systems Research and Development task is developing these algorithms for the Ocean Energy Systems Program. This report describes the status of these algorithms. First we developed or acquired system performance analysis algorithms and then programmed them for use on SERI's CDC Cyber 7600 computer. Cost analysis algorithms will be developed later. SERI personnel have developed a Claude-cycle performance analysis algorithm and acquired a closed-cycle OTEC performance analysis algorithm developed by Abelson of MITRE, Inc. Both of these algorithms have been programmed to run on the SERI Cyber computer. Abelson has described his CC-OTEC performance analysis algorithm (Abelson 1978). This report will describe the Claude-cycle performance analysis algorithm (Sec. 2.0) and its application to an analysis of the effect of deaerating the warm and cold water on the performance of a particular Claude-cycle system using a channel flow evaporator and a horizontal jet condenser (Sec. 3.0).

The Claude-cycle performance analysis algorithm was developed to be flexible enough to accommodate many system designs and yet to be detailed enough to portray a reasonably accurate system performance. A typical system is divided into the components shown in Fig. 1-1 (evaporator, turbine, condenser, deaerators, and cold and warm water pumps). Losses incurred in interconnecting passages were neglected, allowing computations to be independent of a specific system layout. Since the system operates at low pressure (0.1 to 0.5 psia), the sea water in the cold and warm water inlet ducts could rise approximately 10 m above sea level. To avoid large penalties in pumping requirements, the evaporator and condenser should be located at this "barometric level." It was assumed in this analysis that the plant's layout adheres to this barometric principle. The scope of the analysis is limited to the Claude-power cycle and the sea water systems and assumes a temperature distribution through the system as shown in Fig. 1-2. The steam flow required to produce a specified gross generator output is then computed from the available enthalpy drop across the turbine. Sea water flow rates are computed using overall heat balances in the evaporator and condenser. These components are then sized using detailed performance models to determine head losses and pumping power requirements. The performance of the condenser will

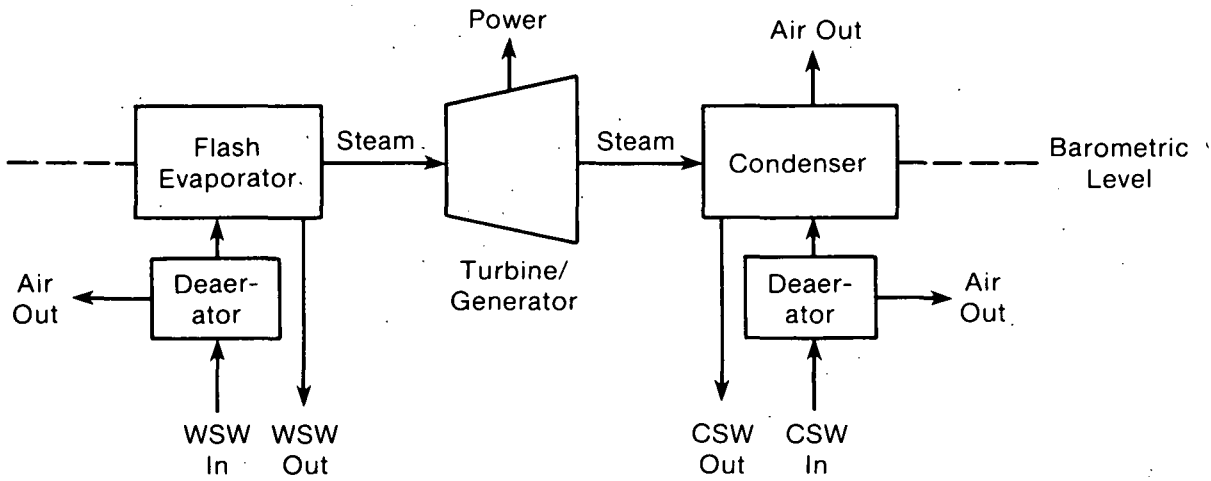


Figure 1-1. Schematic of Claude Cycle

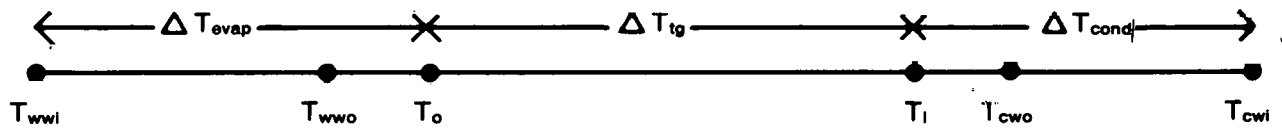


Figure 1-2. System Temperature Distribution

depend on the amount of noncondensable gas present. Deaeration can remove a given fraction of noncondensable gases from the warm or the cold water before it enters the evaporator or condenser respectively. The rest of the gases are assumed to be liberated in the evaporator and condenser and must be removed from the condenser by an exhaust pump. The net power output is then the gross power output minus the sum of the power for the cold water, warm water, deaerator, and condenser exhaust pumps.

In this country, the most completely developed Claude-cycle system is the Westinghouse design (Westinghouse Electric Corp. 1979) that uses a single, vertical-axis turbine with a toroidal channel flow flash evaporator and a shell and tube condenser (Fig. 1-3). The evaporator, sea water and vapor flow passages, and diffuser are integral with the structure. This compact configuration results in minimum losses between components and could produce cost advantages for construction. Because this design serves as a baseline against which other Claude-cycle systems should be compared, we chose first to model a channel-flow flash evaporator and a single, vertical-axis turbine. However, we chose to model a direct contact horizontal jet condenser instead of the Westinghouse shell and tube condenser because it has potential for higher heat transfer coefficients and thus reduced size. Disadvantages of the horizontal jet condenser are a possible increase in the amount of noncondensable gases released in the system owing to the exposed cold water flow and the elimination of a fresh water by-product. Cold and warm water deaerators and condenser gas exhaust component models were also developed. Models of other evaporator and condenser concepts will be developed and used in the performance algorithm. The system model is discussed in Sec. 2.0 of this report.

The Claude-cycle system performance analysis algorithm including the specific component models discussed has been programmed for use on SERI's CDC Cyber 7600 computer. We used this program to study the effects of deaeration on the performance of the system composed of the components previously discussed. Whether to deaerate the warm sea water before the evaporator is always a question applicable to open-cycle OTEC systems. The same question applies to the cold sea water when the system uses a direct contact condenser. The results of this study are discussed in Sec. 3.0.

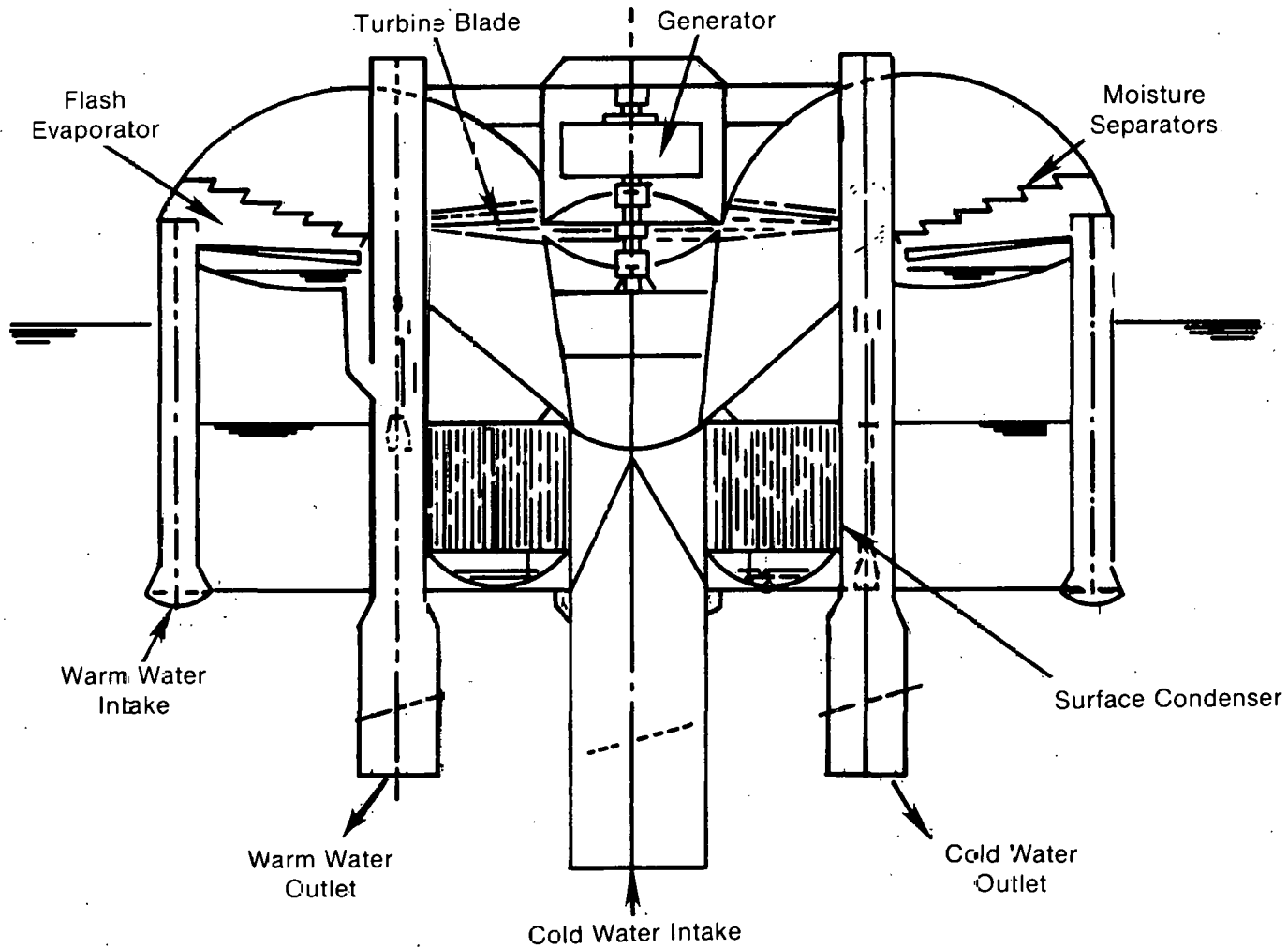


Figure 1-3. Westinghouse OC-OTEC Plant Configuration

SECTION 2.0

SYSTEM MODEL

2.1 INTRODUCTION

The algorithm developed to analyze the performance of Claude-cycle OTEC systems is described in this section. First, the overall modeling approach is explained, and then each component model is developed; i.e., deaerators, the turbine, channel-flow flash evaporator, jet condenser, spray condenser, and condenser exhaust. The deaerators remove air from the warm and cold water streams before they enter the evaporator or condenser; the condenser exhaust removes air liberated in the evaporator and condenser. The turbine and the channel-flow flash evaporator models are based on the work of Westinghouse (Westinghouse Electric Corp. 1979), the jet condenser is based on the model of Bakay and Jaszay (1978), and the spray condenser model is based on the work of the Colorado School of Mines (Watt 1977).

Before discussing the details of the algorithm, the general operation of a Claude-cycle OTEC System will be discussed using a typical temperature/entropy plot as shown in Fig. 2-1. The following temperature distribution through the cycle is assumed for this particular realization: warm water inlet temperature, 25°C; vapor temperature in the evaporator, 20°C; temperature drop across the turbine, 10°C; steam temperature in the condenser, 10°C; cold water exit temperature, 10°C. The diagram depicts the sequence of thermodynamic states occupied by an element of working fluid as it traverses the cycle. The element begins the cycle as subcooled liquid at 25°C and 1 atm pressure. On the diagram this state is indistinguishable from one at 25°C on the saturation curve. The element then expands isentropically to a temperature of 20°C. During this expansion the state of the element crosses the saturation curve and some of the liquid "flashes" into vapor. The element continues to evaporate as it receives heat from the rest of the warm water in the evaporator until it becomes saturated vapor at 20°C. The saturated vapor then isentropically expands through the turbine to a temperature of 10°C. At this point the element is steam with a quality of 97.3%. The steam is condensed as it gives up heat to the cold water in the condenser until it becomes saturated liquid at 10°C. The cycle is closed by an isentropic compression of the liquid to atmospheric pressure and then an isobaric heating by the sun to 25°C. On this diagram these final processes are indistinguishable from a simultaneous compression and heating along the saturation curve. The cycle operates at the foot of the saturation curve and over a narrow temperature range so that its efficiency is very nearly the Carnot efficiency of 3.4% for a Carnot engine operating between 20°C and 10°C.

2.2 MODELING APPROACH

The modeling approach used in the study was to compute subsystem and system performance as a function of a given temperature distribution. Fixed parameters in the analysis include a gross generator output of 100 MW_e, warm sea water inlet temperature of 25°C, cold sea water inlet temperature of 5°C, and a fixed temperature drop across the turbine of 10°C. For a given temperature

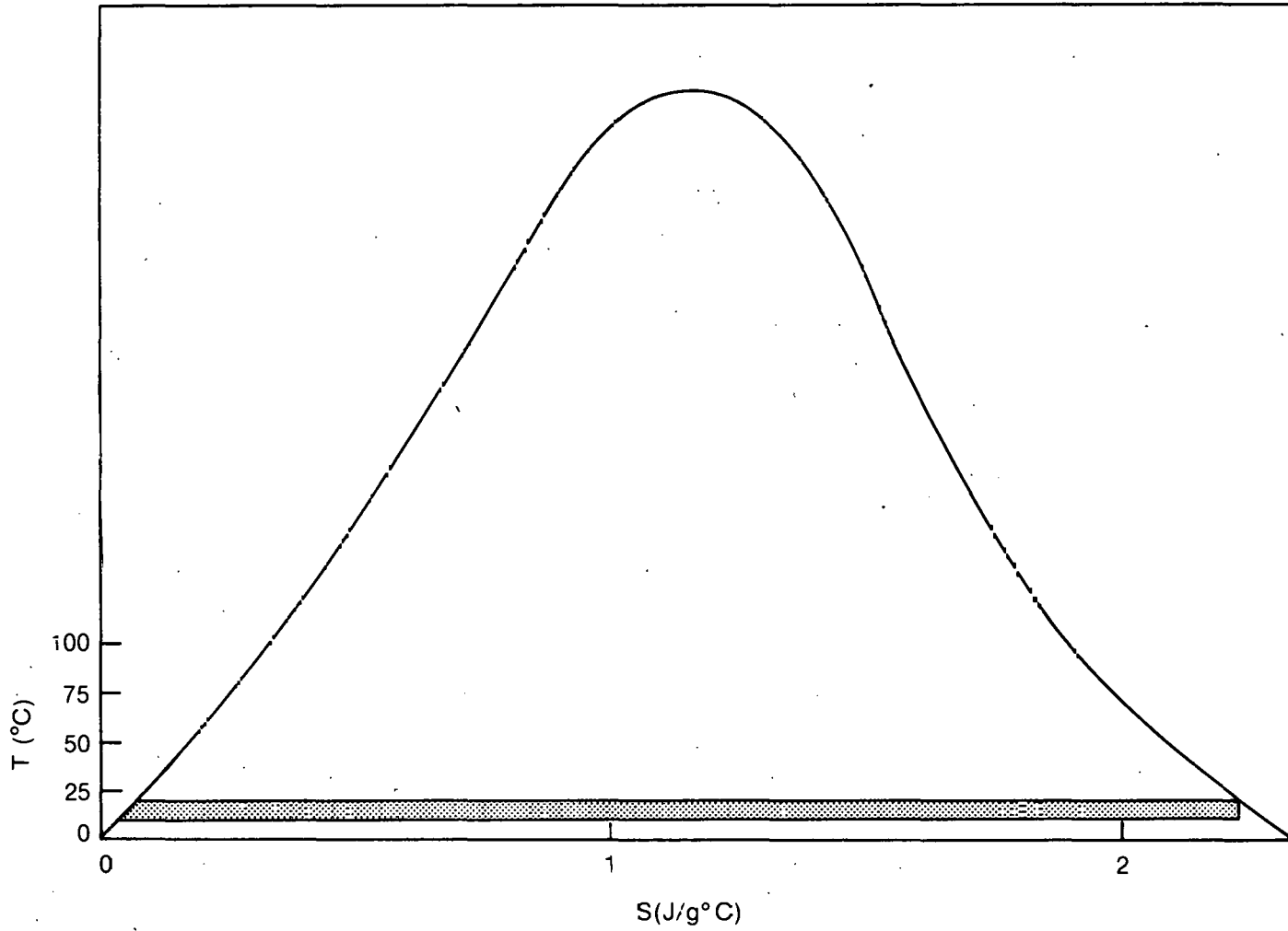


Figure 2-1. Temperature/Entropy Diagram for Claude-OTEC Power Cycles

distribution, the required steam flow is computed from the available enthalpy drop across the turbine. Sea water flows are computed using overall heat balances in the evaporator (warm stream) and condenser (cold stream). Each of the components is then sized to determine head losses and power requirements. The net power output is then the gross output minus the sum of all auxiliary requirements.

A computer program, written in FORTRAN, was developed to use the open-cycle model. A flowchart of the main program is shown in Fig. 2-2, and a listing of the program is given in the Appendix. Most data are passed between the main program and the component subroutines by Common statements. The input parameters are then read into the program from an external file. The parameters are listed in Table A-1 of the Appendix and will be outlined in the details of the model to follow.

For each set of input parameters, a series of temperature distributions is generated by the model (see Fig. 2-3). The temperature differences available to the evaporator and condenser are controlled by the variable R , where

$$R = \frac{\Delta T_{\text{evap}}}{\Delta T_{\text{cond}}} \quad (2.1)$$

R is varied to impose a range of temperature distributions on the model. The warm water outlet temperature is set by the fraction of approach to equilibrium in the evaporator η_e . Perfect equilibrium would be established if the warm water outlet temperature equaled the steam temperature. In the evaporator, the fraction of approach to equilibrium is defined as

$$\eta_e = \frac{T_{\text{wwi}} - T_{\text{wwo}}}{T_{\text{wwi}} - T_0} \quad (2.2)$$

The approach to equilibrium in the condenser is called "approach temperature difference." The parameter η_c is defined as

$$\eta_c = \frac{T_{\text{cwo}} - T_{\text{cwi}}}{T_1 - T_{\text{cwi}}} \quad (2.3)$$

Using the parameters R , η_e , and η_c , we obtain the temperatures throughout the system.

It is instructive to consider numerical values for a particular case. Consider a system for which $R = 1/2$, $\eta_c = 0.9$, and the temperature difference across the turbine is 10°C . Then, for a warm water inlet temperature of 25°C , the temperature of the vapor in the evaporator is 21.67°C and since this is saturated vapor its pressure is 0.376 psi. After a 10°C temperature drop across the turbine, the high quality steam in the condenser has a temperature of 11.67°C and a pressure of 0.199 psi. The pressure drop across the turbine is only 0.177 psi, an indication that the turbine design will be unusual. The temperature of the cold water out will be 11°C .

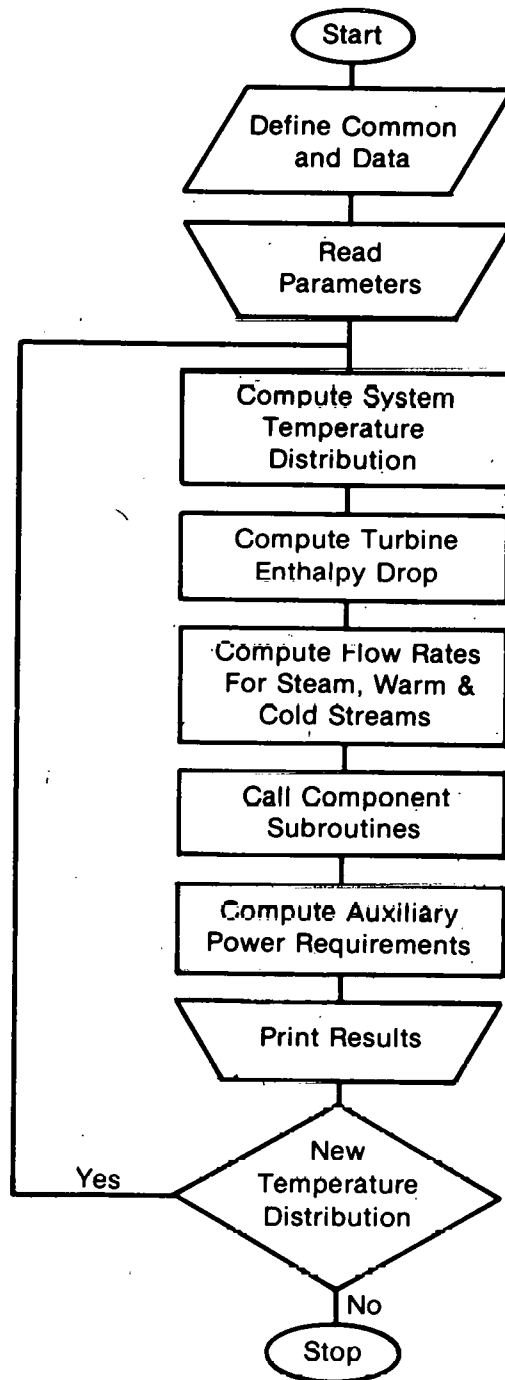


Figure 2-2. Main Program Flowchart, Open-Cycle Computer Model

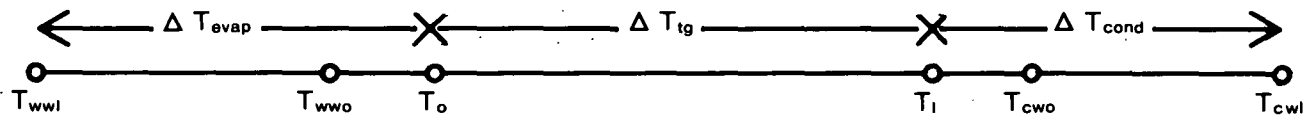


Figure 2-3. Temperature Distribution for the Open-Cycle Model

The next step is to compute the enthalpy available to the turbine. Steam at the inlet is assumed to be saturated. Owing to the slight decrease in steam quality at the exit, the exit enthalpy consists of both liquid and vapor components. If we assume isentropic expansion, the exit enthalpy h_1 is given by

$$h_1 = (1 - x) h_l(T_1) + x h_v(T_1) \quad , \quad (2.4)$$

where the steam quality x is

$$x = \frac{s_v(T_0) - s_l(T_1)}{s_v(T_1) - s_l(T_1)} \quad , \quad (2.5)$$

and s_v and s_l are the entropies of vapor and liquid at the given temperatures.

If we assume that the steam at the turbine inlet is saturated, then the inlet enthalpy h_0 is $h_v(T_0)$, and the isentropic enthalpy drop across the turbine is

$$\Delta h = h_0 - h_1 \quad . \quad (2.6)$$

The amount of steam flow required to generate the gross output W_g is then

$$\dot{m}_s = \frac{W_g}{\eta_{tg} \Delta h} \quad , \quad (2.7)$$

where η_{tg} is the turbine-generator efficiency, which equals the total to static turbine efficiency η_{TS} times the generator efficiency η_g . Heat balances at the evaporator yield the required warm water flow as follows:

$$\dot{m}_w = \frac{\dot{m}_s [h_v(T_0) - h_l(T_{wwo})]}{h_l(T_{wwi}) - h_l(T_{wwo})} \quad . \quad (2.8)$$

Similarly, at the condenser the required cold water flow is

$$\dot{m}_c = \frac{f \dot{m}_s [h_1 - h_l(T_{cwo})]}{h_l(T_{cwo}) - h_l(T_{cwi})} \quad , \quad (2.9)$$

where f is the fraction of steam condensed, which is set at $f = 0.99$, based on the capabilities of a direct contact condenser.

Then each component routine is called with appropriate control parameters and inputs. The routines return with power requirements, head losses, or dimensions, as appropriate. Pumping power W_c requirements for a component are computed from total head losses H_t and flow rates m as follows:

$$W_c = \frac{\dot{m} g H_t}{\eta_p} \quad , \quad (2.10)$$

where g = gravitational constant, 9.8 m/s^2 , and η_p = pump efficiency.

Net power for the plant is the gross power less pumping power for the warm and cold loop (including head losses in any deaerators), condenser air removal, and deaerator air removal.

2.3 COMPONENT MODELS

Six component models were generated for this study: deaerators (serving both warm and cold streams), flash evaporator, turbine, two condenser models, and condenser air removal. In any particular run, deaeration can be selected with a control variable. When deaeration is selected, both warm and cold streams are deaerated with a variable number of stages and head loss per stage. The model computes the power to remove air from the water streams. In the flash evaporator, turbine and condenser routines, the models compute size as a function of the specified performance parameters and temperature distribution. The condenser air removal model computes power requirements for compression of the noncondensable gases and uncondensed vapor.

2.3.1 Deaerators

The deaeration system consists of a series of stages, each stage including a deaerator, a vent condenser, and a compressor. Operation of the system can be understood through the schematic of Fig. 2-4. Aerated sea water, consisting of dissolved air and water, enters at stage N . The vent condenser maintains a pressure above the stage larger than the vapor saturation pressure at the water temperature, forcing air out of the sea water. Each successive deaerator stage operates at a lower pressure (but still greater than the vapor saturation pressure), as more air is driven out of the sea water. The pressures in the stages are fixed by the vent condensers. Air and water vapor enter the first vent condenser from the last stage in the train. Much of the liberated water vapor is condensed by the intercoolers, reducing the amount of gas that must be compressed. A compressor pumps the remaining mixture to the next vent condenser, fixing its operating pressure and the stage 2 deaerator operating pressure (higher than stage 1). Air and water vapor are added from the stage 2 deaerator, compressed to the next vent condenser, and so on down the line. The main purpose of a staged system is to reduce the amount of air removed at low pressure. Compression efficiency decreases with decreasing pressure, and therefore a greater penalty is applied to the low pressure stages.

Figure 2-5 shows a flowchart of the deaeration subroutine, which requires that only the number of stages N and the stream (warm or cold) to deaerate be input. All other inputs are passed via Common. If deaeration is not selected, the analysis is bypassed, and all air dissolved in the sea water stream is assumed to be liberated to the evaporator or condenser, as appropriate.

In each deaerator stage, the pressure $P_{s,i}$ consists of water vapor partial pressure P_{vs} and air partial pressure $P_{as,i}$. The water vapor partial pressure is set to the saturation pressure at the temperature of the water stream being deaerated, $P_{sat}(T_{wwi}$ or $T_{cwi})$. The first stage pressure is set by a parameter

14

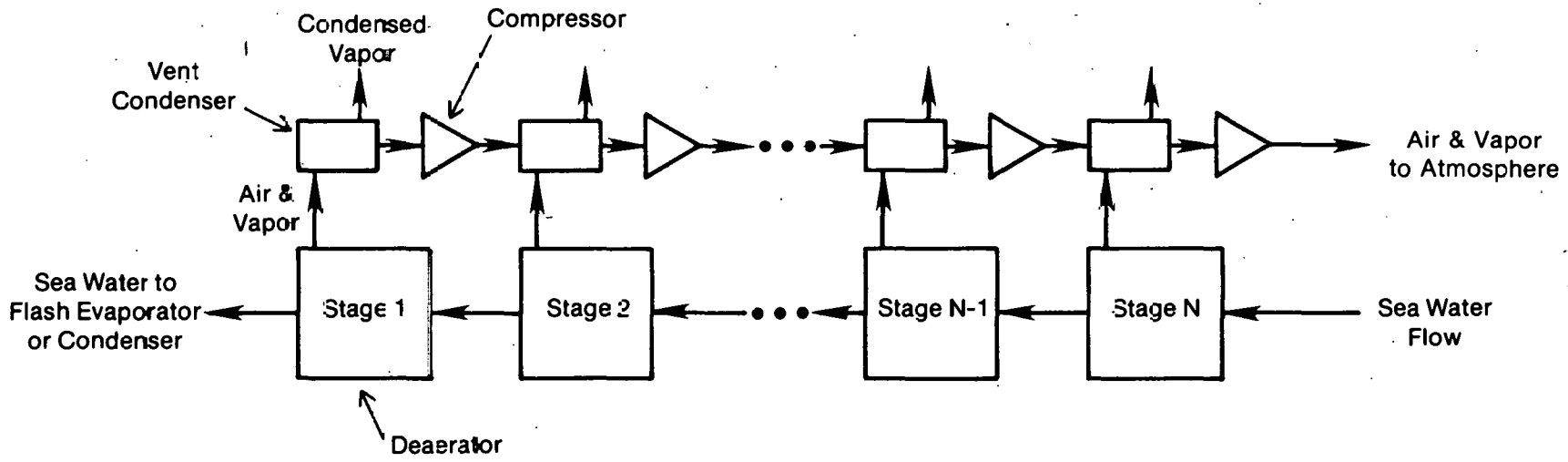


Figure 2-4. Deaeration System Schematic

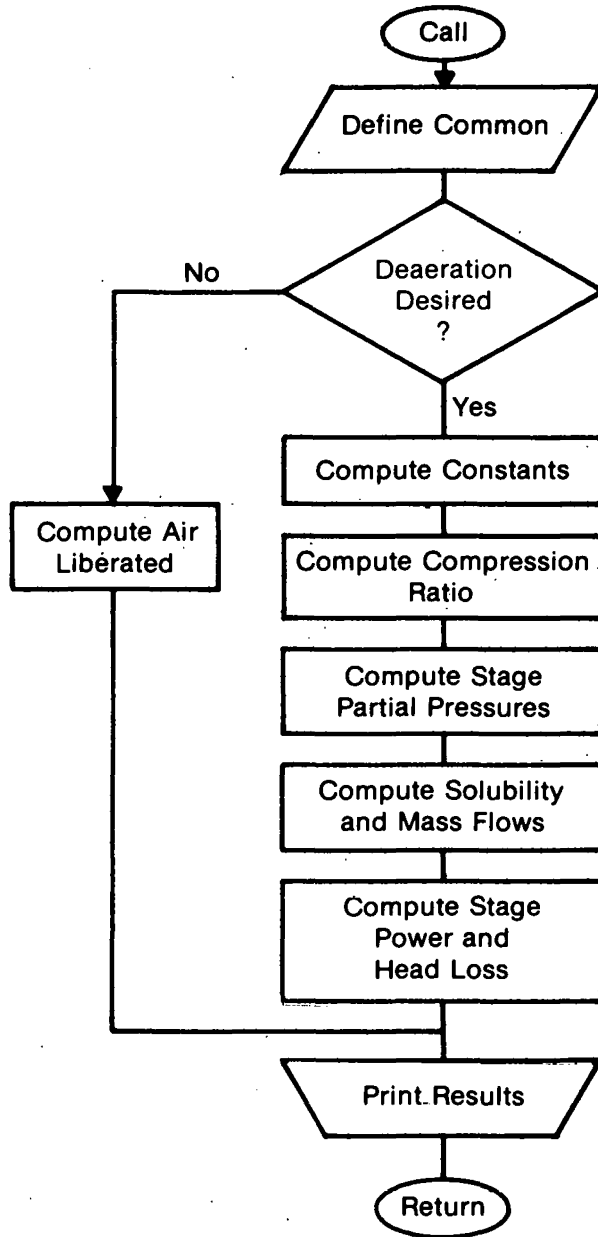


Figure 2-5. Deaeration Subroutine Flowchart

f_g , which is the ratio of vapor pressure to total pressure in the stage. The pressure in stage 1 is given by

$$P_{s,1} = \frac{P_{vs}}{f_g} \quad (2.11)$$

where $P_{vs} = P_{sat}(T_{wwi} \text{ or } T_{cwi})$.

When the first stage pressure is set, it is possible to compute the compression ratio per stage r required to compress the gases to slightly above atmospheric pressure. After some algebraic manipulation, we can generate an expression for the compression ratio:

$$r^N = \frac{P_o + \Delta P \sum_{i=1}^N r^i}{P_{s,1}} \quad (2.12)$$

where

P_o = outlet pressure, slightly above atmospheric;

ΔP = vent condenser pressure drop; and

N = number of deaerator stages.

Equation 2.12 lends itself to an iterative solution and converges quickly. When the cold stream is being deaerated, the first vent condenser is not functional since it operates at the same temperature as the incoming water vapor. In this case, the compression ratio is

$$r^N = \frac{P_o + \Delta P \sum_{i=1}^{N-1} r^i}{P_{s,1}} \quad (2.13)$$

When the first stage partial pressures and compression ratio are known, the pressures throughout the system can be calculated. Vent condenser performance is assumed sufficient to maintain a vapor pressure at the compressor inlet $P_{vc,in}$ equal to saturated water vapor pressure at 7°C, $P_{sat}(7^\circ\text{C})$, with a pressure drop through the condenser ΔP of 0.276 kPa. The air pressure at the compressor inlet is for stage i

$$P_{ac,in,i} = P_{c,in,i} - P_{sat}(7^\circ) \quad (2.14)$$

where

$$P_{c,in,i} = P_{s,i} - \Delta P \quad .$$

The compressor outlet pressure $P_{c,out,i}$ is the inlet pressure multiplied by the compression ratio:

$$P_{c,out,i} = P_{c,in,i} \cdot r \quad (2.15)$$

The pressure of stage $i + 1$ is the stage i compressor outlet pressure:

$$P_{s,i+1} = P_{c,out,i} \quad (2.16)$$

The partial pressure of water vapor P_{sat} (T_{wwi} or T_{cwi}) is known, and thus the air partial pressure can be calculated by

$$P_{as,i+1} = P_{s,i+1} - P_{sat}(T_{wwi} \text{ or } T_{cwi}) \quad (2.17)$$

The procedure (Eqs. 2.14 to 2.17) can be repeated until water vapor and air pressures are computed for all stages of deaeration.

Next, solubilities and air and water mass flow rates are calculated for each deaerator stage. The solubility of air in water x_a and the partial pressure of air at the interface between liquid and vapor phases in equilibrium are related by the Henry number H_e and the relationship is expressed by

$$x_a = \frac{P_a}{P_o H_e} \quad (2.18)$$

where x_a = mole fraction of air dissolved in water. The equilibrium mass fraction m_{ea} and mole fraction are related by the familiar equation

$$m_{ea} = \frac{x_a M_a}{x_a M_a + x_w M_w} \quad ,$$

and since $x_w \approx 1 \gg x_a$, then

$$m_{ea} \approx x_a \frac{M_a}{M_w} = 1.60 \cdot x_a \quad (2.19)$$

Data for the Henry number were fit with a linear function of temperature. Combining Eqs. 2.18 and 2.19 yields an expression for the outlet equilibrium mass fraction of air in water for any stage i :

$$m_{ea,i} = \frac{1.60 \cdot P_{as,i}}{P_o \cdot H_e} \quad (2.20)$$

The mass flow rate of air leaving a stage $\dot{m}_{a,i}$ is the difference in inlet and outlet mass fractions multiplied by the mass flow of water. To allow for less than this "equilibrium" release of air, a parameter of value less than or equal to one, f_l , is applied. However, when less than the equilibrium amount of air is released, the outlet mass fraction is increased above that computed in Eq. 2.20. The outlet mass fraction for stage i updated as a function of the parameter f_l becomes

$$m_{a,i} = (1 - f_l) \cdot m_{a,i+1} + f_l \cdot m_{ea,i}, \quad i = N, \dots, 2, 1 \quad (2.21)$$

where $m_{a,N+1} = m_{ea,N+1} = 1.60/H_e$. If we assume that f is the same for all stages, the mass flow of air from stage i is computed using

$$\dot{m}_{a,i} = (m_{a,i+1} - m_{a,i}) \cdot \dot{m}_{(w \text{ or } c)} \quad (2.22)$$

The amount of vapor flowing through a deaerator stage is proportional to its mass fraction in the stage, and the mass fraction of vapor in the stage can be related to the mass fraction of air through the perfect gas law. After some manipulation, the following expression can be derived:

$$\dot{m}_{v,i} = \frac{P_{\text{sat}}(7^\circ)}{1.60 \cdot P_{ac,in,i}} \sum_{j=1}^i \dot{m}_{a,j} \quad (2.23)$$

The total flow of gas through a compressor $\dot{m}_{t,i}$ is

$$\dot{m}_{t,i} = \dot{m}_{v,i} + \dot{m}_{a,i} \quad (2.24)$$

Any air remaining in the stream exiting to the evaporator or condenser is assumed to be released. In the case of no deaeration, all the air originally in the dissolved water stream is released in the evaporator or condenser. The amount of air released \dot{m}_r is

$$\dot{m}_r = m_{a,1} \cdot \dot{m}_{(w \text{ or } c)} \quad (2.25)$$

where $m_{a,1}$ = the air remaining in the first deaerator stage or $m_{a,1} = 1.60/H_e$, if there is no deaeration.

The power required to compress the gas in any stage i can be computed from thermodynamic relationships. The result for stage power $W_{s,i}$ is

$$W_{s,i} = \frac{293 \cdot T_{in} \cdot r^{0.3} \ln r \cdot \dot{m}_{t,i}}{\eta_{cp} \eta_m} \quad (2.26)$$

where T_{in} = inlet temperature = 280°K, and η_m = motor efficiency = 0.9,

and the compressor efficiency is

$$\eta_{cp} = \frac{1.7 P_{c,in,i}}{P_o} \quad , \quad \eta_{cp} \leq 0.8 \quad (2.27)$$

The factor of 1.7 comes from a more detailed analysis of the fluid dynamic behavior of compressors (Watt, Matthews, and Hathaway 1977). The total power to remove the gas from the deaerators is the sum of the individual compressor power requirements:

$$W_d = \sum_{i=1}^N W_{s,i} \quad (2.28)$$

Associated with each stage of deaeration is a head loss H_s needed to provide sufficient surface area for the air to diffuse towards. The method of deaeration is not specified in the study, but could be a packed bed, spray, or film. The total head required H_{td} in the deaerators is the head loss per stage multiplied by the number of stages:

$$H_{td} = N \cdot H_s \quad (2.29)$$

The parameter H_s is specified as an input to the model. Both the total power and the total head required are passed back to the main program, and the details of the deaeration analysis are printed.

2.3.2 Turbine

A complete calculation of turbine performance and geometry is a complex, iterative process that maximizes turbine efficiency by varying the many parameters of turbine design. For this system study, however, a detailed design is not necessary. Instead, what is required is the basic relationship between turbine performance and turbine size (outer diameter). Therefore, a number of simplifying assumptions are used to formulate the turbine subroutine. The assumptions used here, as well as the formulas that follow, were supplied by Westinghouse and are similar to those used in their recently completed open-cycle study (Westinghouse Electric Corp. 1979).

The assumptions related to the mathematical description of the problem are:

- o steady-state flow;
- o one-dimensional flow with axisymmetric stream surfaces;
- o symmetric velocity diagram (50% reaction), (see Fig. 2-6);
- o incompressible flow; and
- o stream surface at the mean diameter is representative of the whole stage.

These additional assumptions will be made:

- o diagram angle α_1 and $\beta_2 = 23.6^\circ$ (see Fig. 2-6);
- o blade-loss coefficient $\zeta = 0.1$;
- o hub-to-tip ratio $r_t = 0.44$; and
- o total to static efficiency $\eta_{TS} = 75\%$, 80% , and 85% .

These inputs are based on experience in turbine design. A range of efficiency values will be used to determine system sensitivity to this parameter. A flow chart of the subroutine is shown in Fig. 2-7.

The turbine velocity diagram is shown in Fig. 2-6. Vertical velocity components in the diagram represent axial components in the turbine; horizontal components in the diagram represent tangential components in the turbine. The incoming vapor flow, exiting from the evaporator, streams axially downward with velocity C_0 . The stationary stator gives the flow a tangential component; C_1 is the velocity at the stator exit and rotor inlet. Relative to the rotating rotor, the velocity is W_1 . The rotor extracts energy from the flow, reversing the tangential component of the velocity. The flow leaves the rotor with velocity C_2 , and velocity relative to the rotor of W_2 .

The definition of efficiency is the actual work divided by actual work plus losses and is represented as,

$$\eta_{TS} = \frac{\bar{W}}{\bar{W} + \zeta \frac{C_1^2}{2} + \zeta \frac{W_2^2}{2} + \frac{C_2^2}{2}} \quad (2.30)$$

The frictional loss owing to the stator blade is $\zeta C_1^2/2$; the frictional loss resulting from the rotor blade is $\zeta W_2^2/2$; and the remaining kinetic energy in the flow exiting at the rotor that has not been converted to work is $C_2^2/2$.

Work per unit mass \bar{W} can be defined using conservation of angular momentum:

$$\bar{W} = U(C_{u1} + C_{u2}) \quad , \quad (2.31)$$

which after substitution and manipulation can be rearranged as

$$\bar{W} = \frac{C_1^2}{2} v_1 (2 \cos \alpha_1 - v_1) + \frac{W_2^2}{2} v_2 (2 \cos \beta_2 - v_2) \quad , \quad (2.32)$$

where $v_1 = \frac{U}{C_1}$ and $v_2 = \frac{U}{W_2}$.

If we let $\epsilon_1 = v_1(2 \cos \alpha_1 - v_1)$ and $\epsilon_2 = v_2(2 \cos \beta_2 - v_2)$, Eq. 2.32 becomes,

$$\bar{W} = \epsilon_1 \left(\frac{C_1^2}{2}\right) + \epsilon_2 \left(\frac{W_2^2}{2}\right) \quad . \quad (2.33)$$

For a symmetric stage we have:

$$C_1 = W_2, \alpha_1 = \beta_2, \epsilon_1 = \epsilon_2 = \epsilon \quad ;$$

therefore,

$$\bar{W} = \epsilon W_2^2 \quad . \quad (2.34)$$

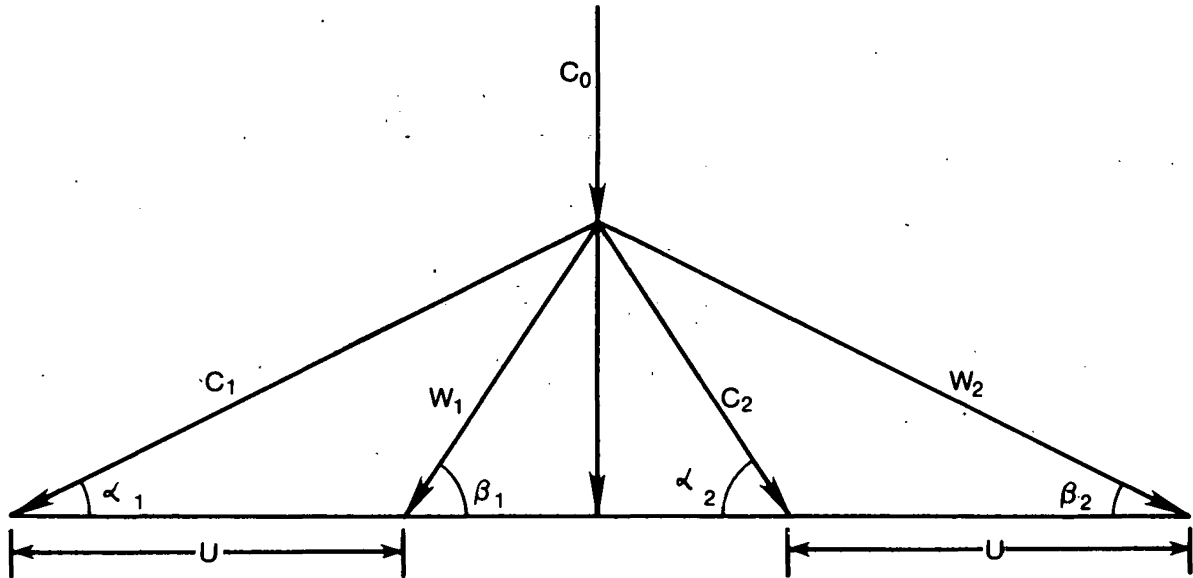


Figure 2-6. Turbine Velocity Diagram

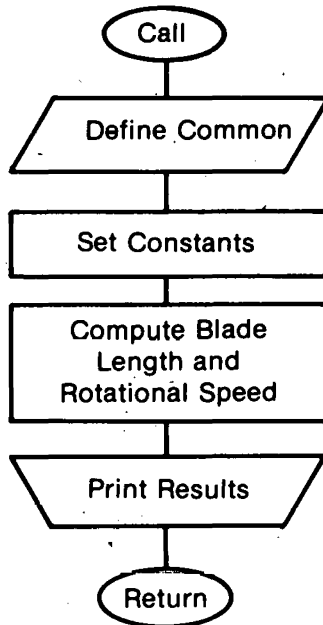


Figure 2-7. Turbine Subroutine Flowchart

By substituting Eq. 2.34 into Eq. 2.30 we obtain an efficiency of

$$\eta_{TS} = \frac{\epsilon W_2^2}{\epsilon W_2^2 + \zeta \frac{C_1^2}{2} + \zeta \frac{W_2^2}{2} + \frac{C_2^2}{2}}$$

or

$$\eta_{TS} = \frac{1}{1 + \left(\frac{\zeta}{\epsilon}\right) + \left(\frac{C_2^2}{2\epsilon W_2^2}\right)} \quad (2.35)$$

From the velocity diagram (Fig. 2-7), it can be shown that

$$C_2^2 = W_2^2 - v_2 W_2^2 (2 \cos \beta_2 - v_2) \text{ and}$$

$$C_2^2 = W_2^2 (1 - \epsilon) \quad .$$

Therefore, Eq. 2.35 becomes

$$\eta_{TS} = \frac{1}{1 + \left(\frac{\zeta}{\epsilon}\right) + \left(\frac{1 - \epsilon}{2\epsilon}\right)} \quad (2.36)$$

Solving Eq. 2.36 for ϵ gives

$$\epsilon = (1 + 2\zeta) / (2/\eta_{TS} - 1) \quad (2.37)$$

Conservation of mass yields

$$\dot{m}_s \Lambda_2 = W_{a2} A$$

and

$$W_2 = \frac{\dot{m}_s \Lambda_2}{A \sin \beta_2} \quad .$$

Substituting this equation into Eq. 2.34 gives

$$\bar{W} = \epsilon \left(\frac{\dot{m}_s \Lambda_2}{A \sin \beta_2} \right)^2 \quad (2.38)$$

Conservation of energy gives

$$\bar{W} = \eta_{TS} \Delta h \quad (2.39)$$

Then by eliminating \bar{W} in Eqs. 2.38 and 2.39 and solving for the cross-sectional area for flow A we obtain

$$A = \frac{\dot{m}_s \Lambda_2}{\sin \beta_2} \left(\frac{\epsilon}{\eta_{TS} \Delta h} \right)^{1/2} . \quad (2.40)$$

Equation 2.40 gives the area of vapor flow through the turbine based on the given operating conditions. By assuming a value for the hub-to-tip ratio and by knowing this area we can calculate the size of the turbine. The blade length is

$$L = \left(\frac{A}{\pi} \frac{1 - r_t}{1 + r_t} \right)^{1/2} ;$$

the mean diameter is

$$D_m = L \frac{1 + r_t}{1 - r_t} ;$$

the outer diameter is

$$D_o = D_m + L ; \text{ and}$$

the hub diameter is

$$D_h = D_m - L .$$

In addition, the turbine speed n (in rpm) can be calculated from the peripheral wheel speed U . The peripheral wheel speed is

$$U = \frac{\dot{m} \Lambda_2}{A \sin \beta_2} \cdot \left(\cos \beta_2 - \frac{1}{2} [(2 \cos \beta_2)^2 - 4\epsilon]^{1/2} \right) . \quad (2.41)$$

The rotational speed is

$$n = \frac{U}{\frac{1}{2} D_m} \cdot \frac{1 \text{ revolution}}{2\pi \text{ radians}} \cdot \frac{60 \text{ s}}{1 \text{ min.}} \text{ and}$$

$$n = 19.099 \frac{U}{D_m} . \quad (2.42)$$

The outer diameter is returned to the main program to size the remaining components, and the details of the turbine analysis are printed.

2.3.3 Channel-Flow Flash Evaporator

The flash evaporator is a toroidal, open-channel flow type. The turbine is located on the center of the vertical axis and above the plane of the toroid. Steam released in the flashing process flows vertically upward from the open channel and then inward and down to the turbine. This flow path can be seen in Fig. 2-8.

Flash evaporation can be characterized by the degree of thermal nonequilibrium in the process. At equilibrium, the sea water outlet temperature is equal to the steam temperature. The steam temperature is equal to the saturation temperature associated with the chamber pressure. However, for any real flash evaporator of this type, equilibrium is not likely to be reached (without paying enormous penalties in cost and head losses), and the sea water outlet temperature will be higher than the steam temperature. The fraction of nonequilibrium is a function of the length, depth, and velocity of flow in an open channel.

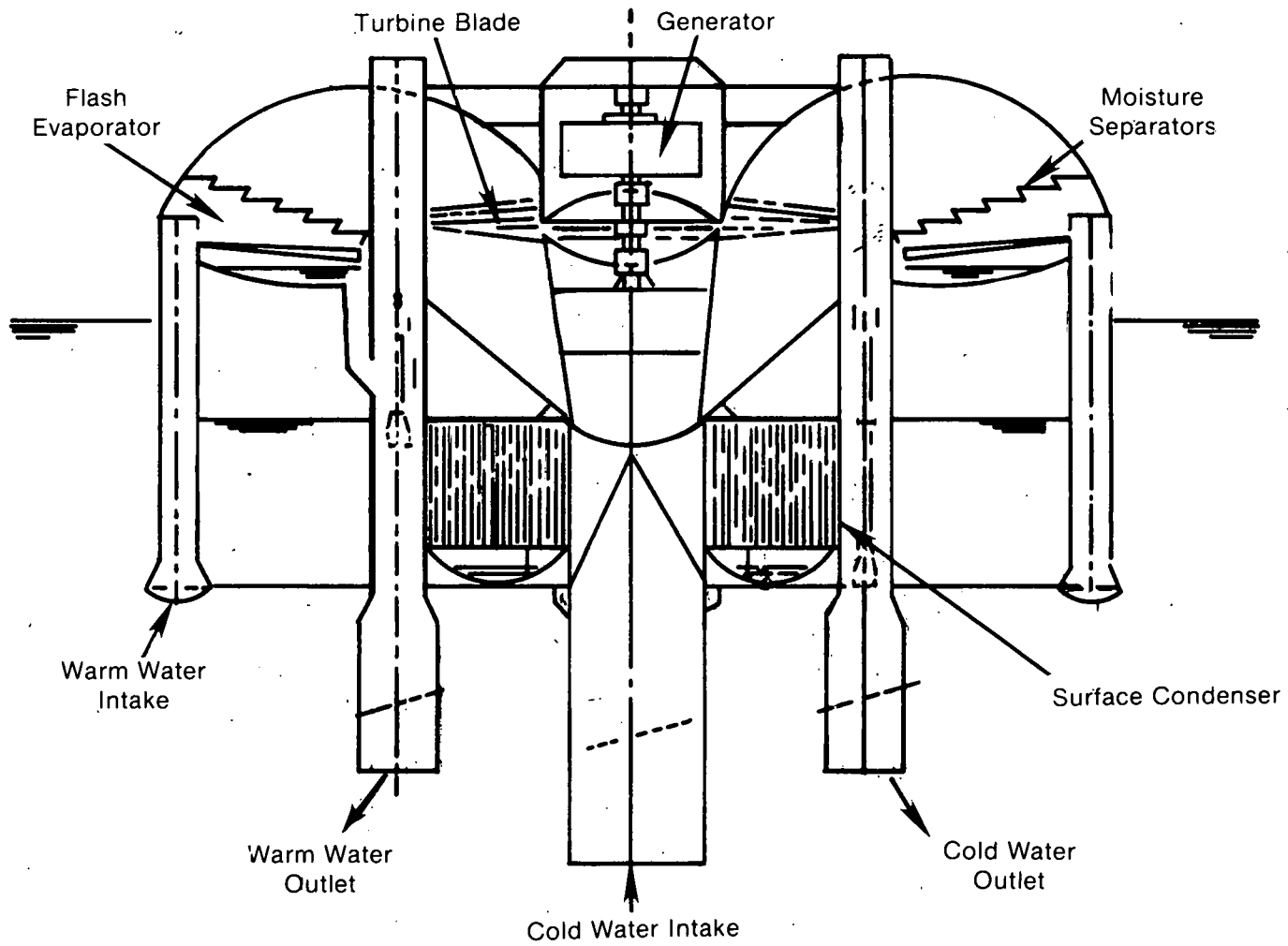
In an open-channel evaporator operating under the conditions existing within an OC-OTEC plant (except for very near the surface of the flow), hydrostatic head suppresses bubble formation. At the low pressures and temperatures experienced in an open-cycle OTEC plant, flashing can be conservatively conceived as a surface evaporation process. Using this assumption, Westinghouse (Westinghouse Electric Corp. 1979) obtained results for a rectangular, open-channel flow with a turbulent velocity profile (see Fig. 2-9) upon which we based the model used in this study.

A flowchart of the calculation scheme is shown in Fig. 2-10. The routine requires that the fraction of nonequilibrium β_e be input. All other parameters are passed by Common. The fraction of nonequilibrium is defined as

$$\beta_e = \frac{T_{wwo} - T_o}{T_{wwi} - T_o} = 1 - \eta_e \quad , \quad (2.43)$$

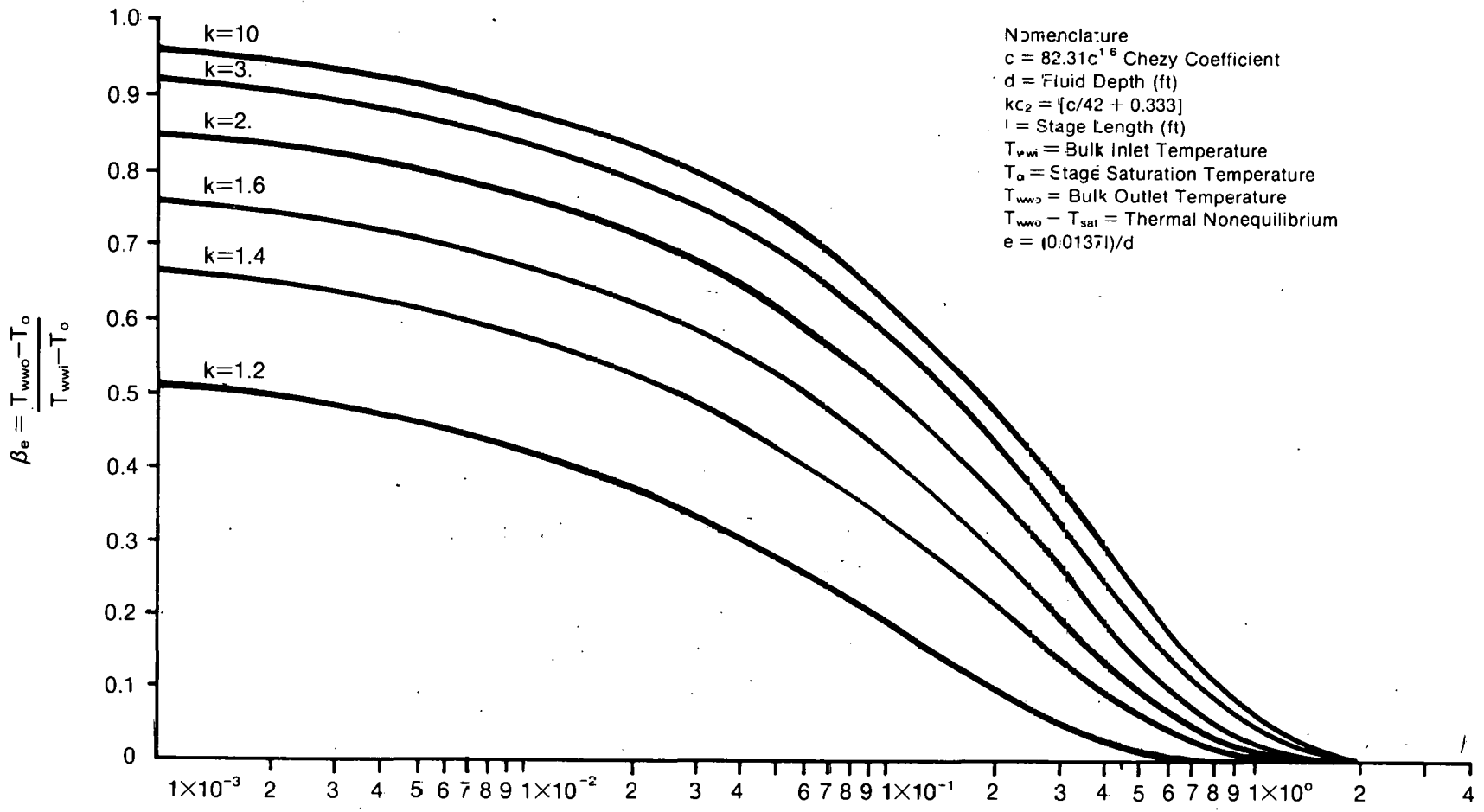
which is identical to the ordinate in Fig. 2-9. Inspection of this figure reveals that if the depth d is known, then the parameter k_c can be calculated. Only the length of the channel l remains unknown. The well-known Manning formula for steady, uniform flow in a channel can be used to relate volumetric flow with cross-sectional area and hydraulic radius. After some manipulation of the formula, depth can be found as a function of mass flow per unit width and channel slope:

$$d = \left(\frac{f_r \cdot \dot{m}_w}{\rho_w w \sin^2 \theta} \right)^{0.6} \quad , \quad (2.44)$$



25

Figure 2-8. Westinghouse OC-OTEC Plant Configuration



Nomenclature
 c = 82.31c^{1.6} Chezy Coefficient
 d = Fluid Depth (ft)
 kc₂ = [c/42 + 0.333]
 l = Stage Length (ft)
 T_{wwi} = Bulk Inlet Temperature
 T_o = Stage Saturation Temperature
 T_{wwo} = Bulk Outlet Temperature
 T_{wwo} - T_{sat} = Thermal Nonequilibrium
 e = (0.0137l)/d

Note: Logarithmic Scale

$$e/k_s^2 = \frac{(0.0137l)}{d} \left(\frac{l}{\frac{c}{42 + 0.333}} \right)$$

Figure 2-9. Thermal Nonequilibrium for Open Channel Flow

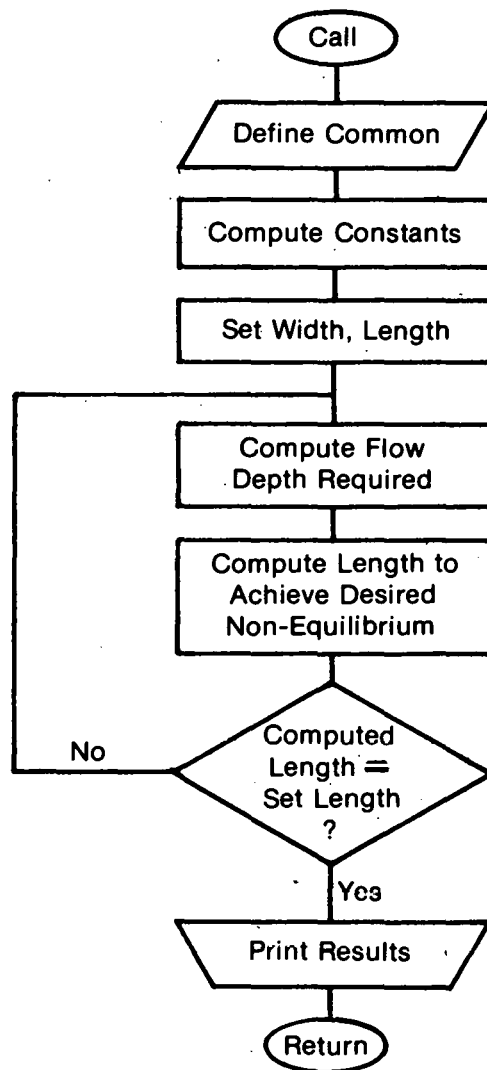


Figure 2-10. Channel-Flow Flash Evaporator Subroutine Flowchart

where

f_r = surface roughness factor (0.014 for concrete),

\dot{m}_w = warm sea water flow,

ρ_w = warm sea water density,

w = width of flow, and

θ = slope of the channel, taken as 2° .

The width and length of flow are related for a toroidal shape when the inner diameter is specified. The turbine analysis computes an outer diameter for the turbine blades, and a 4-m cushion is added to obtain an inner diameter for the flash evaporator. The calculation proceeds by assuming a length (and consequently a width) for the flow with a fixed slope of 2° on the channel. Eq. 2.44 yields the required depth. Figure 2-9 was modified to be a plot of the fraction of nonequilibrium versus the variable e , with k_c as a parameter. Then the curves in the figure were fit by fourth order polynomials. The length is calculated as

$$l = \frac{e \cdot d}{0.0137} \quad (2.45)$$

and compared with the assumed length. This procedure is repeated until the assumed and calculated length converge within acceptable limits.

The total head required for the flash evaporator is the sum of the free-fall head and the sluice gate loss. The free-fall head H_e is

$$H_e = l \sin \theta + d \cos \theta \quad , \quad (2.46)$$

and the sluice gate loss H_g is fixed at 0.15 m. The total head loss H_{Te} is

$$H_{Te} = H_e + H_g \quad . \quad (2.47)$$

This head loss is returned to the main program, and details of the flash evaporator analysis are printed.

2.3.4 Jet Condenser

Direct-contact condensers have the potential for higher heat transfer rates than surface condensers, owing to the lack of an intervening surface between the condensing steam and cold water flow. Until recently there have been little data available on direct contact condenser performance. Bakay and Jaszay (1978) have reported experience with turbulent, flat-jet condensers in Hungary for steam turbines of 100-200 MW_e capacity. They describe a calculation procedure for sizing the flat jets that includes the influence of increasing air concentration on heat transfer coefficients during the condensation process. Their analysis was used in this study. A flow-chart of the subroutine is shown in Fig. 2-11.

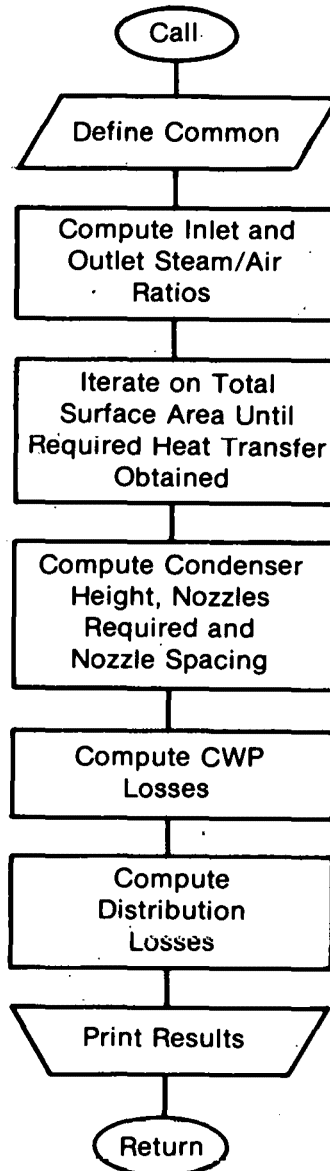


Figure 2-11. Jet Condenser Subroutine Flowchart

The design of the jet condenser consists of a flat, vertical sheet of water in which the velocity is horizontal. The steam flows vertically downward between these jets. We assume a homogeneous, continuous water sheet (evenly distributed vertically) that does not absorb air. We also assume that all air dissolved in the cold water is released immediately upon entering the condenser. After the analysis of Bakay and Jaszay, an equation is developed relating flow, temperature, air concentration, and heat transfer:

$$\frac{\dot{m}_c c_p (T_1 - T_{cwi})}{h_{lv} \cdot \dot{m}_a} = \int_{\sigma_1}^{\sigma_2} \frac{d\sigma}{1 - e^{-Bk}} \quad (2.48)$$

where

c_p = specific heat of sea water,

h_{lv} = latent heat of vaporization,

σ = steam to air ratio (1: condenser inlet, 2: outlet),

k = heat transfer coefficient = $k(\sigma)$,

and

$$B = \frac{a}{\dot{m}_c c_p} \quad (2.49)$$

where a = total surface area.

The heat transfer coefficient k is given as a function of the steam-to-air ratio. A series of polynomials were fit to this function over the range of interest in σ . The mass flow of air is the sum of the air liberated by the warm and cold sea water streams. All air is assumed to be liberated before it reaches the condenser steam inlet. Consistent with the comments in Bakay and Jaszay, the amount of steam condensed, f , was set at 99%, thus making the steam/air ratio cover a 100:1 range through the condenser.

The left side of Eq. 2.48 is constant, and the only unknown in the right side integral is B . A modified method of bisection was used to solve for B . The total surface area required is

$$a = R \cdot \dot{m}_c \cdot c_p \quad (2.50)$$

For a fixed spacing and width of jets, the number of channels and the height of the condenser H_c can be easily calculated. A typical, large-flow, flat spray nozzle was used to estimate the nozzle losses and required spacing. Nozzle losses of 2.6 m were estimated based on a nozzle flow rate of 4.5 g/s.

Included in the analysis were losses for the cold water pipe H_p that consisted of a loss owing to density difference between sea water at 1000-m depth and the surface (~1.0 m) and frictional losses in the 10-m diameter, 1000-m-long pipe (with an assumed roughness factor of 0.01). A small loss for the distribution H_d was included in the total cold water loop head requirements H_{tc} :

$$H_{tc} = H_c + H_p + H_d \quad (2.51)$$

This total loss was returned to the main program, and details of the condenser analysis were printed.

2.3.5 Spray Condenser

This direct-contact condenser analysis was based on work referenced by Colorado School of Mines (Watt et al. 1977). The condenser type is described as either a spray or cascade/baffle design. An overall, volumetric mass transfer coefficient approach is employed. A flowchart of the subroutine is shown in Fig. 2-12. The mass transfer coefficient k_m varied over a range of 0.1 to 0.4 kg/s·m³·K, presumably accounting for effects of varying noncondensable gas concentrations; however, no explanation is given for the range. Because the functional dependence of the heat transfer coefficient is not clarified, any results from this component model must be carefully evaluated.

The effect of subatmospheric pressure on the heat transfer coefficient k_o is accounted for by

$$k = k_o \left[\frac{P_{\text{sat}}(T_1)}{P_o} \right]^{0.2} \quad (2.52)$$

Additionally, the analysis is based on a log-mean temperature difference ΔT_{LM} where

$$\Delta T_{\text{LM}} = \frac{T_{\text{cwo}} - T_{\text{cwi}}}{\ln \frac{T_1 - T_{\text{cwi}}}{T_1 - T_{\text{cwo}}}} \quad (2.53)$$

The required volume of the condenser is then

$$V = \frac{f \cdot \dot{m}_s}{k_m \Delta T_{\text{LM}}} \quad (2.54)$$

where f = fraction of steam condensed.

The height of the condenser is calculated based on a fixed cross-sectional area A_c . The cross-section is toroidal: the outer diameter is equal to the turbine diameter and the inner diameter to the cold water pipe diameter. The condenser height H_c is

$$H_c = \frac{V}{A_c} \quad (2.55)$$

Nozzle losses, distribution losses, and cold water pipe losses are computed similarly to those in Sec. 2.3.4. Total head requirements are passed back to the main program, and details of the condenser analysis are printed to complete the routine.

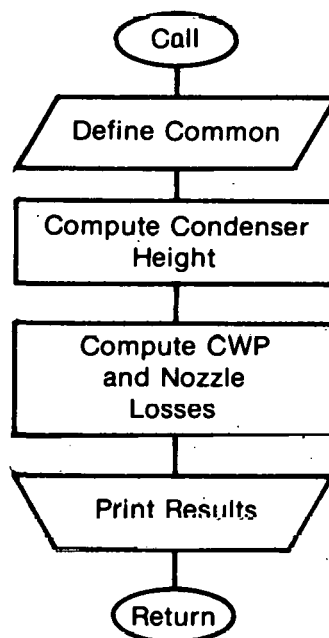


Figure 2-12. Spray Condenser Subroutine Flowchart

2.3.6 Condenser Exhaust

Any condenser type used requires an air removal system to purge the system of noncondensable gases, remove uncondensed vapor, and maintain vacuum. The analysis parallels that of Sec. 2.3.1 for the deaeration air removal. The exception is the absence of deaerator stages, and the similarity is an identical compression train, shown in Fig. 2-13. A flowchart of the subroutine is shown in Fig. 2-14.

The system consists of four compressors with three vent condensers located between them. There is no vent condenser before the first stage, since it operates at the same temperature as the incoming water vapor.

All inputs to the routine are passed through Common and include the amount of uncondensed steam and the mass flow of air. When the condenser pressure P_c is known, the compression ratio can be calculated using Eq. 2.13, with $N = 4$ and $P_{s,1} = P_c$. The total mass flow through the first compressor $\dot{m}_{t,1}$ is the sum of air flow \dot{m}_a and uncondensed vapor $\dot{m}_{v,0}$:

$$\dot{m}_{t,1} = \dot{m}_a + \dot{m}_{v,0} \quad (2.56)$$

The flow of vapor through subsequent compressors is reduced by the vent condensers. The vapor flow for compressor i is given by

$$\dot{m}_{v,i} = \frac{\dot{m}_a \cdot P_{vc,in}}{1.60 \cdot P_{a,i}} \quad (2.57)$$

where

$$P_{vc,in} = P_{sat}(7^\circ) \text{ as in Sec. 2.3.1 and}$$

$$P_{a,i} \text{ is calculated using Eqs. 2.14 to 2.16.}$$

The total flow through any compressor $\dot{m}_{t,i}$ is

$$\dot{m}_{t,i} = \dot{m}_a + \dot{m}_{v,i} = \dot{m}_a \left(1 + \frac{P_{vc,in}}{1.60 \cdot P_{a,i}} \right) \quad (2.58)$$

Power required to compress this flow is calculated using Eq. 2.26. The power required for each compressor is summed and passed back to the main program, and details of the air removal analysis are printed.

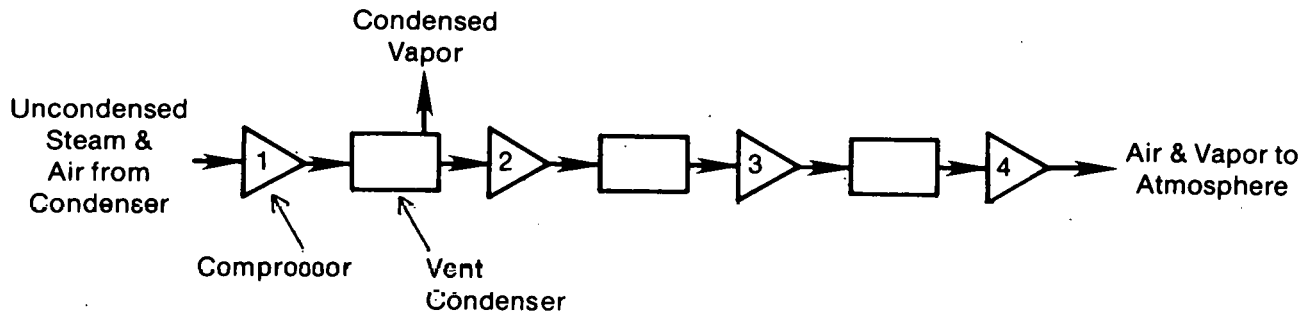


Figure 2-13. Condenser Exhaust Schematic

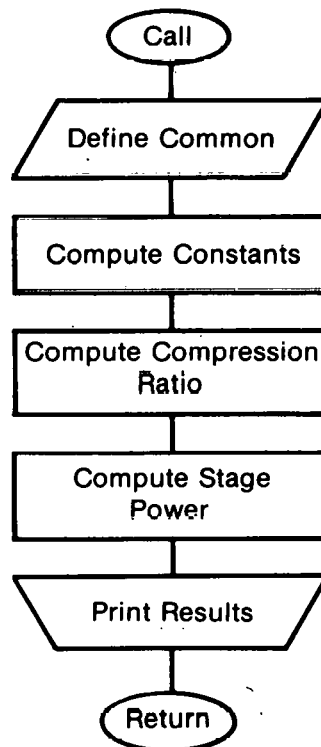


Figure 2-14. Condenser Exhaust Subroutine Flowchart

SECTION 3.0

RESULTS

3.1 INTRODUCTION

The Claude-cycle OTEC systems performance program was run 17 times for this study, and the results of the simulations are presented in this section. The input parameters for the 17 runs are listed in Table A-1 of the Appendix (numbered as runs 1 through 17). For each set of input parameters, the performance of the system was analyzed as R varied from 0.2 to 2.0, in increments of 0.2. The first simulation was a baseline study, and the runs that followed studied the effect of varying one or two of the input parameters from its baseline value. The results are summarized in Table A-2 of the Appendix, and the sections that follow discuss the most important results from the simulations.

3.2 BASELINE STUDY

The results of the baseline study are plotted in Figs. 3-1 through 3-4. This simulation had no deaeration and used the jet condenser. Figure 3-1 shows the net power of the cycle together with the three auxiliary components (condenser air removal and cold and warm loop requirements) that subtract power from the 100-MW_e gross output. Each parameter is plotted against R , where R is the temperature drop across the evaporator divided by the temperature drop across the condenser as discussed in Sec. 2.2. High R indicates most of the temperature drop occurred in the evaporator; low R indicates most of the temperature drop occurred in the condenser. Condenser air removal power is the power required to pump the air and uncondensed steam out of the condenser. Cold-loop power is the pumping power required to overcome head losses in the cold water loop: losses through the cold water pipe, losses in the water distribution system, nozzle losses, and the lost head in the condenser. Warm-loop power is the similar pumping power required to overcome head losses in the warm water side, losses in the evaporator, and losses through the warm water distribution system.

In the baseline study, the maximum net power is about 70 MW, corresponding to an R of 0.6. At this R , the turbine inlet temperature is 21.25°C and the turbine outlet temperature is 11.25°C. For lower or higher values of R , the net power decreases. At the optimal operating conditions, the major component of the auxiliary power requirement is the power for air removal in the condenser. Cold-loop and warm-loop power requirements are much less; cold loop power is larger than warm-loop power. Cold-loop power increases as R increases, whereas warm-loop power decreases as R increases. Cold-loop power is greater than warm-loop power primarily because of the head losses from the long cold water pipe and condenser height.

The trends for the warm- and cold-loop power requirements can be understood through Fig. 3-2, which plots the warm water, cold water, and steam mass flow rates for the baseline simulation as a function of R . At high R (small ΔT across the condenser), higher cold water mass flow rates are required to

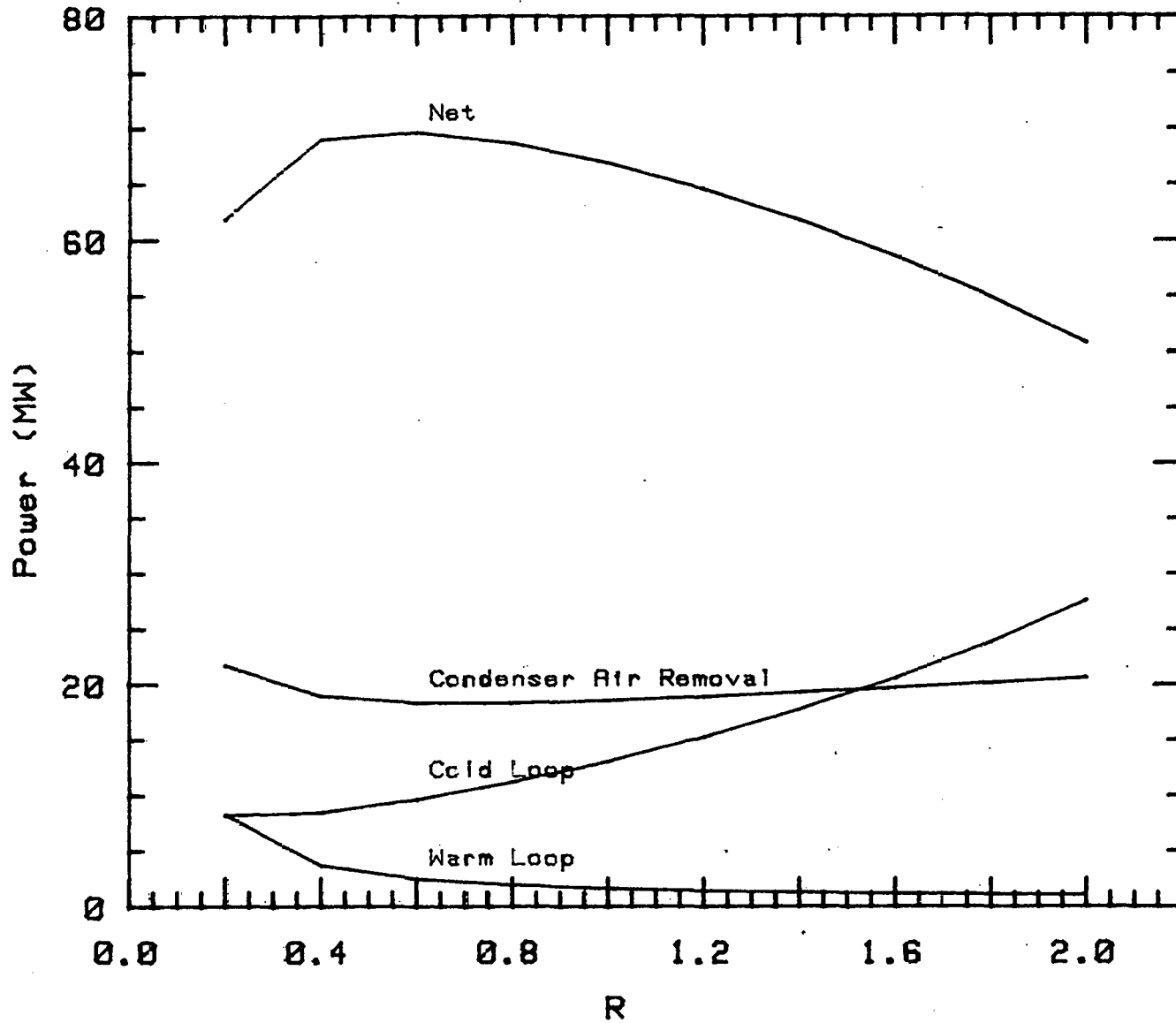


Figure 3-1. Baseline Study Results

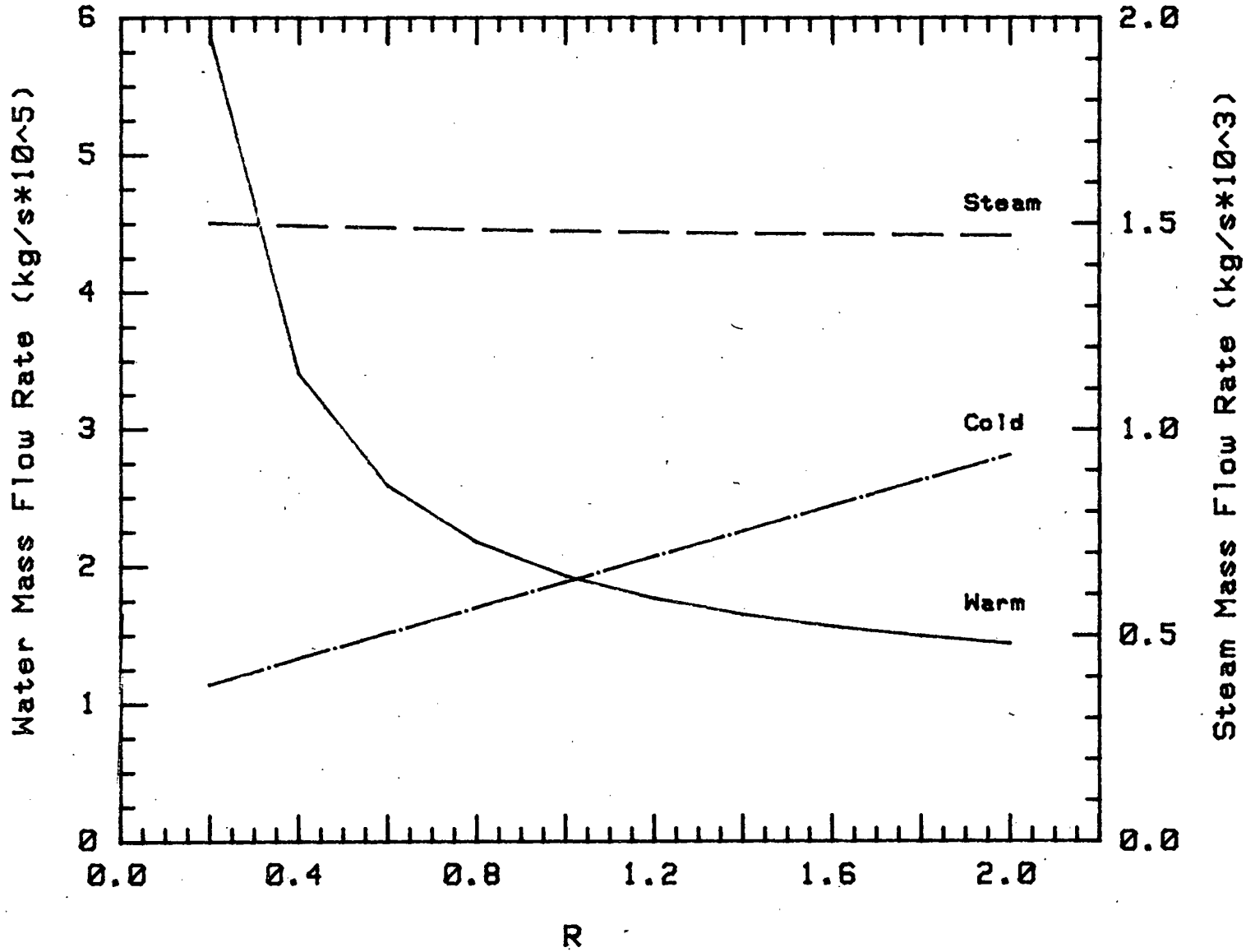


Figure 3-2. Baseline Simulation Flow Rates

accomplish the necessary cooling in the condenser. Because cold-loop power requirements equal the mass flow rate times the head losses, cold-loop power goes up as R increases. Similarly, at low R values (small ΔT across the evaporator), higher warm water mass flow rates are required to evaporate the water, and hence the power goes up. The steam mass flow rate remains roughly constant with respect to R since the enthalpy difference associated with $\Delta T_{\text{turbine}} = 10^\circ\text{C}$ varies little with absolute temperature.

The trend for condenser air removal power becomes clear by inspecting Eq. 2.26, which is the relation for computing stage power in the compressors that remove air from the condenser. Stage power is a strong function of the amount of air plus steam that must be compressed. The amount of steam present in the compressors is virtually constant as R varies, since it is assumed that 1% of the total steam flow must be removed by the compressors and the total steam flow does not change significantly with R . The air mass flow is proportional to the water stream flows because it is assumed that all the dissolved air in the water flows is liberated in the evaporator and condenser. Hence, at small R , the warm water flow rate is high, large amounts of air are liberated, and condenser air removal power is highest. As R increases, the warm water flow decreases, but the cold water flow increases; the larger amounts of air liberated from the cold stream balance decrease in air liberated from the warm stream, keeping condenser air removal power roughly constant.

Figure 3-3 shows the evaporator length, and Fig. 3-4 shows the plant outer diameter as a function of R for the baseline study. The shape of the curves is similar to the warm-loop power requirement. The dimensions decrease for higher values of R and increase for lower values of R . The evaporator length increases as R decreases because the available temperature drop is smaller, requiring larger warm water flows and, therefore, more surface area for evaporation. The plant's outer diameter is one crude estimate of plant cost; as the diameter increases so will the cost of the plant.

3.3 COMPARISON OF BASELINE STUDY WITH DEAERATION

The relative effects of deaeration and of no deaeration are shown in Figs. 3-5 through 3-7, which compare a simulation without deaeration (baseline) to one using deaerators. For the deaeration simulation, parameters include 4 warm stream stages and 5 cold stream stages with head loss at 0.5 m per stage. The plot of net power versus R in Fig. 3-5 shows that no significant overall improvements are gained by deaerating the warm and cold streams before they enter the evaporator and condenser, respectively. At the optimal R of 0.6, the deaeration simulation produces slightly less net power than the baseline simulation. For high values of R , deaeration is slightly better than no deaeration, but not better than the baseline case at the optimum value of R . The total deaeration power is the total power used to remove air from the system, including the pumping power to remove air in the cold and warm water deaerators, the pumping power to remove air from the condenser, and the water stream head losses resulting from deaeration. For the baseline study, the only component is the condenser air removal power. As can be seen from Fig. 3-6, the total deaeration power is slightly greater for the deaeration simulation. The air liberated by the cold and warm water streams has to be

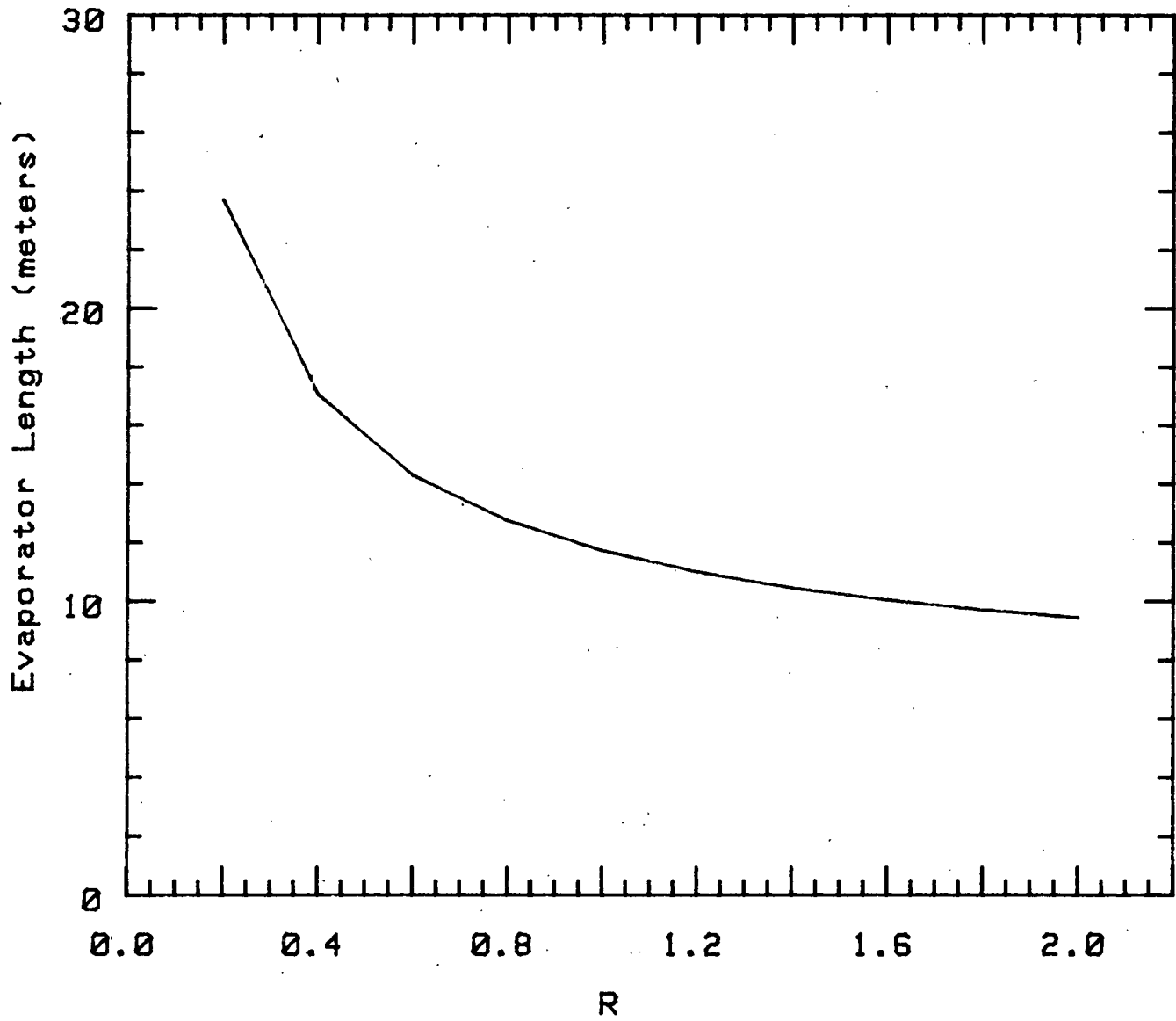


Figure 3-3. Baseline Study Evaporator Length

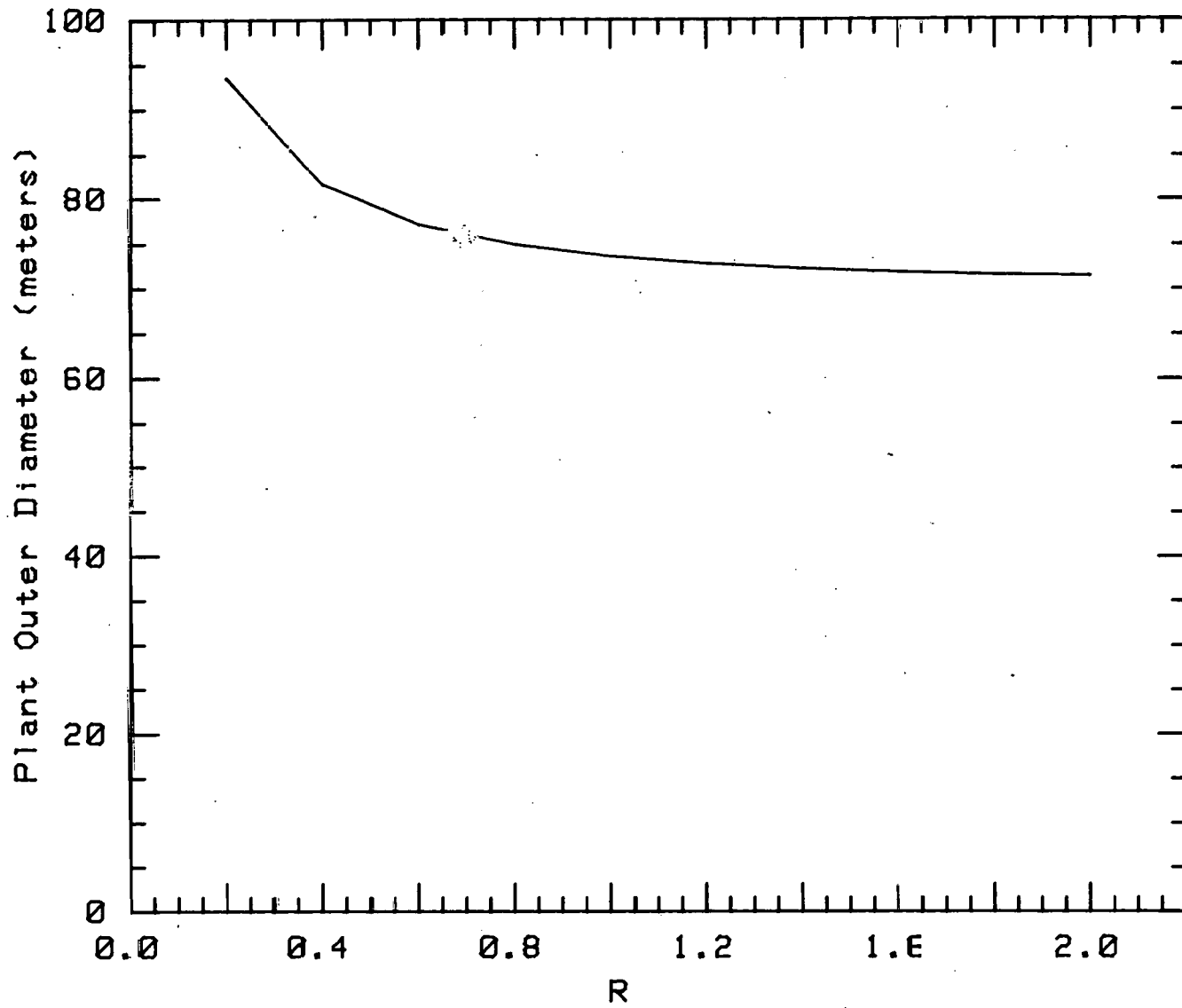


Figure 3-4. Baseline Study Plant Outer Diameter

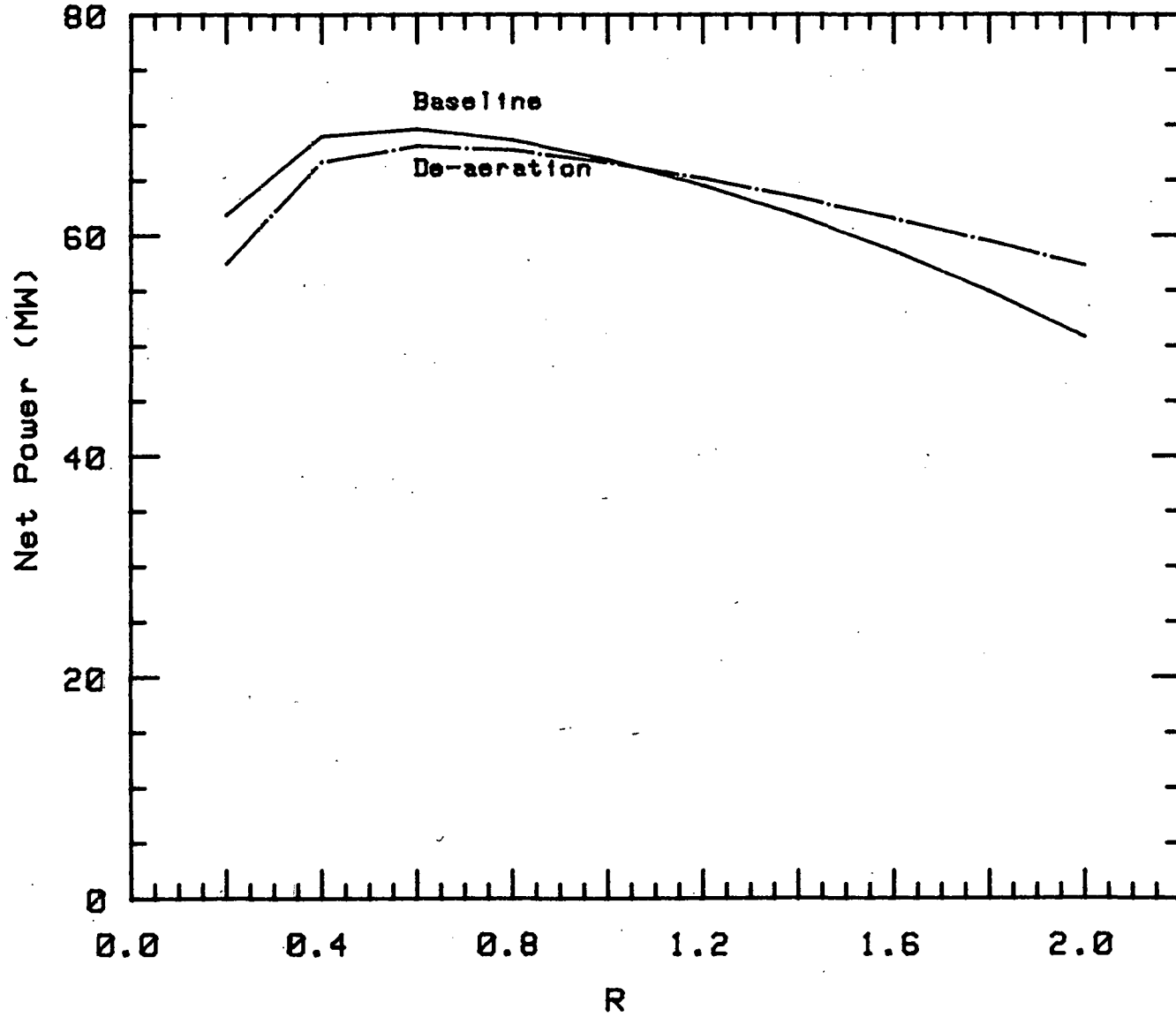


Figure 3-5. Comparison of Predeaeration and Baseline Studies

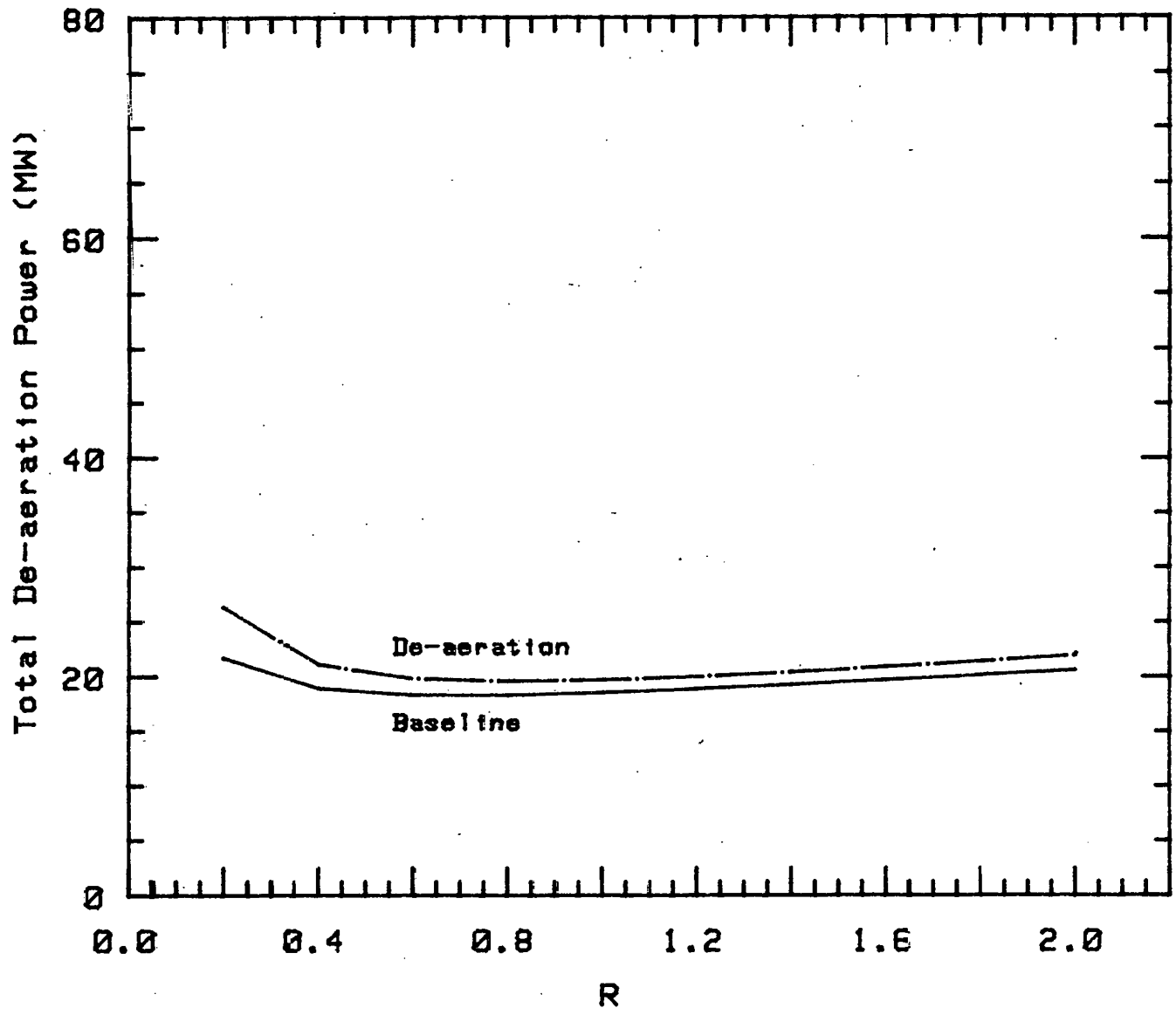


Figure 3-6. Comparison of Total Deaeration Power for Predeaeration and Baseline Studies

removed at some point during the cycle; the results for these simulations show that it does not matter where the air is removed. It can be pumped out before it reaches the condenser (deaeration) or after the steam is condensed (baseline); the net effect is about the same. It is important to remember that this model assumes all the air in both the cold and warm water streams is liberated and must be removed regardless of the system parameters chosen. This may not be a good assumption, especially for the cold water stream.

The advantage of deaeration can be seen in Fig. 3-7, which shows condenser height as a function of R for the deaeration and baseline runs. The baseline run requires a larger condenser, owing to reduced performance resulting from larger air concentrations. Deaeration reduces condenser size and, therefore, condenser head losses. One meter was assumed to be the minimum allowable condenser height. If the jet condenser algorithm calculated condenser heights of less than 1 m, the height was set to 1 m. However, the deaerators introduce additional head losses in the water streams, which are at least as great as any savings in condenser performance. The overall effect of deaeration is that it does not improve cycle performance. But it may reduce cost if the size is reduced.

3.3.1 Stage Head Loss Effects

Figures 3-8 and 3-9 show the effect of head loss in the deaerator stages on total deaeration power and maximum net power, respectively. As can be seen in both figures, larger stage head losses dramatically reduce performance. Stage head loss was found to be the most sensitive parameter of system performance of those tested in this model. Although a cycle with efficient deaerators is nearly as good as a cycle without deaeration, inefficient deaerators drastically reduce the net power. If deaerators are used they must be efficient and have minimal stage head losses.

3.3.2 Effects of Steam Partial Pressure to Total Pressure Ratio

One parameter measuring how much air the deaerators must remove from the water streams is the ratio of steam partial pressure to total pressure; i.e., the partial pressure of the steam divided by the total pressure in the last stage of the deaerator train. High values indicate very pure mixtures, and low values represent steam with greater amounts of air. The range of values tested was 0.8, 0.9, and 0.98. Figures 3-10 and 3-11 show that as the steam-partial-pressure to total-pressure ratio is increased, total deaeration power increases slightly and maximum net power decreases very slightly, respectively. Over this range of the ratio, there is no significant effect on cycle performance.

3.3.3 Effect of Air Fraction Liberated

Figure 3-12 shows the effect of the fraction of air liberated per deaerator stage on total deaeration power. The fraction of air liberated per deaerator stage is a measure of how efficiently each deaerator stage operates. Total deaeration power decreases very slightly as the fraction increases. The

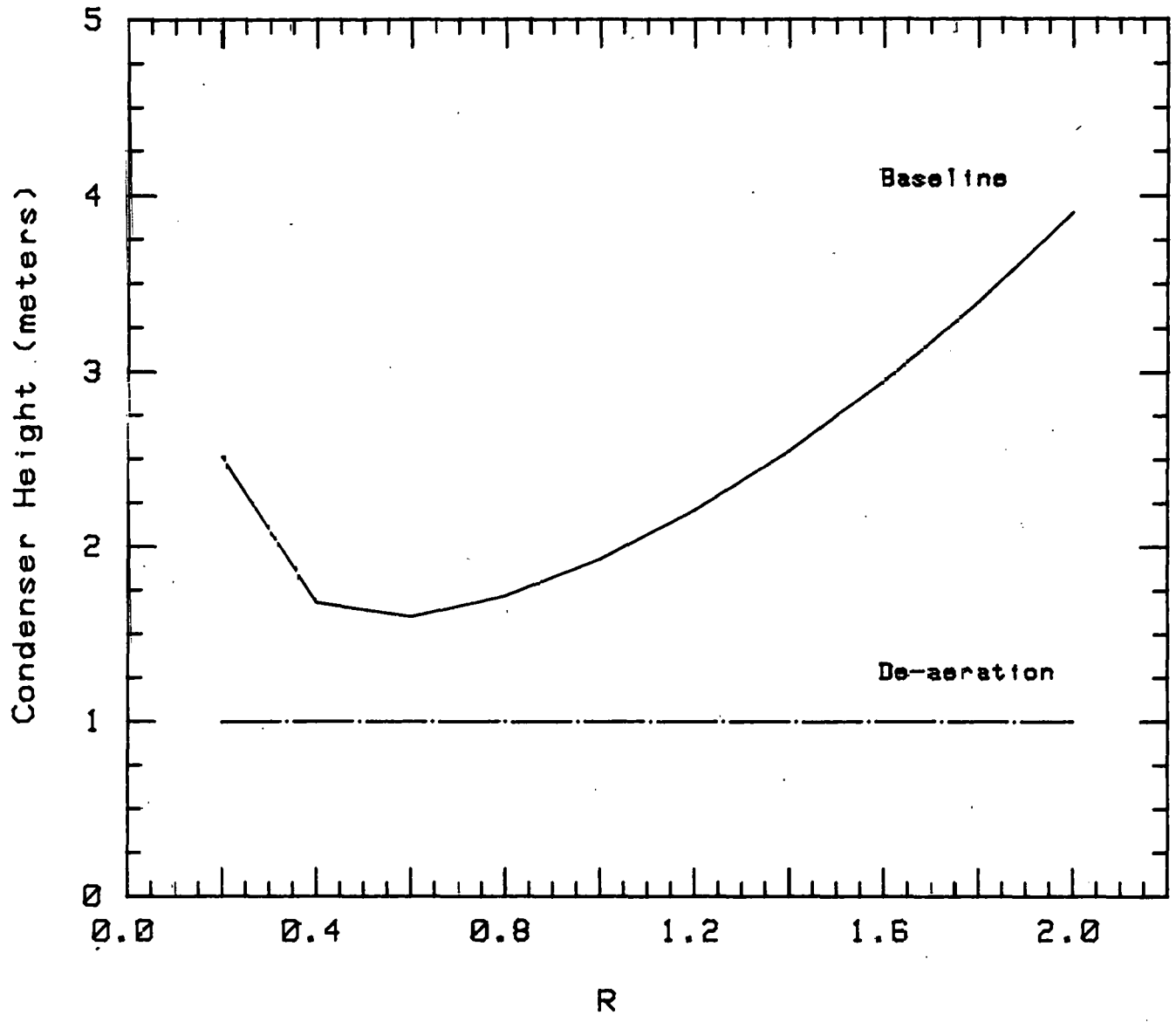


Figure 3-7. Comparison of Condenser Height for Predeaeration and Baseline Studies

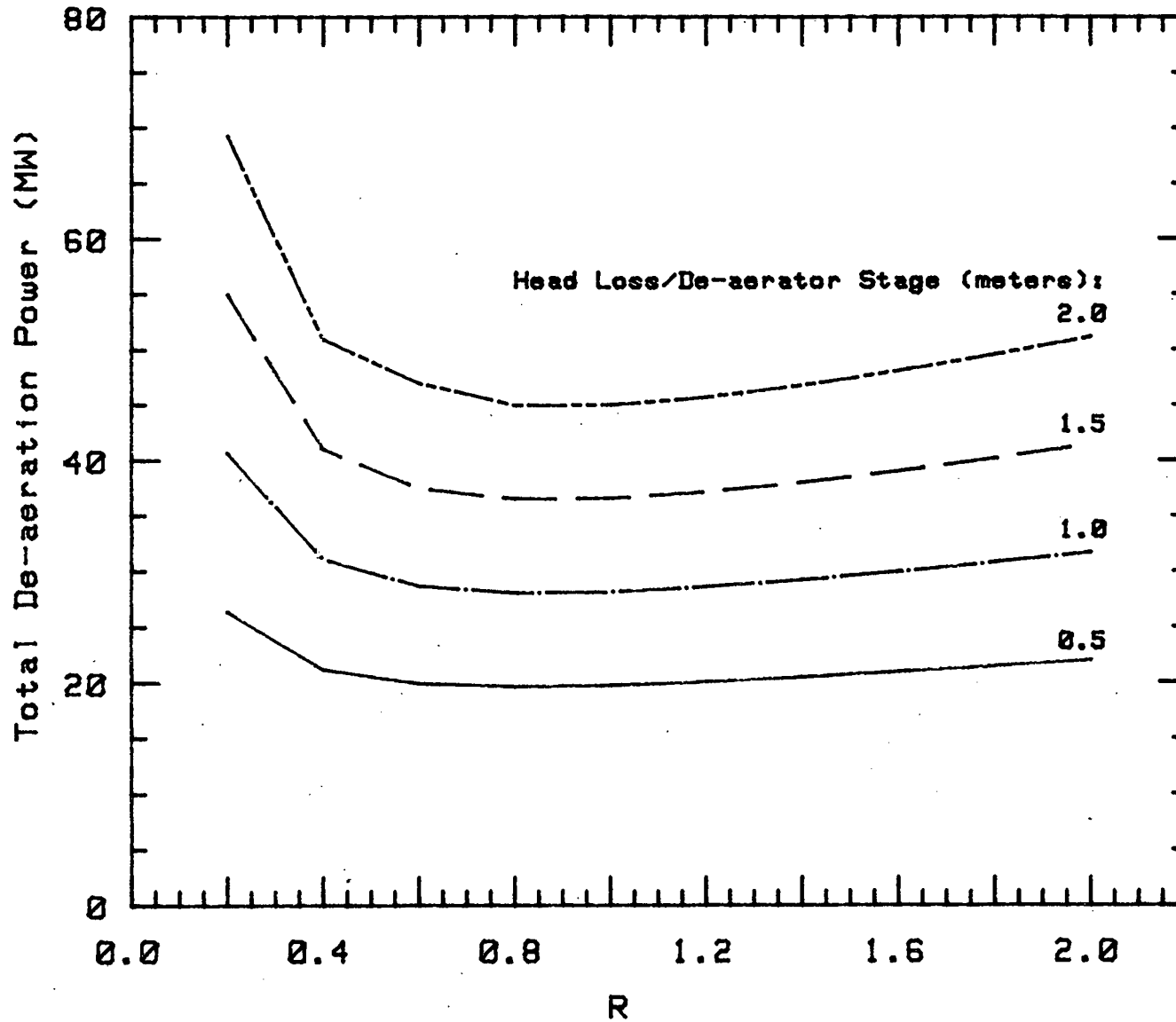


Figure 3-8. Deaeration Stage Head Loss Effect on Total Deaeration Power

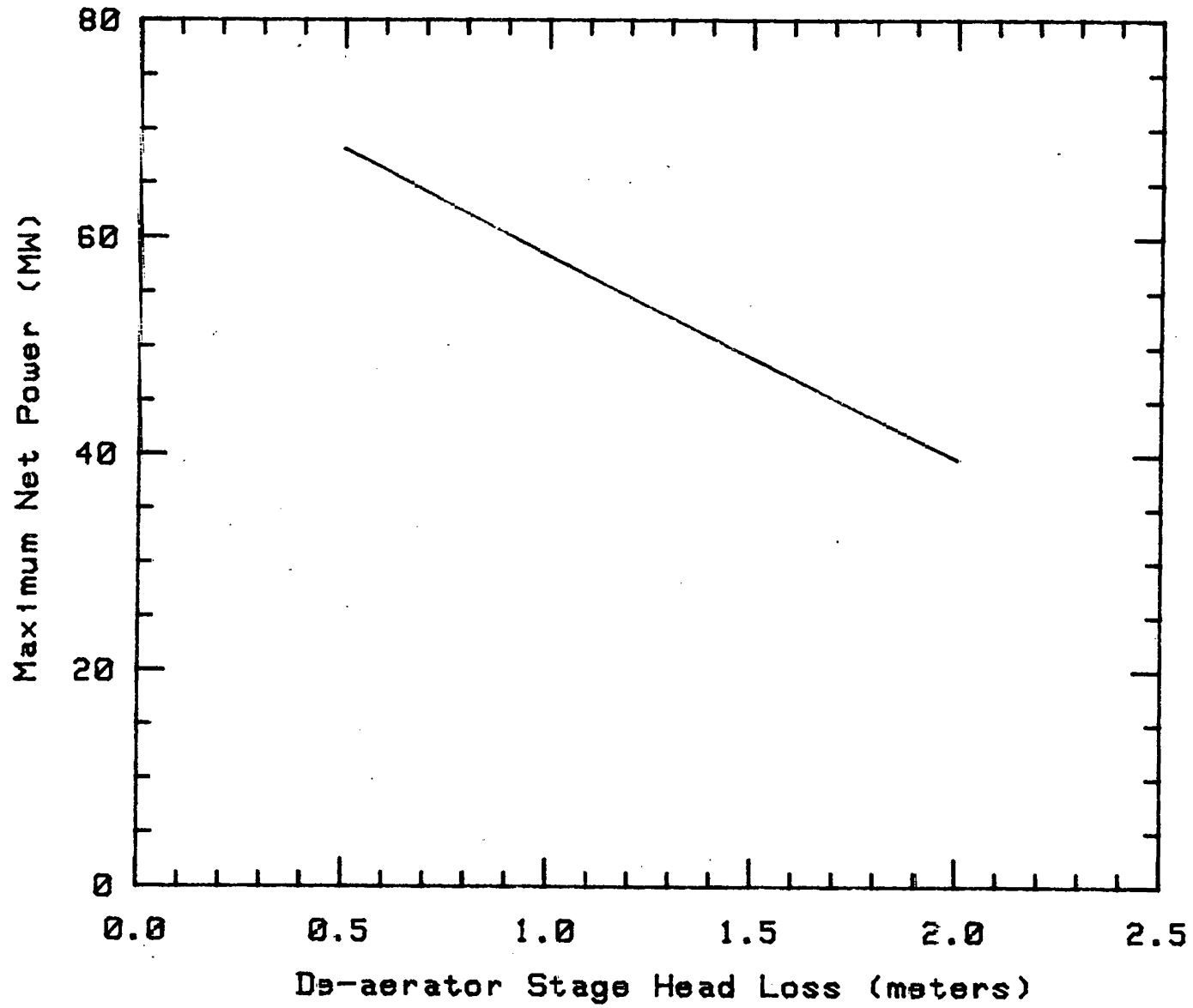


Figure 3-9. Deaeration Stage Head Loss Effect on Net Power

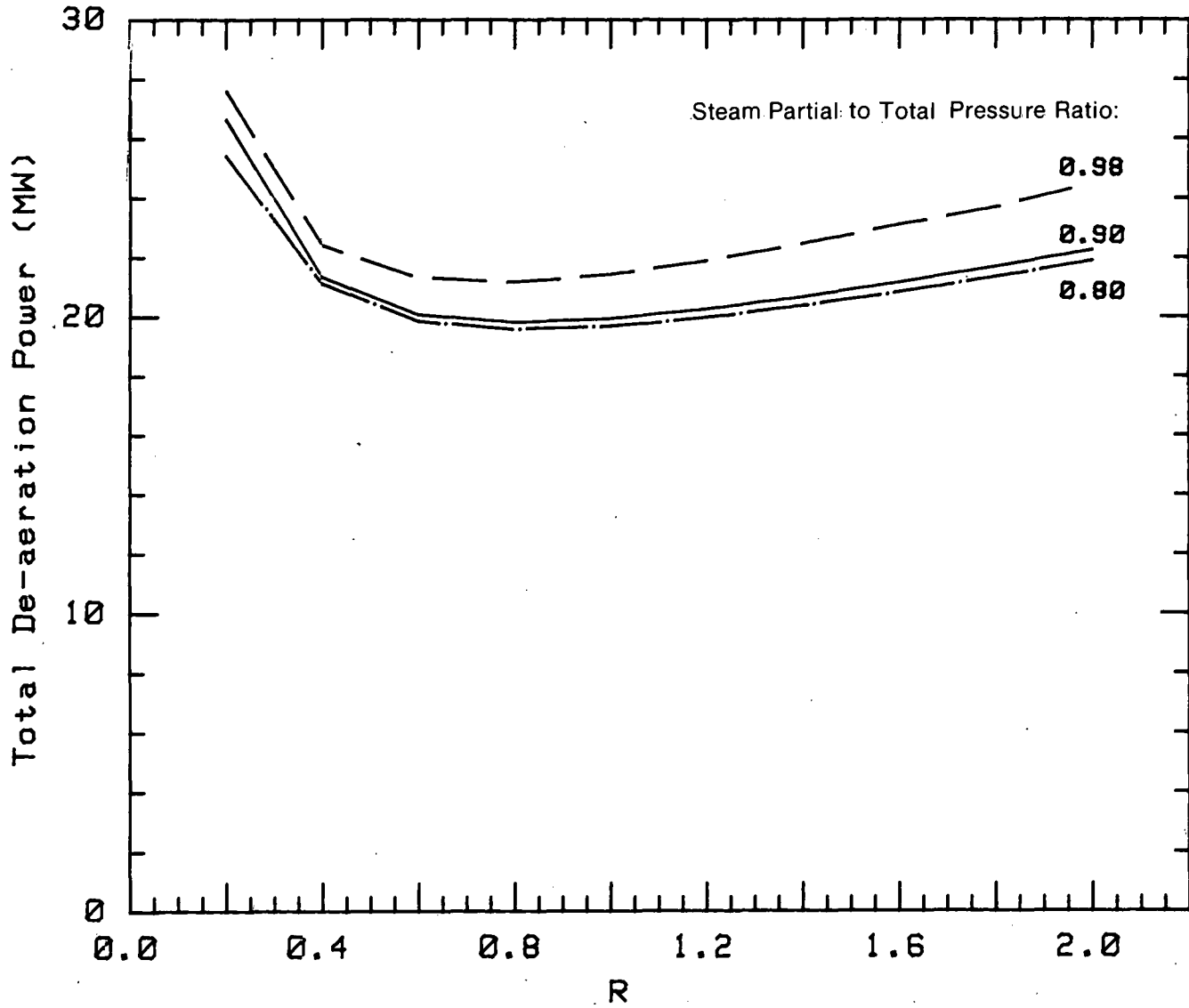


Figure 3-10. Steam Partial to Total Pressure Ratio Effect on Total Deaerator Power

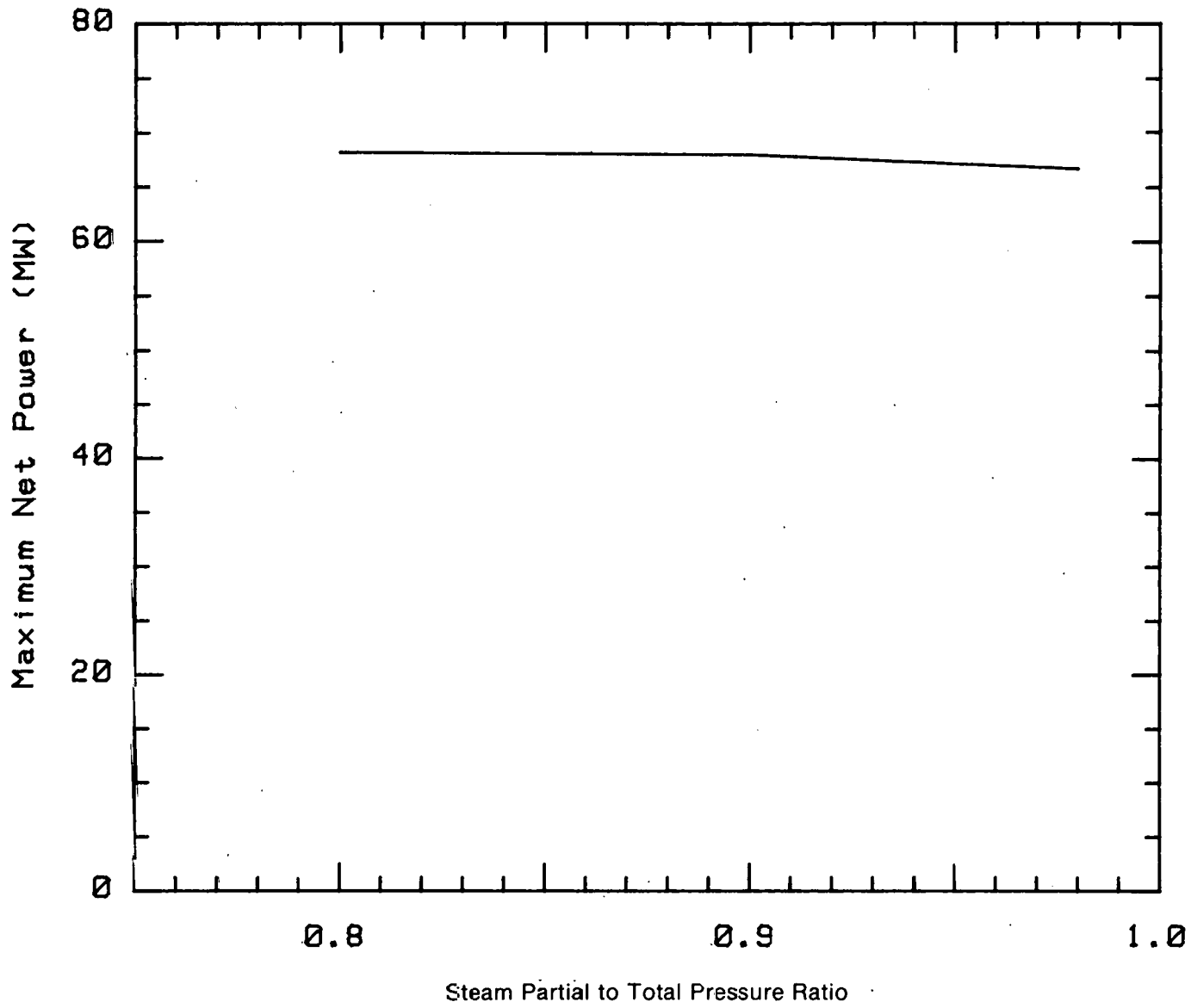


Figure 3-11. Steam Partial to Total Pressure Ratio Effect on Net Power

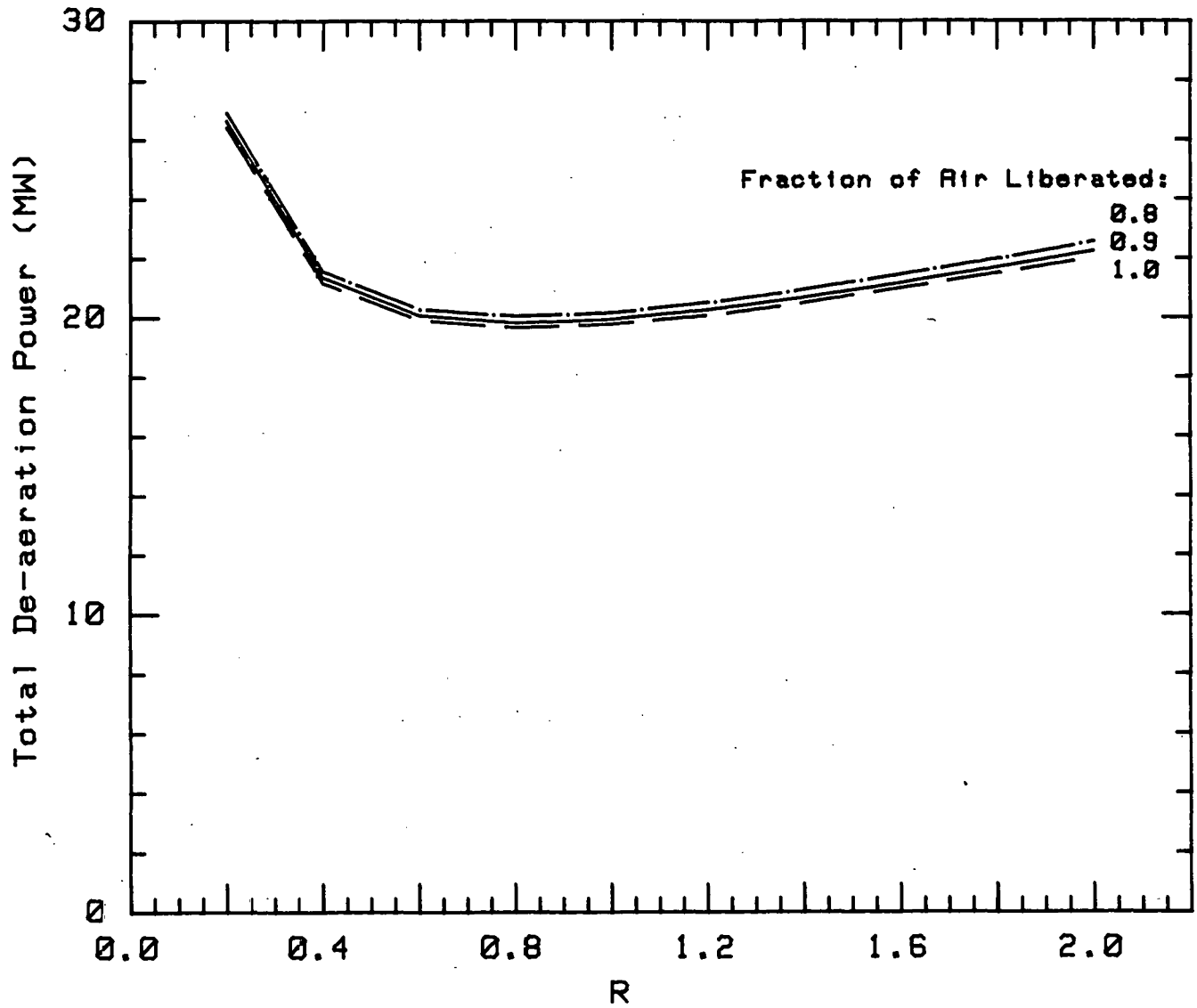


Figure 3-12. Effect of Air Fraction Liberated on Total Deaerator Power

effect of air liberated per deaerator stage on maximum net power was also studied. It was found that the maximum net power is virtually constant. The total deaeration power decreases for higher values because more of the air is liberated in the first few stages of deaeration when pump efficiencies are higher and less power is required to compress the air and vapor. Both the fraction of air liberated per deaerator stage and the steam-partial-pressure to total-pressure ratio simulations show the relative insensitivity of the model to efficiencies of deaerator air removal. It does not make much difference where air is removed.

3.3.4 Number of Deaeration Stages

Figures 3-13 and 3-14 show the effect of varying the number of deaerator stages on net power and total deaeration power, respectively. As the figures show, maximum net power decreases and total deaeration power requirements increase as the number of stages increases. Increasing the number of stages improves the efficiency of the deaeration process, reducing the power to pump air out of the cycle. However, as the number of stages increases, the deaerator water stream head losses increase at a faster rate than the pumping power decreases. Additional deaerator stages will be beneficial only if they have small head losses.

3.4 EQUILIBRIUM APPROACH FRACTION

The equilibrium approach fraction is a measure of the closeness of the warm stream to thermodynamic equilibrium with the vapor when it leaves the evaporator and of the closeness of the cold stream to thermodynamic equilibrium with the vapor when it leaves the condenser. Simulations for which the equilibrium approach fraction was varied used the jet condenser and no deaeration. Both the condenser and the evaporator used the same value for the approach fraction as it was varied.

Figure 3-15 shows the effect of equilibrium approach fraction on maximum net power. As the equilibrium approach fraction increases from 0.85 to 0.95, maximum net power also increases. The more efficient evaporators or condensers (higher approach fractions) allow the required heating and cooling at lower water flow rates. The net power increases because the auxiliary pumping power (mass flow rate times head loss) decreases for decreasing water flow rates. The increase in maximum net power is slight--a 10% increase in the equilibrium approach fraction produces only a 3.5% increase in net power. Acceptable data do not yet exist for channel-flow flash evaporators operating at temperatures and flow rates per unit width expected in OTEC plants. The Westinghouse model used in this study is based on an analytical prediction of an assumed evaporator design, not on experimental data. It would be beneficial to study the effect of a lower evaporator approach fraction on system performance, for the value could be as low as 0.5 or 0.6. Also, provision should be made to vary the evaporator and condenser approach fractions independently. It is likely the optimal operating point would move to higher values of R if the equilibrium approach fraction were lower for the evaporator than for the condenser (a larger ΔT across the evaporator would compensate for the lower equilibrium approach fraction).

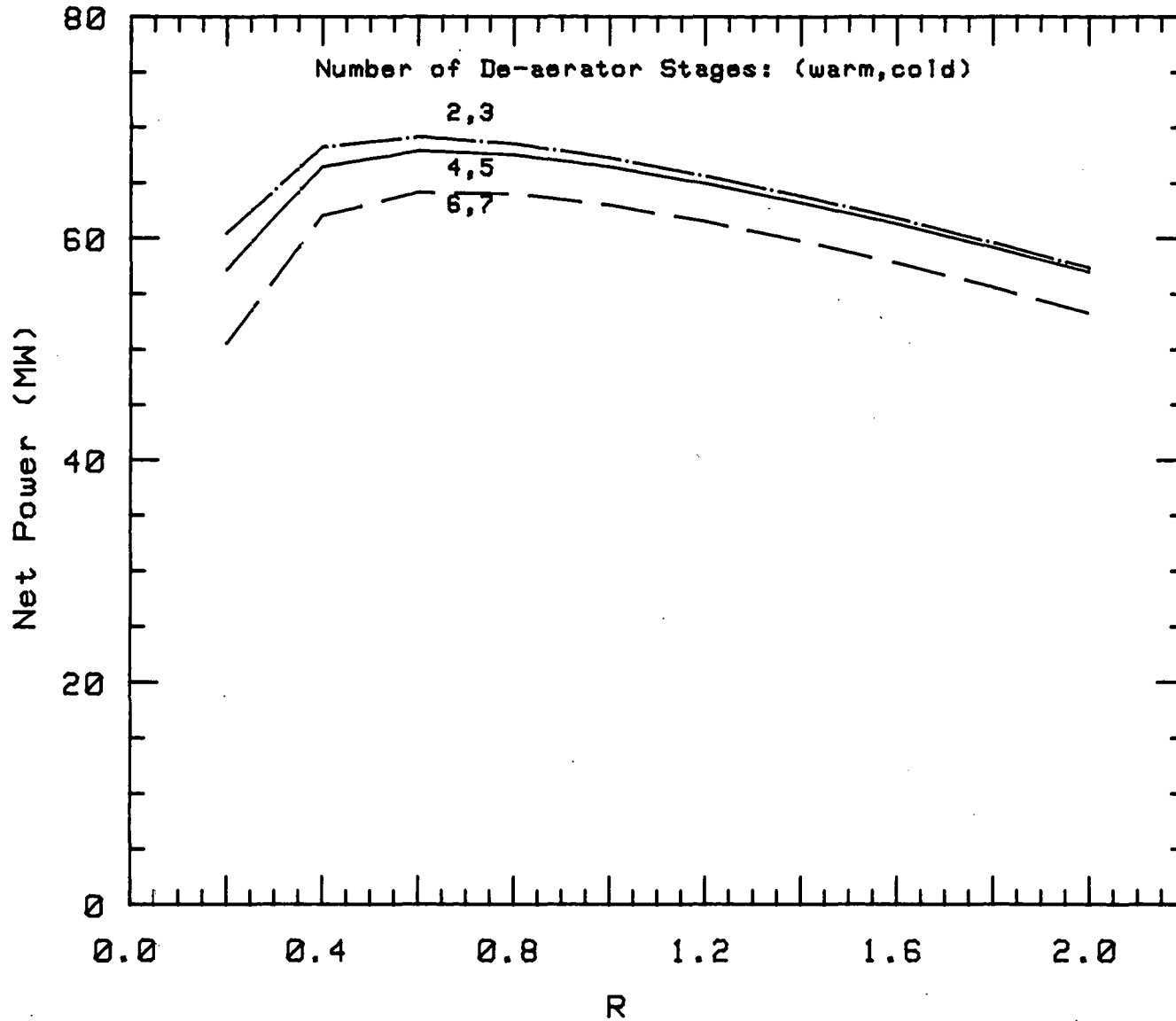


Figure 3-13. Effect of the Number of Deaeration Stages on Net Power

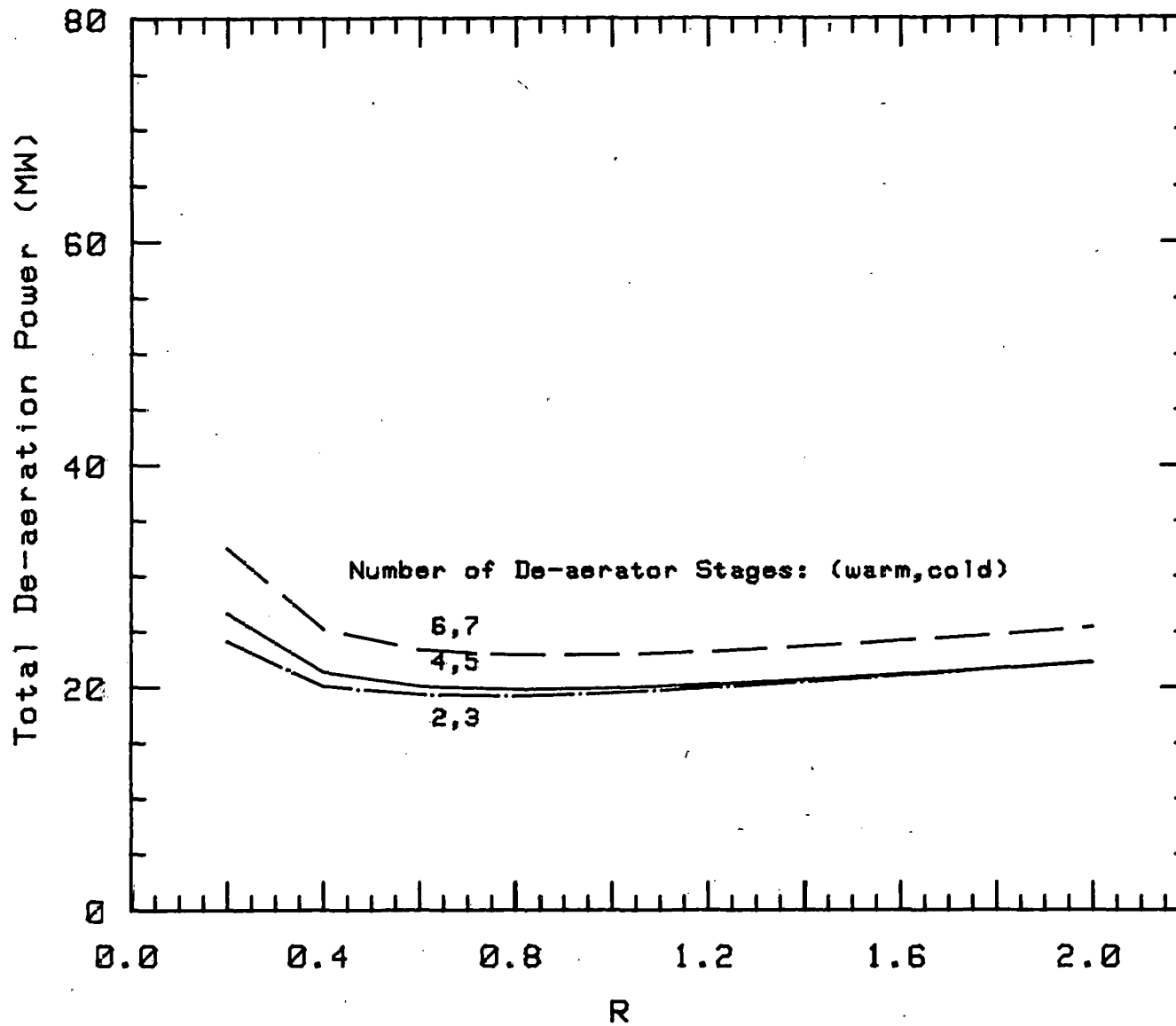


Figure 3-14. Effect of the Number of Deaeration Stages on Total Deaeration Power

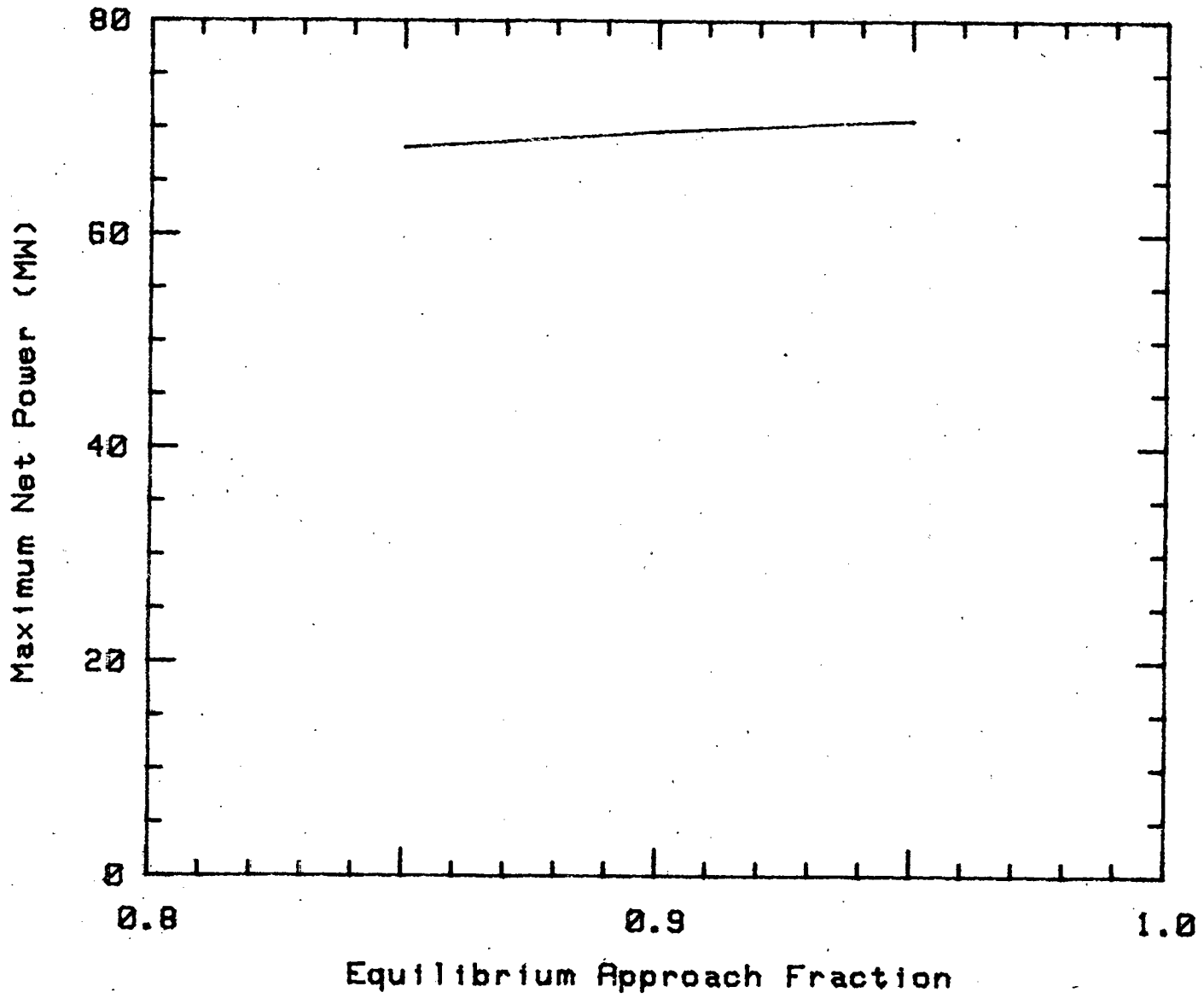


Figure 3-15. Effect of Equilibrium Approach Fraction on Net Power

3.5 TURBINE - GENERATOR EFFICIENCY

Figure 3-16 shows the effect of increasing the turbine-generator efficiency on maximum net power. The simulations used the jet condenser with no deaeration. As the efficiency is increased from 0.75 to 0.85, maximum net power increases by 6% to 7%. More efficient turbines require lower steam flow rates to produce the gross power and, therefore, lower cold and warm water flow rates. The lower cold and warm water flow rates reduce auxiliary power requirements.

3.6 SPRAY CONDENSATION

Several simulations were performed using the CSM spray condenser model rather than the jet condenser. These results were accepted with much less confidence, owing to the uncertainty of the condenser performance in the presence of noncondensable gases. A range of 0.1 to 0.4 was given by CSM (Watt et al. 1977) for the condenser volumetric heat transfer coefficient. The wide range presumably results from the effect of noncondensable gases on condenser performance. For the entire range of this parameter used in the studies, the net power using spray condensation was always less than the net power using the jet condenser. For the study using the lowest value for the heat transfer coefficient, the cycle actually required power to operate at high R. Spray condensers required much greater height to condense the steam than the jet condenser. This added height, and correspondingly greater head loss, predominantly reduced the net power.

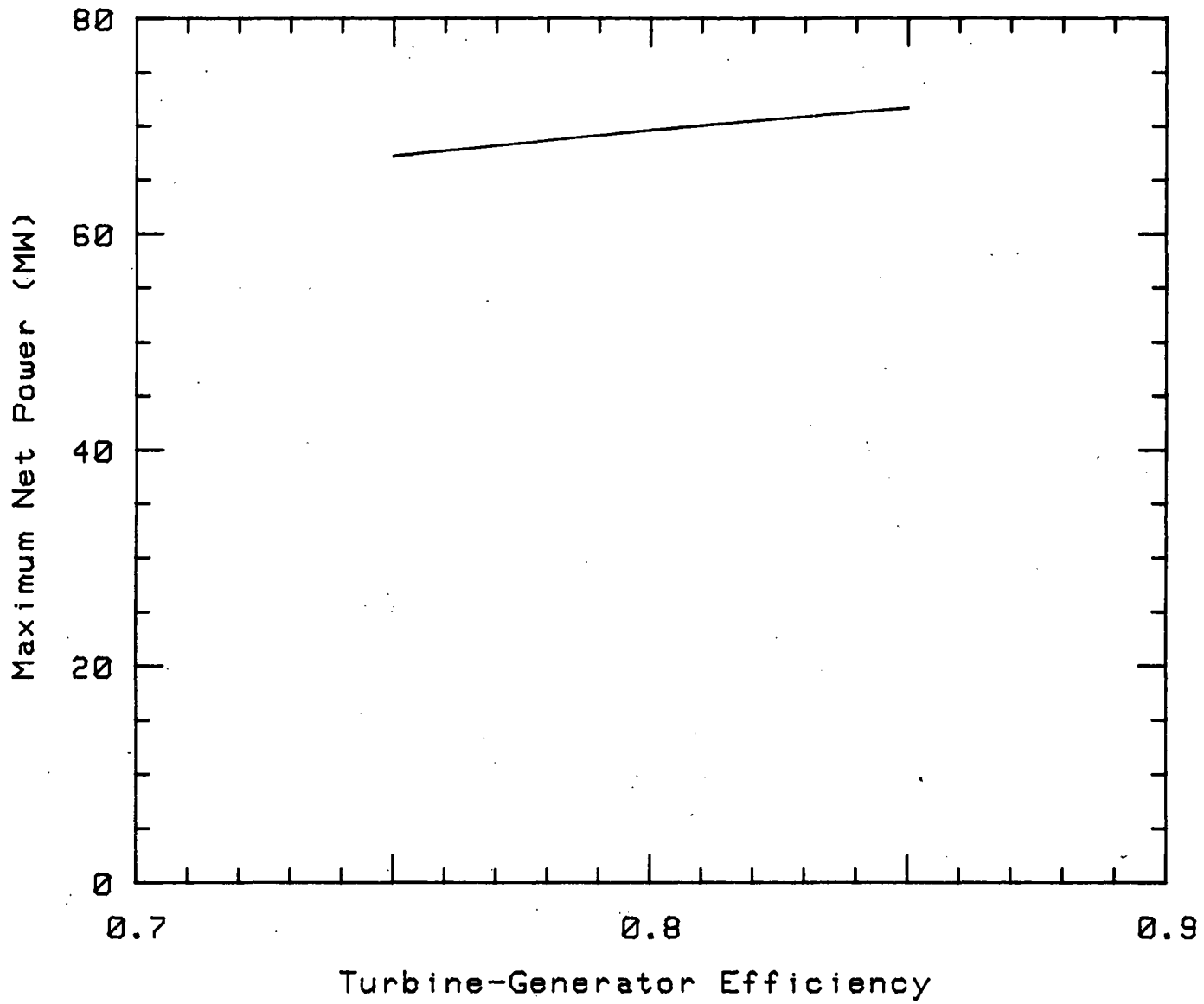


Figure 3-16. Effect of Turbine-Generator Efficiency on Net Power

SERIO 

SECTION 4.0

CONCLUSIONS AND RECOMMENDATIONS

4.1 CONCLUSIONS

Conclusions about the developed algorithm and the resulting baseline, deaeration, and sensitivity studies will be discussed.

4.1.1 Conclusions About the Algorithm

All component algorithms discussed in this report are simple and assume that the component will achieve a given level of performance independent of operating conditions. For example, the deaerator algorithm assumes that each deaeration stage will liberate a fixed fraction of the amount of air that would be liberated under equilibrium conditions, independent of the flow rate of water through it. The turbine algorithm assumes that the turbine operates with a fixed efficiency independent of the absolute magnitude of the inlet and outlet temperatures or vapor velocities. In this approach each component is assumed to be designed for the particular operating condition under study, implying that the design changes as the operating conditions change. Thus, the algorithm cannot be used to analyze the off-design performance of a particular system, but it can be used to compare the performance of two systems, each operating at their design point. In particular, it will be used to compare the performance of different evaporator and condenser designs at their common design point. For this application, we must be concerned whether the simplifying assumptions made in the other component models might unfairly favor the performance of one type of evaporator or condenser versus another. The following sections discuss this possibility for each component other than the evaporator and condenser. We concluded that the approach will allow some of the penalties of inefficiency to show up in cost rather than performance.

4.1.1.1 Conclusions About the Deaerator Algorithm

A more efficient evaporator or condenser would require a lower warm or cold water flow rate than a less efficient one. The fractional approach to equilibrium air removal per stage in the deaerator might depend on flow rate (or more directly, on residence time of a given volume of fluid in a deaerator stage). However, according to the philosophy of the adopted approach, we will assume that the deaerator is designed to remove a given fraction of the air dissolved in water under equilibrium conditions, whatever the water flow rate. Thus, two different evaporators or condensers would require the same amount of pumping power to deaerate the warm or cold water streams regardless of efficiency. The effect of efficiency would show up in the design and thus in the cost of the deaerator, not in the performance of the system.

4.1.1.2 Conclusions About the Turbine Algorithm

The turbine algorithm calculates the turbine size required to produce a given amount of gross power. The turbine size depends upon the minus $3/2$ power of the enthalpy drop across the turbine. A more efficient evaporator or condenser would allow a greater enthalpy drop across the turbine for a given sea water temperature difference across the plant. However, according to our adopted approach, we will compare the performance of different evaporators and condensers with a fixed temperature drop across the turbine. Thus, the effect of evaporator and condenser efficiency will show up in the size of these components required to produce or condense a given flow rate of steam, rather than the size of the turbine. Increased evaporator or condenser size affects performance through increased losses and cost through increased materials and fabrication time.

4.1.1.3 Conclusions About the Condenser Exhaust Algorithm

The pumping power required by the condenser exhaust depends on the rate of flow of uncondensed vapor in the condenser. A more efficient condenser would condense more vapor than a less efficient one. However, consistent with our approach, we will assume that condensers are designed to obtain a given fraction of steam condensed. Thus, the rate of flow of uncondensed vapor in the condenser is independent of condenser efficiency. The effect of efficiency will show up in condenser size. A less efficient condenser must be larger than a more efficient one to yield the same rate of flow of uncondensed vapor. Condenser size influences performance through increased losses and cost through increased materials and fabrication expenses.

4.1.2 Conclusions About Baseline, Deaeration, and Sensitivity Studies

4.1.2.1 Baseline Study

The baseline study shows that the peak net power output occurs at $R \approx 0.6$. It is to be expected that the net power will peak at some intermediate value of R , because at low R (low temperature drop across the evaporator) a high mass flow rate is required in the evaporator, implying higher losses there, and at high R (low temperature drop across the condenser) a high mass flow rate of cold water is required in the condenser, implying higher losses there. Losses will be minimized at some intermediate value of R . The optimum value occurs for $R < 1$ (lower temperature drop across the evaporator than the condenser) because the evaporator has smaller losses than the condenser; hence the plant needs to be operated with lower cold-water flow rate than warm-water flow rate. Reduced cold water flow rate occurs when ΔT_{cond} is large.

The plant's outer diameter decreases as R increases, first rapidly and then more slowly, because the required length of the channel-flow flash evaporator decreases as the temperature difference across the evaporator increases. The outer diameter is close to its minimum value at the optimum value of R from the point of view of performance. The relation of the outer diameter to cost (the larger the plant, the more it costs) implies that the best performing plant may also be close to the cheapest.

4.1.2.2 Deaeration Study

The baseline study shows that condenser exhaust power is a significant requirement of the system. The deaeration study was made to determine if removing air from the warm and cold water streams before their entrance into the evaporator and condenser would reduce this loss. At the optimum value of R , deaeration produces slightly less net power than the baseline case. For higher values of R , deaeration is slightly better than the baseline case at the same value of R , but not better than the baseline at optimum R . Therefore, air has to be removed from the system, and where it is removed does not significantly alter system performance. However, the condenser height is reduced with deaeration so that the value of deaeration may be to reduce cost rather than improve performance.

Effect of Deaeration Stage Head Loss and Increased Number of Stages. The deaerator stage head loss is the parameter that most affects system performance. A system with efficient deaerators is nearly as good as one without deaerators as far as performance is concerned, but inefficient deaerators drastically reduce performance.

Increasing the number of deaerator stages decreases the net output power because the additional head losses overcome the increased deaerator pumping efficiency.

Effect of Parameters Which Influence the Amount of Air Removed by the Deaerators. Two parameters which influence the amount of air removed by the deaerators are the ratio of the vapor partial pressure to the total pressure in the first deaerator stage (f_g) and the fraction of air liberated per stage of the deaerator (f_l). Varying these parameters had little effect on the performance of the system; with regard to performance, it does not matter where the air is removed.

4.1.2.3 Sensitivity Study

Two other parameters that influence system performance are the equilibrium approach fraction for the evaporator and condenser and the turbine generator efficiency. In this study, both the evaporator and condenser were assumed to achieve the same equilibrium approach fraction. Variation of this number from 0.85 to 0.95 (10%) increased the net power by 3.5%, because of reduced warm and cold water flow rates. The size of the channel-flow flash evaporator required to achieve these values of the equilibrium approach fraction was calculated using data extrapolated from higher temperatures and pressures than will exist in an OTEC plant. These extrapolations are very uncertain. An evaporator sized according to them may actually achieve an equilibrium approach fraction of only 0.5 to 0.6. It is also not necessarily true that the evaporator and condenser would be designed to give the same value of this parameter.

Increasing the turbine generator efficiency from 0.75 to 0.85 increases the net power by 6%-7%, because the increased efficiency means a lower steam mass flow rate is required for the same gross power output. The warm and cold water flow rates are reduced concomitantly, requiring less pumping power.

4.2 RECOMMENDATIONS

The present algorithm is constructed so that many of the consequences of inefficient evaporator or condenser design show up as increased component size. Increased size sometimes, but not always, means poorer performance. To determine the full impact of inefficient evaporator or condenser design, the economic penalty of increased size must also be assessed. The main effect of deaeration is to reduce the condenser size but not greatly affect performance. To assess the importance of deaeration, the economic consequences of a smaller condenser must be considered.

An alternative approach would be to hold the cost of competing systems approximately constant, while comparing their performance. This approach would require more sophisticated performance models of the components than the ones developed so far. For example, cost is related to amount of materials used in construction, which, in turn, is related to size. Thus, if size is kept constant, cost will be approximately constant. If size is kept constant, then performance will vary with changes in the design point. For example, if the turbine size is kept constant, then the gross power produced will vary with changes in the design point. Also, if the deaerator cost is kept constant by freezing the design, then the fraction of air liberated per stage will vary with water flow rate.

We recommend that one or the other approach be decided upon and efforts be initiated to provide a cost analysis of each system or to improve the component performance analysis algorithms.

Of course, some improvements to the component performance analysis algorithms would be desirable even if the present approach is adhered to. The conclusion that deaeration does not greatly affect performance rests on the assumption that all air dissolved in the sea water when it enters the evaporator or condenser is liberated there. If this does not happen, which especially might be true in the condenser, then the effect of deaeration on performance might be quite different. A parametric study of this possibility should be performed, and if it is important, a method of calculating the amount of air liberated in the evaporator or condenser should be developed.

Another parametric study that should be undertaken is the effect of different equilibrium approach fractions in the evaporator and condenser. If cost is held constant, different evaporators and condensers, each with the same cost, are not likely to have the same value for the equilibrium approach fraction.

Finally, better data are needed for channel-flow flash evaporators and jet or spray condensers operating in OTEC conditions, but this information cannot be obtained from an analytical study and requires an experimental program.

SECTION 5.0

REFERENCES

- Abelson, H. 1978 (Aug.). OTEC Power System Performance Model. MITRE Report Number MTR-7924. McLean, VA.
- Westinghouse Electric Corporation. 1979 (Mar.). 100 MW_e OTEC Alternate Power Systems. DOE Contract EG-77-C-05-1473. Lester, PA.
- Bakay, A.; Jaszay, T. 1978 (Aug.). "High Performance Jet Condensers for Steam Turbines." Paper EC10. VI International Heat Transfer Conference. Toronto, Canada.
- Watt, A. D.; Mathews, F. S.; Hathaway, R. E. 1977 (Dec.). Open Cycle Energy Conversion. A Preliminary Engineering Evaluation. DOE Report Number ALO/3723-7613. Golden, CO: Colorado School of Mines.

SERIO 

APPENDIX

The Appendix includes two tables and a printout of the computer program. Table A-1 lists the values of the input parameters for the 17 runs of the program. An underlined value indicates that the effect of varying the parameter from its run 0 value was studied. Table A-2 lists the values of the output parameters for the 17 runs of the program. For each run, the program calculates the output parameter as R ranges from 0.2 to 2.0.

Table A-1. PARAMETER MATRIX FOR OC-OTEC SYSTEMS MODEL

Parameter description	Run Number																	
	1	2	3	4	5	6	7	8	9	10	11	12	13	14	15	16	17	
Equilibrium approach fraction in evaporator	0.9	0.9	0.9	0.9	0.9	0.9	0.9	0.9	0.9	0.9	0.9	0.9	0.9	<u>0.85</u>	<u>0.95</u>	0.9	0.9	
Equilibrium approach fraction in condenser	0.9	0.9	0.9	0.9	0.9	0.9	0.9	0.9	0.9	0.9	0.9	0.9	0.9	<u>0.85</u>	<u>0.95</u>	0.9	0.9	
Turbine-generator efficiency	0.8	0.8	0.8	0.8	0.3	0.8	0.8	0.8	0.8	0.8	0.8	<u>0.75</u>	<u>0.85</u>	0.8	0.8	0.8	0.8	
Deaeration	No	<u>Yes</u>	Yes	Yes	Yes	Yes	Yes	Yes	Yes	Yes	Yes	No	No	No	No	No	<u>Yes</u>	
Ratio of steam pressure to total pressure in last stage of deaerator	--	0.9	0.9	0.9	0.9	0.9	0.9	<u>0.8</u>	<u>0.98</u>	0.9	0.9	--	--	--	--	--	0.9	
Fraction of equilibrium air liberated/ deaerator stage	--	0.9	0.9	0.9	0.9	<u>0.8</u>	<u>1.0</u>	0.9	0.9	0.9	0.9	--	--	--	--	--	0.9	
Number of warm deaeration stages	--	4	4	4	4	4	4	4	4	<u>2</u>	<u>6</u>	--	--	--	--	--	4	
Number of cold deaeration stages	--	5	5	5	5	5	5	5	5	<u>3</u>	<u>7</u>	--	--	--	--	--	5	
Deaerator stage head loss (m)	--	0.5	<u>1.0</u>	<u>1.5</u>	<u>2.0</u>	0.5	0.5	0.5	0.5	0.5	0.5	--	--	--	--	--	0.5	
Condenser type	Jet	Jet	Jet	Jet	Jet	Jet	Jet	Jet	Jet	Jet	Jet	Jet	Jet	Jet	Jet	Jet	<u>Spray</u>	<u>Spray</u>
Volumetric heat transfer coefficient in condenser	--	--	--	--	--	--	--	--	--	--	--	--	--	--	--	--	0.1	<u>0.4</u>

64



Table A-2. RESULTS OF OC-OTEC SYSTEMS MODEL

Run #	R	Net Power (MW)	Warm Loop Power (MW)	Cold Loop Power (MW)	Condenser		
					Air Removal Power (MW)	Warm Deaeration Power (MW)	Cold Deaeration Power (MW)
1	0.2	61.85	8.25	8.20	21.70	--	--
	0.4	68.96	3.68	8.44	18.92	--	--
	0.6	69.63	2.44	9.62	18.32	--	--
	0.8	68.62	1.88	11.18	18.32	--	--
	1.0	66.83	1.57	13.05	18.55	--	--
	1.2	64.51	1.37	15.23	18.89	--	--
	1.4	61.75	1.23	17.73	19.29	--	--
	1.6	58.54	1.14	20.06	19.72	--	--
	1.8	54.89	1.06	23.87	20.17	--	--
	2.0	50.79	1.00	27.58	20.63	--	--
2	0.2	57.21	21.02	9.44	8.08	2.98	1.26
	0.4	66.43	11.10	11.08	8.20	1.73	1.46
	0.6	67.89	8.07	12.75	8.31	1.32	1.66
	0.8	67.52	6.62	14.48	8.40	1.11	1.87
	1.0	66.42	5.77	16.27	8.48	0.98	2.07
	1.2	64.94	5.22	18.13	8.55	0.90	2.27
	1.4	63.20	4.83	20.06	8.60	0.84	2.47
	1.6	61.28	4.54	22.06	8.65	0.79	2.68
	1.8	59.20	4.31	24.16	8.69	0.76	2.88
	2.0	56.98	4.14	26.35	8.73	0.73	3.08
3	0.2	41.32	33.79	12.57	8.08	2.98	1.26
	0.4	55.38	18.52	14.70	8.20	1.73	1.46
	0.6	58.12	13.71	16.88	8.31	1.32	1.66
	0.8	58.14	11.36	19.12	8.40	1.11	1.87
	1.0	57.08	9.98	21.41	8.48	0.98	2.07
	1.2	55.45	9.07	23.77	8.55	0.90	2.27
	1.4	53.46	8.42	26.20	8.60	0.84	2.47
	1.6	51.23	7.94	28.71	8.65	0.79	2.68
	1.8	48.79	7.57	21.31	8.69	0.76	2.88
	2.0	46.19	7.27	34.00	8.73	0.73	3.08
4	0.2	25.42	45.56	15.69	8.08	2.98	1.26
	0.4	44.34	25.94	18.33	8.20	1.73	1.46
	0.6	48.35	19.34	21.02	8.31	1.32	1.66
	0.8	48.76	16.11	23.75	8.40	1.11	1.87
	1.0	47.73	14.19	26.55	8.48	0.98	2.07
	1.2	45.96	12.92	29.41	8.55	0.90	2.27
	1.4	43.73	12.01	32.35	8.60	0.84	2.47
	1.6	41.18	11.34	35.36	8.65	0.79	2.68
	1.8	38.39	10.82	38.46	8.69	0.76	2.88
	2.0	35.40	10.40	41.65	8.73	0.73	3.08

Table A-2. RESULTS OF OC-OTEC SYSTEMS MODEL (continued)

5	0.2	9.53	59.33	18.81	8.08	2.98	1.26
	0.4	33.29	33.36	21.96	8.20	1.73	1.46
	0.6	38.59	24.98	25.15	8.31	1.32	1.66
	0.8	39.39	20.85	28.39	8.40	1.11	1.87
	1.0	38.39	18.39	31.69	8.48	0.98	2.07
	1.2	36.47	16.77	35.05	8.55	0.90	2.27
	1.4	33.99	15.61	38.49	8.60	0.84	2.47
	1.6	31.13	14.74	42.01	8.65	0.79	2.68
	1.8	27.99	14.07	45.61	8.69	0.76	2.88
2.0	24.62	13.54	49.31	8.73	0.73	3.08	
6	0.2	56.94	21.02	9.44	8.23	3.02	1.35
	0.4	66.21	11.12	11.08	8.30	1.76	1.56
	0.6	67.67	8.07	12.75	8.39	1.33	1.78
	0.8	67.29	6.62	14.48	8.48	1.12	2.00
	1.0	66.19	5.77	16.27	8.56	1.00	2.21
	1.2	64.69	5.22	18.13	8.62	0.91	2.43
	1.4	62.94	4.83	20.06	8.68	0.85	2.65
	1.6	61.00	4.54	22.06	8.72	0.81	2.86
	1.8	58.91	4.31	24.16	8.77	0.77	3.08
2.0	56.67	4.14	26.35	8.81	0.74	3.30	
7	0.2	57.42	21.02	9.44	7.99	2.93	1.19
	0.4	66.60	11.10	11.08	8.14	1.70	1.38
	0.6	68.05	8.07	12.75	8.26	1.29	1.58
	0.8	67.68	6.62	14.48	8.36	1.09	1.77
	1.0	66.59	5.77	16.27	8.44	0.96	1.96
	1.2	65.12	5.22	18.13	8.50	0.88	2.15
	1.4	63.39	4.83	20.06	8.56	0.82	2.34
	1.6	61.48	4.54	22.06	8.61	0.80	2.54
	1.8	59.41	4.31	24.16	8.65	0.75	2.73
2.0	57.20	4.14	26.35	8.68	0.72	2.92	
8	0.2	57.43	21.02	9.44	8.16	2.84	1.11
	0.4	66.64	11.10	11.08	8.25	1.65	1.29
	0.6	68.11	8.07	12.75	8.35	1.25	1.47
	0.8	67.75	6.62	14.48	8.44	1.06	1.64
	1.0	66.68	5.77	16.27	8.52	0.94	1.82
	1.2	65.21	5.22	18.13	8.58	0.86	2.00
	1.4	63.50	4.83	20.06	8.64	0.80	2.18
	1.6	61.60	4.54	22.06	8.68	0.76	2.36
	1.8	59.54	4.31	24.16	8.73	0.72	2.54
2.0	57.34	4.14	26.35	8.76	0.70	2.71	
9	0.2	56.25	21.02	9.44	8.03	3.09	2.17
	0.4	65.35	11.02	11.08	8.17	1.79	2.52
	0.6	66.67	8.07	12.75	8.29	1.36	2.86
	0.8	66.16	6.62	14.48	8.38	1.15	3.21
	1.0	64.92	5.77	16.27	8.46	1.02	3.56
	1.2	63.29	5.22	18.13	8.52	0.93	3.91
	1.4	61.41	4.83	20.06	8.58	0.87	4.26
	1.6	59.34	4.54	22.06	8.63	0.82	4.61
	1.8	57.11	4.31	24.16	8.67	0.79	4.96
2.0	54.75	4.14	26.35	8.71	0.76	5.31	

Table A-2. RESULTS OF OC-OTEC SYSTEMS MODEL (continued)

10	0.2	60.48	14.64	8.19	8.23	5.77	2.68
	0.4	68.22	7.39	9.62	8.30	3.35	3.11
	0.6	69.16	5.25	11.10	8.39	2.55	3.55
	0.8	68.52	4.25	12.63	8.48	2.14	3.98
	1.0	67.25	3.67	14.22	8.55	1.90	4.41
	1.2	65.63	3.29	15.87	8.62	1.74	4.84
	1.4	63.80	3.03	17.60	8.67	1.62	5.27
	1.6	61.79	2.84	19.41	8.72	1.54	5.71
	1.8	59.64	2.69	21.30	8.76	1.47	6.14
2.0	57.36	2.57	23.29	8.80	1.42	6.57	
11	0.2	50.56	27.41	10.69	8.04	2.35	0.94
	0.4	62.03	14.81	12.53	8.17	1.37	1.10
	0.6	64.13	10.89	14.41	8.29	1.04	1.25
	0.8	64.01	8.99	16.34	8.38	0.87	1.40
	1.0	63.00	7.88	18.33	8.46	0.77	1.55
	1.2	61.53	7.14	20.38	8.53	0.71	1.71
	1.4	59.76	6.62	22.51	8.58	0.66	1.86
	1.6	57.77	6.24	24.72	8.63	0.63	2.01
	1.8	55.61	5.94	27.02	8.67	0.60	2.16
2.0	53.29	5.70	29.41	8.71	0.58	2.32	
12	0.2	58.78	9.04	9.03	23.15	--	--
	0.4	66.53	4.03	9.26	20.19	--	--
	0.6	67.23	2.66	10.56	19.55	--	--
	0.8	66.09	2.05	12.31	19.55	--	--
	1.0	64.08	1.71	14.41	19.79	--	--
	1.2	61.47	1.50	16.87	20.16	--	--
	1.4	58.35	1.35	19.71	20.59	--	--
	1.6	54.74	1.24	22.97	21.05	--	--
	1.8	50.61	1.16	26.70	21.53	--	--
2.0	45.97	1.09	30.92	22.02	--	--	
13	0.2	64.50	7.58	7.50	20.42	--	--
	0.4	71.01	3.38	7.75	17.80	--	--
	0.6	71.70	2.24	8.82	17.24	--	--
	0.8	70.80	1.73	10.23	17.23	--	--
	1.0	69.20	1.44	11.91	17.45	--	--
	1.2	67.12	1.26	13.85	17.77	--	--
	1.4	64.64	1.14	16.08	18.15	--	--
	1.6	61.77	1.04	18.63	18.55	--	--
	1.8	58.53	0.98	21.52	18.98	--	--
2.0	54.89	0.92	24.79	19.40	--	--	
14	0.2	60.40	8.08	9.01	22.51	--	--
	0.4	67.56	3.60	9.26	19.58	--	--
	0.6	68.13	2.38	10.55	18.93	--	--
	0.8	66.95	1.84	12.31	18.91	--	--
	1.0	64.92	1.53	14.41	19.14	--	--
	1.2	62.31	1.34	16.87	19.48	--	--
	1.4	59.18	1.21	19.73	19.89	--	--
	1.6	55.56	1.11	22.99	20.33	--	--
	1.8	51.45	1.04	26.73	20.79	--	--
2.0	46.79	0.98	30.97	21.26	--	--	

Table A-2. RESULTS OF OC-OTEC SYSTEMS MODEL (continued)

15	0.2	62.46	9.07	7.51	20.95	--	--
	0.4	69.89	4.05	7.74	18.31	--	--
	0.6	70.72	2.69	8.83	17.76	--	--
	0.8	69.91	2.07	10.24	17.77	--	--
	1.0	68.35	1.73	11.92	18.01	--	--
	1.2	66.28	1.51	13.86	18.35	--	--
	1.4	63.82	1.36	16.08	18.74	--	--
	1.6	60.98	1.25	18.61	19.17	--	--
	1.8	57.74	1.17	21.49	19.60	--	--
	2.0	54.10	1.10	24.74	20.05	--	--
16	0.2	51.13	8.25	18.91	21.70	--	--
	0.4	52.36	3.68	25.04	18.92	--	--
	0.6	47.20	2.44	32.04	18.32	--	--
	0.8	39.87	1.88	39.93	18.32	--	--
	1.0	31.17	1.57	48.71	18.55	--	--
	1.2	21.34	1.37	58.40	18.89	--	--
	1.4	10.47	1.23	69.00	19.29	--	--
	1.6	-1.38	1.14	80.52	19.72	--	--
	1.8	-14.21	1.06	92.98	20.17	--	--
	2.0	-28.00	1.00	106.37	20.63	--	--
17	0.2	55.43	21.02	11.50	8.08	2.80	1.17
	0.4	63.48	11.10	14.24	8.20	1.62	1.36
	0.6	63.59	8.07	17.24	8.31	1.23	1.55
	0.8	61.67	6.62	20.52	8.40	1.04	1.74
	1.0	58.80	5.77	24.09	8.48	0.92	1.93
	1.2	55.32	5.22	27.96	8.55	0.84	2.12
	1.4	51.35	4.83	32.13	8.60	0.79	2.30
	1.6	46.97	4.54	36.61	8.65	0.74	2.49
	1.8	42.18	4.31	41.42	8.69	0.71	2.68
	2.0	37.02	4.14	46.56	8.73	0.69	2.87

Table A-2. RESULTS OF OC-OTEC SYSTEMS MODEL (continued)

Run #	Total Deaeration Power (MW)	Warm Water Mass Flow Rate (kg/s X 10 ⁵)	Cold Water Mass Flow Rate (kg/s X 10 ⁵)	Steam Mass Flow Rate (kg/s X 10 ³)	Evaporator Length (m)	Condenser Height (m)	Plant Outer Diameter (m)
1	21.70	5.864	1.147	1.503	23.69	2.51	93.48
	18.92	3.407	1.333	1.496	17.06	1.68	81.62
	18.32	2.587	1.518	1.490	14.28	1.60	77.16
	18.32	2.177	1.703	1.486	12.73	1.72	74.96
	18.55	1.931	1.888	1.482	11.71	1.93	73.62
	18.89	1.767	2.072	1.479	10.99	2.21	72.78
	19.29	1.650	2.257	1.476	10.45	2.55	72.20
	19.72	1.562	2.442	1.474	10.04	2.95	71.78
	20.17	1.494	2.627	1.472	9.71	3.40	71.52
	20.63	1.439	2.811	1.470	9.44	3.90	71.38
2	26.62	5.864	1.147	1.503	23.69	1.00	93.48
	21.34	3.407	1.333	1.496	12.06	1.00	81.62
	20.07	2.587	1.518	1.490	14.28	1.00	77.16
	19.81	2.177	1.703	1.486	12.73	1.00	74.96
	19.94	1.931	1.888	1.482	11.71	1.00	73.62
	20.26	1.767	2.072	1.479	10.99	1.00	72.78
	20.67	1.650	2.257	1.476	10.45	1.00	72.20
	21.16	1.562	2.442	1.474	10.04	1.00	71.78
	21.69	1.494	2.627	1.472	9.71	1.00	71.52
	22.24	1.439	2.811	1.470	9.44	1.00	71.38
3	40.93	5.864	1.147	1.503	23.69	1.00	93.48
	31.28	3.407	1.333	1.496	17.06	1.00	81.62
	28.87	2.587	1.518	1.490	14.28	1.00	77.16
	28.25	2.177	1.703	1.486	12.73	1.00	74.96
	28.35	1.931	1.888	1.482	11.71	1.00	73.62
	28.80	1.767	2.072	1.479	10.99	1.00	72.78
	29.44	1.650	2.257	1.476	10.45	1.00	72.20
	30.21	1.562	2.442	1.474	10.04	1.00	71.78
	31.06	1.494	2.627	1.472	9.71	1.00	71.52
	31.96	1.439	2.811	1.470	9.44	1.00	71.38
4	55.24	5.864	1.147	1.503	23.69	1.00	93.48
	41.21	3.407	1.333	1.496	17.06	1.00	81.62
	37.66	2.587	1.518	1.490	14.28	1.00	77.16
	36.70	2.177	1.703	1.486	12.73	1.00	74.96
	36.77	1.931	1.888	1.482	11.71	1.00	73.62
	37.34	1.767	2.072	1.479	10.99	1.00	72.78
	38.20	1.650	2.257	1.476	10.45	1.00	72.20
	39.24	1.562	2.442	1.474	10.04	1.00	71.78
	40.42	1.494	2.627	1.472	9.71	1.00	71.52
	41.67	1.439	2.811	1.470	9.44	1.00	71.38

Table A-2. RESULTS OF OC-OTEC SYSTEMS MODEL (continued)

5	69.53	5.864	1.147	1.503	23.69	1.00	93.48
	51.17	3.407	1.333	1.496	17.06	1.00	81.62
	47.16	2.587	1.518	1.490	14.28	1.00	77.16
	45.12	2.177	1.703	1.486	12.73	1.00	74.96
	45.17	1.931	1.888	1.482	11.71	1.00	73.62
	45.88	1.767	2.072	1.479	10.99	1.00	72.78
	46.97	1.650	2.257	1.476	10.45	1.00	72.20
	48.30	1.562	2.442	1.474	10.04	1.00	71.78
	49.78	1.494	2.627	1.472	9.71	1.00	71.52
	51.37	1.439	2.811	1.470	9.44	1.00	71.38
6	26.91	5.864	1.147	1.503	23.69	1.00	93.48
	21.56	3.407	1.333	1.496	17.06	1.00	81.62
	20.29	2.587	1.518	1.490	14.28	1.00	77.16
	20.05	2.177	1.703	1.486	12.73	1.00	74.96
	20.17	1.931	1.888	1.482	11.71	1.00	73.62
	20.51	1.767	2.072	1.479	10.99	1.00	72.78
	20.94	1.650	2.257	1.476	10.45	1.00	72.20
	21.45	1.562	2.442	1.474	10.04	1.00	71.78
	21.98	1.494	2.627	1.472	9.71	1.00	71.52
	22.56	1.439	2.811	1.470	9.44	1.00	71.38
7	26.41	5.864	1.147	1.503	23.69	1.00	93.48
	21.17	3.407	1.333	1.496	17.06	1.00	81.62
	19.92	2.587	1.518	1.490	14.28	1.00	77.16
	19.65	2.177	1.703	1.486	12.73	1.00	74.96
	19.78	1.931	1.888	1.482	11.71	1.00	73.62
	20.07	1.767	2.072	1.479	10.99	1.00	72.78
	20.49	1.650	2.257	1.476	10.45	1.00	72.20
	20.99	1.562	2.442	1.474	10.04	1.00	71.78
	21.49	1.494	2.627	1.472	9.71	1.00	71.52
	22.03	1.439	2.811	1.470	9.44	1.00	71.38
8	25.41	5.864	1.147	1.503	23.69	1.00	93.48
	21.13	3.407	1.333	1.496	17.06	1.00	81.62
	19.85	2.587	1.518	1.490	14.28	1.00	77.16
	19.58	2.177	1.703	1.486	12.73	1.00	74.96
	19.69	1.931	1.888	1.482	11.71	1.00	73.62
	19.98	1.767	2.072	1.479	10.99	1.00	72.78
	20.38	1.650	2.257	1.476	10.45	1.00	72.20
	20.84	1.562	2.442	1.474	10.04	1.00	71.78
	21.35	1.494	2.627	1.472	9.71	1.00	71.52
	21.89	1.439	2.811	1.470	9.44	1.00	71.38
9	27.58	5.864	1.147	1.503	23.69	1.00	93.48
	22.42	3.407	1.333	1.496	17.06	1.00	81.62
	21.31	2.587	1.518	1.490	14.78	1.00	77.16
	21.18	2.177	1.703	1.486	12.73	1.00	74.96
	21.44	1.931	1.888	1.482	11.71	1.00	73.62
	21.89	1.767	2.072	1.479	10.99	1.00	72.78
	22.46	1.650	2.257	1.476	10.45	1.00	72.20
	23.10	1.562	2.442	1.474	10.04	1.00	71.78
	23.68	1.494	2.627	1.472	9.71	1.00	71.52
	24.49	1.439	2.811	1.470	9.44	1.00	71.38

Table A-2. RESULTS OF OC-OTEC SYSTEMS MODEL (continued)

10	24.12	5.864	1.147	1.503	23.69	1.00	93.48
	20.07	3.407	1.333	1.496	17.06	1.00	81.62
	19.35	2.587	1.518	1.490	14.28	1.00	77.16
	19.23	2.177	1.703	1.486	12.73	1.00	74.96
	19.52	1.931	1.888	1.482	11.71	1.00	73.62
	19.99	1.767	2.072	1.479	10.99	1.00	72.78
	20.50	1.650	2.257	1.476	10.45	1.00	72.20
	21.09	1.562	2.442	1.474	10.04	1.00	71.78
	21.71	1.494	2.627	1.472	9.71	1.00	71.52
	22.33	1.439	2.811	1.470	9.44	1.00	71.38
11	32.51	5.864	1.147	1.503	23.69	1.00	93.48
	25.22	3.407	1.333	1.496	17.06	1.00	81.62
	23.39	2.587	1.518	1.490	14.28	1.00	77.16
	22.90	2.177	1.703	1.486	12.73	1.00	74.96
	22.94	1.931	1.888	1.482	11.71	1.00	73.62
	23.24	1.767	2.072	1.479	10.99	1.00	72.78
	23.69	1.650	2.257	1.476	10.45	1.00	72.20
	24.24	1.562	2.442	1.474	10.04	1.00	71.78
	24.82	1.494	2.627	1.472	9.71	1.00	71.52
	25.47	1.439	2.811	1.470	9.44	1.00	71.38
12	23.15	6.255	1.266	1.604	24.46	2.68	95.92
	20.19	3.634	1.424	1.596	17.62	1.80	83.64
	19.55	2.760	1.622	1.590	14.74	1.71	79.08
	19.55	2.323	1.819	1.585	13.13	1.84	76.76
	19.79	2.060	2.017	1.581	12.10	2.07	75.40
	20.16	1.885	2.214	1.577	11.36	2.37	74.52
	20.59	1.760	2.412	1.574	10.81	2.73	74.02
	21.05	1.666	2.609	1.572	10.38	3.15	73.56
	21.53	1.593	2.807	1.570	10.04	3.63	73.28
	22.02	1.535	3.004	1.568	9.76	4.17	73.02
13	20.42	5.519	1.078	1.415	23.00	2.36	91.20
	17.80	3.206	1.252	1.408	16.55	1.58	79.70
	17.24	2.435	1.426	1.403	13.84	1.51	75.38
	17.23	2.049	1.600	1.398	12.33	1.62	73.26
	17.45	1.818	1.774	1.395	11.34	1.82	71.98
	17.77	1.663	1.947	1.392	10.65	2.08	71.20
	18.15	1.553	2.121	1.389	10.13	2.40	70.66
	18.55	1.470	2.294	1.387	9.73	2.77	70.26
	18.98	1.406	2.468	1.385	9.40	3.19	70.00
	19.40	1.354	2.640	1.384	9.14	3.66	69.78
14	22.51	6.208	1.216	1.503	20.12	2.72	86.12
	19.58	3.606	1.412	1.496	14.31	1.86	61.81
	18.93	2.739	1.608	1.490	11.91	1.77	72.42
	18.91	2.305	1.804	1.486	10.56	1.90	70.62
	19.14	2.044	1.999	1.482	9.67	2.13	69.54
	19.48	1.870	2.195	1.479	9.05	2.44	68.90
	19.89	1.746	2.391	1.476	8.60	2.82	68.50
	20.33	1.653	2.586	1.474	8.25	3.25	68.20
	20.79	1.581	2.782	1.472	7.96	3.74	68.02
	21.26	1.523	1.978	1.470	7.73	4.29	67.96

Table A-2. RESULTS OF OC-OTEC SYSTEMS MODEL (continued)

15	20.95	5.556	1.086	1.503	30.62	2.31	107.34
	18.31	3.228	1.262	1.496	22.38	1.53	92.26
	17.76	2.452	1.437	1.490	18.93	1.46	86.46
	17.77	2.064	1.612	1.486	16.96	1.57	83.42
	18.01	1.830	1.788	1.482	15.67	1.76	81.54
	18.35	1.675	1.963	1.479	14.76	2.02	80.32
	18.74	1.564	2.138	1.476	14.09	2.33	79.48
	19.17	1.481	2.313	1.474	13.56	2.69	78.82
	19.60	1.416	2.488	1.472	13.15	3.10	78.40
	20.05	1.364	2.663	1.470	12.80	3.56	78.10
16	21.70	5.864	1.147	1.503	23.69	11.25	93.48
	18.92	3.407	1.333	1.496	17.06	13.26	81.62
	18.32	2.587	1.518	1.490	14.28	15.28	77.16
	18.32	2.177	1.703	1.486	12.73	17.29	74.96
	18.55	1.931	1.888	1.482	11.71	19.31	73.62
	18.89	1.767	2.072	1.479	10.99	21.32	72.78
	19.29	1.650	2.257	1.476	10.45	23.34	72.20
	19.72	1.562	2.442	1.474	10.04	25.35	71.78
	20.17	1.494	2.627	1.472	9.71	27.37	71.52
	20.63	1.439	2.811	1.470	9.44	29.38	71.38
17	26.35	5.864	1.147	1.503	23.69	2.81	93.48
	21.12	3.407	1.333	1.496	17.06	3.32	81.62
	19.88	2.587	1.518	1.490	14.28	3.82	77.16
	19.62	2.177	1.703	1.486	12.73	4.32	74.96
	19.74	1.931	1.888	1.482	11.71	4.83	73.62
	20.05	1.767	2.072	1.479	10.99	5.33	72.78
	20.45	1.650	2.257	1.476	10.45	5.83	72.20
	20.92	1.562	2.442	1.474	10.04	6.34	71.78
	21.44	1.494	2.627	1.472	9.71	6.84	71.52
	22.00	1.439	2.811	1.470	9.44	7.35	71.38

```

1      PROGRAM OTEC(INPUT,OUTPUT,TAPE1,TAPE7,TAPE9)
      REAL L,MFCW,MFGCOND,MFGEVAP,MFS,MFW,MFSO
      C
      C      COMMON STATEMENTS
      C
      COMMON/CONST/PI,P0,G
      COMMON/FLOW/MFW,MFCW,MFS,MFSO
      COMMON/DEAER/FG,FL,HLD
      COMMON/TEMP/TWWI,TCWI,TCWD,T1,TO,TWO
      COMMON/EVAP/RHOWW
      COMMON/COND/CKM,RHOCW,D,L,EPS
      COMMON/TURB/ETATG,DTTG,DHS
      COMMON/AIR/MFGEVAP,MFGCOND
      COMMON/AIR1/SIGMA1,SIGMA0,TEST
      COMMON/SIZE/DO
      C
      C      DATA STATEMENTS
      C
      DATA TWWI,TCWI,RHOCW,RHOWW,D,L,EPS,ETAPUMP,PGR/
      *25.0,5.0,1027.5,1023.0,10.0,1000.0,0.01,0.9,100.0/
      DATA G,P0,PI,IMAX/9.8,101.325,3.1416,10/
      C
      C      READ INPUT DATA FROM TAPE 1
      C
      NAMELIST/INPUT1/EFFE,EFFC,FG,FL,ETATG,CKM,KDWM,KDCW,KCND,
      *HLD,NW,NC
      READ (1,INPUT1)
      WRITE(7,701) PGR
      WRITE(9,704)
      C
      C      LOOP THRU VALUES OF R
      C
      DO 100 I1=1,IMAX
      R = 0.20*I1
      C
      C      SET DTTG = 10.0
      C
      DTTG = 10.0
      C
      C      COMPUTE SYSTEM TEMPERATURES
      C
      DTEVAP = (TWWI - TCWI - DTTG)/(1. + 1./R)
      TO = TWWI - DTEVAP
      FDNE = (1.0 - EFPE1)*DTEVAP
      TWWO = TO + FDNE
      T1 = TO - DTTG
      DTCOND = DTEVAP/R
      DTA = (1.0 - EFFC)*DTCOND
      TCWO = T1 - DTA
      C
      C      COMPUTE ENTHALPY DROP ACROSS TURBINE AND STEAM FLOW RATE
      C
      X = (SG(TO) - SF(T1))/(SG(T1) - SF(T1))
      HEXS = HF(T1) + X*(HG(T1) - HF(T1))
      DHS = HG(TO) - HEXS
      MFS = PGR/(ETATG + DHS)*1.0E6
      C

```

Figure A-1. Program OTEC

```

C   COMPUTE WATER FLOW RATES WITH ASSUMPTION 0.99 STEAM CONDENSED
C
60  HEX = HG(TD) - (ETATG*DHS)
    MFCW = (0.99*MFS*(HEX-HF(TCWD)))/(HF(TCWO)-HF(TCWI))
    MFWW = MFS*(HG(TO)-HF(TWVO))/(HF(TWWI)-HF(TWVO))
    MFSO = 0.01*MFS
C
65  C   OUTPUT TO TAPE 7
    C
    WRITE(7.702) R.TWWI,TWVO,TO,TI,TCWO,TCWI
    WRITE(7.703) MFWW,MFS,MFCW
C
70  C   WARM WATER PRE-DEAERATION ROUTINE
    C   KD=-2 INDICATES NO PRE-DEAERATION
    C   KD=2 INDICATES PRE-DEAERATION
    C
    CALL DEAIR(NW,KDWW,PDAIRW,MFGEVAP,HDAE)
75  C
    C   TURBINE ROUTINE
    C
    CALL TURBIN
C
80  C   EVAPORATOR SIZING ROUTINE
    C
    CALL FLASH(1.0-EFFE,HZEVAP)
C
85  C   COLD WATER PRE-DEAERATION ROUTINE
    C   KD=-1 INDICATES NO PRE-DEAERATION
    C   KD=1 INDICATES PRE-DEAERATION
    C
    CALL DEAIR(NC,KDCW,PDAIRC,MFGCOND,HDAC)
90  C
    C   CONDENSER SIZING AND COLD WATER LOOP LOSS ROUTINE.
    C   CONDEN1=JET CONDENSER. CONDEN2=BAFFLE/SPRAY(CSM)
    C
    IF (KCOND.EQ.1) CALL CONDEN1(HZCOND,HDIST,HPIPE,PDCOND)
    IF (KCOND.EQ.2) CALL CONDEN2(HZCOND,HDIST,HPIPE,PDCOND)
95  C
    C   COMPUTE PARASITIC POWER REQUIREMENTS
    C
    PCWL = MFCW * G * (HZCOND + HDIST + HPIPE + HDAC)/ETAPUMP
    ?/1.0E6
    PWWL = MFWW*G*(HZEVAP+HDAE)/ETAPUMP/1.0E6
    PDAIR = (PDAIRW+PDAIRC+PDCOND)/1.0E6
    PNET = PGR - PCWL - PWWL - PDAIR
    WRITE(7.705) PCWL,PWWL,PDAIR,PNET
100  PDCOND=PDCOND/1.0E6
    PDAIRW=PDAIRW/1.0E6
    PDAIRC=PDAIRC/1.0E6
    WRITE(9.706) PWWL,PCWL,PDAIRW,PDAIRC,PDCOND,PNET
105  CONTINUE
C
110  C   FORMAT STATEMENTS
    C
    701. FORMAT(1H1,25(/),20X,45(1H*),2(/20X,1H*.43X,1H*),
    */.2X,1H*.* QTEC-OPEN CYCLE MODEL-VERSION 3*.
    *7X,1H*.2(/.20X,1H*.43X,1H*).8X./,20X,1H*.

```

```

115      *.6X.* GROSS POWER OUTPUT=*.F6.1.* MW*.8X.1H*./ .20X.1H*.
      *.6X.*OPEN-CHANNEL FLASH EVAPORATOR*.8X.1H*./ .20X.1H*.
      *.9X.*VERTICAL AXIS TURBINE*.13X.1H*./ .20X.1H*.8X.
      **.DIRECT CONTACT CONDENSER*.11X.1H*.2(/.20X.1H*.43X.1H*).
      */.20X.45(1H*)
120      702 FCRMAT(1H1.* TEMPERATURES. DEG C FOR R=*.F5.2./ /.
      *.14X.* WARM WATER INLET:*.F6.2./ .13X.* WARM WATER OUTLET:*.F6.2./ .
      *.17X.* TURBINE INLET:*.F6.2./ .16X.* TURBINE OUTLET:*.F6.2./ .
      *.13X.* COLD WATER OUTLET:*.F6.2./ .14X.* COLD WATER INLET:*.F6.2)
125      703 FORMAT(//.* MASS FLOWS. KG/S*./ /.20X.* WARM WATER:*.1PE10.3./ .
      *.25X.* STEAM:*.E10.3./ .20X.* COLD WATER:*.E10.3)
      704 FORMAT(1H1.* SUMMARY OF NET OUTPUT FOR THIS RUN*./ .1X.
      **.WARM LOOP COLD LOOP WARM DEAIR COLD DEAIR COND DEAIR NET*)
      705 FORMAT(///.* COLD WATER POWER*.5X.* WARM WATER POWER*.5X.
      **.DEAERATION POWER*.8X.* NET POWER*./ .8X.* MW*.19X.* MW*.19X.
      **.MW*.19X.* MW*./ .4X.F7.2.14X.F7.2.14X.F7.2.14X.F7.2)
130      706 FORMAT(1X.F6.2.F11.2.3(F12.2).F10.2)
      STOP
      END
    
```

SYMBOLIC REFERENCE MAP (R=1)

ENTRY POINTS
12267 OTEC

VARIABLES	SN	TYPE	RELOCATION				
0	CKM	REAL	COND	2	D	REAL	COND
2	DHS	REAL	TURB	0	DO	REAL	SIZE
13035	DTA	REAL		13034	DTCOND	REAL	
13032	DTEVAP	REAL		1	DTTG	REAL	TURB
13022	EFFC	REAL		13021	EFFE	REAL	
4	EPS	REAL	COND	12534	ETAPUMP	REAL	
0	ETATG	REAL	TURB	13033	FDNE	REAL	
0	FG	REAL	DEAER	1	FL	REAL	DEAER
2	G	REAL	CONST	13045	HDAC	REAL	
13042	HDAE	REAL		13047	HDIST	REAL	
13040	HEX	REAL		13037	HEXS	REAL	
2	HLD	REAL	DEAER	13050	HPIPE	REAL	
13046	HZCOND	REAL		13043	HZEVAP	REAL	
12536	IMAX	INTEGER		13030	I1	INTEGER	
13025	KCND	INTEGER		13024	KDCW	INTEGER	
13023	KDWW	INTEGER		3	L	REAL	COND
1	MFCW	REAL	FLOW	1	MFGCOND	REAL	AIR
0	MFGEVAP	REAL	AIR	2	MFS	REAL	FLOW
3	MFSO	REAL	FLOW	0	MFWW	REAL	FLOW
13027	NC	INTEGER		13026	NW	INTEGER	
13052	PCWL	REAL		13054	PDAIR	REAL	
13044	PDAIRC	REAL		13041	PDAIRW	REAL	
13051	PDCOND	REAL		12535	PGR	REAL	
0	PI	REAL	CONST	13055	PNET	REAL	
13053	PWWL	REAL		1	PO	REAL	CONST
13031	R	REAL		1	RHOCW	REAL	COND
0	RHODWW	REAL	EVAP	0	SIGMAI	REAL	AIR1

VARIABLES	SM	TYPE	RELLOCATION				
1	SIGMA0	REAL	AIR	1	TCWI	REAL	TEMP
2	TCW0	REAL	TEMP	2	TEST	REAL	AIR1
0	TWVI	REAL	TEMP	5	TWVO	REAL	TEMP
4	TO	REAL	TEMP	3	T1	REAL	TEMP
13036	X	REAL					

FILE NAMES	MODE						
0	INPUT		2043	OUTPUT	4106	TAPE1	NAME
10214	TAPE9	FMT					6151 TAPE7 FMT

EXTERNALS	TYPE	ARGS			
CONDEN1		4	CONDEN2		4
DEAIR		5	FLASH		2
HF	REAL	1	HG	REAL	1
SF	REAL	1	SG	REAL	1
TURBIN		0			

NAMELISTS
INPUT1

STATEMENT LABELS							
0	100		12644	701	FMT	12705	702 FMT
12734	703	FMT	12747	704	FMT	12764	705 FMT
13005	706	FMT					

LOOPS	LABEL	INDEX	FROM-TO	LENGTH	PROPERTIES
12277	100	* I1	33 10E	170B	EXT REFS

COMMON	BLOCKS	LENGTH
	CONST	3
	FLOW	4
	DEAER	3
	TEMP	6
	EVAP	1
	COND	5
	TURB	3
	AIR	2
	AIR1	3
	SIZE	1

STATISTICS			
PROGRAM	LENGTH	577B	383
BUFFER	LENGTH	12257B	5295
COMMON	LABELLED COMMON LENGTH	37B	31

```
1      SUBROUTINE DEAIR(N,K,PT,MDOTL,H)
      REAL MFW,MAS,MDOTL,MDOTA,MDOTAT,MDOTV,MDOTT,MFWW,MFCW,MFS
      DIMENSION DP(10),PS(10),PAS(10),PCIN(10),PCOUT(10),PAIN(10),
5      *MAS(11),MDOTA(10),MDOTAT(10),MDOTV(10),MDOTT(10),ETAC(10),
      *PWRC(10)
      C
      C      COMMON STATEMENTS
      C
      COMMON/CONST/PI,P0,G
10     COMMON/TEMP/TWWI,TCWI,TCWO,T1,TO,TWWD
      COMMON/FLOW/MFWW,MFCW,MFS,MFSO
      COMMON/DEAER/FG,F,HLD
      C
      C      MODE=1 IS PREDEAERATION OF COLD WATER LOOP
      C      MODE=2 IS PREDEAERATION OF WARM WATER LOOP
      C      A "--" INDICATES NO PRE-DEAERATION
      C
      MODE=IABS(K)
      IF (MODE.EQ.2) GO TO 1
20     CHAR=4HCOLD
      T=TCWI
      MFW=MFCW
      GO TO 2
      1 CHAR=4HWARM
25     T=TWWI
      MFW=MFWW
      C
      C      CONSTANTS
      C
      C
30     2 IF (K.LT.0) GO TO 90
      HD=HLD
      ETAM=0.9
      DELTA=0.276
      PA=P0+1.01
35     TC=7.0
      PVS=PSAT(T)
      PS(1)=PVS/FG
      PVC=PSAT(TC)
      NP1=N+1
      NM1=N-1
40     DO 5, I=1,N
      5 DP(I)=DELTA
      NSUM=N
      IF (MODE.EQ.1) DP(1)=0.0
45     IF (MODE.EQ.1) NSUM=NM1
      C
      C      COMPUTE COMPRESSION RATIO
      C
      C
50     RS=2.0
      10 RSTEST=RS
      SUM=0.0
      DO 20 I=1,NSUM
      20 SUM=SUM+RS*I
      RS=((PA+DELTA*SUM)/PS(1))**(1.0/N)
55     IF (ABS(RSTEST-RS)/RS.GT.0.01) GO TO 10
      C
      C      COMPUTE PRESSURES AND PARTIAL PRESSURES OF AIR AND VAPOR
```



```

C
60 PAS(1)=PS(1)-PVS
   PCIN(1)=PS(1)-DP(1)
   PAIN(1)=PCIN(1)-PVC
   IF (MCDE.EQ.1) PAIN(1)=PAS(1)
   PCOUT(1)=PCIN(1)*RS
   DO 30 I=2,N
65 PS(I)=PCOUT(I-1)
   PAS(I)=PS(I)-PVS
   PCIN(I)=PS(I)-DP(I)
   PAIN(I)=PCIN(I)-PVC
70 30 PCOUT(I)=PCIN(I)*RS
   PAS(NP1)=P0
C
C COMPUTE MASS FLOWS AND SOLUBILITY
C
75 HE=(4.350+0.114*T)*1.0E4
   DO 40 I=1,NP1
   J=NP1-I+1
40 MAS(J)=1.602*PAS(J)/PO/HE
   DO 50 I=2,N
   J=NP1-I
80 50 MAS(J)=(1.0-FL)*MAS(J+1)+FL*MAS(J)
   DO 55 I=1,N
   J=NP1-I
   MDOAT(J)=(MAS(J+1)-MAS(J))*MFW
55 CONTINUE
85 MDOAT(1)=MDOAT(1)
   MDOTV(1)=PVC/PAIN(1)/1.602*MDCTAT(1)
   MDOTT(1)=MDOTV(1)+MDOAT(1)
   DO 60 I=2,N
   MDOAT(I)=MDOTAT(I-1)+MDOAT(I)
90 MDOTV(I)=PVC/PAIN(I)/1.602*MDCTAT(I)
60 MDOTT(I)=MDOTAT(I)+MDOTV(I)
C
C COMPUTE STAGE POWER REQUIRED
C
95 PT=0.0
   CRS=RS**0.3*ALOG(RS)
   DO 70 I=1,N
   ETAC(I)=1.7*(PCIN(I)/PO)**0.4
100 IF (ETAC(I).GT.0.8) ETAC(I)=0.8
   PWRC(I)=293.0*(TC+273.0)*CRS*MDOTT(I)/ETAC(I)/ETAM/1.0E6
70 PT=PT+PWRC(I)
   H=N*HD
C
C ASSUMPTION: ALL REMAINING AIR IN LIQUID STREAM IS LIBERATED
C
105 MDOTL=MAS(1)*MFW
   DO 80 I=1,NP1
80 MAS(I)=MAS(I)*1.0E6
C
110 C OUTPUT TO TAPE 7
C
   WRITE(7.900) CHAR
   WRITE(7.901) T,MFW,TC,DELTA,D,N,RS,ETAM,FG,FL
   WRITE(7.902) (I,MAS(I),PCIN(I),MDOAT(I),MDOTV(I),MDOTT(I),

```

```

115      * ETAC(I).PWR(I).I=1.N)
          WRITE(7.903) PT.MDOTL.H
          PT=PT*1.0E6
          GO TO 999
C
120      C NO PRE-DEAERATION - ALL AIR IN LIQUID STREAM IS LIBERATED
          C
          90 HE=(4.35+0.114*T)*1.0E4
             PPM=1.602/HE
             MDOTL=PPM*MFW
125      PPM=PPM*1.0E6
             PT=0.0
             H=0.0
             WRITE(7.900) CHAR
             WRITE(7.904) PPM.MFW.MDOTL
130      904 FORMAT(10X.*NO PRE-DEAERATION OF THIS STREAM*./ .10X.
             **ALL AIR IS LIBERATED*./ .27X.*PPM:*.F7.3./ .
             *10X.*MASS FLOW RATE WATER:*.1PE10.2./ .
             *21X.*MF OF AIR:*.0PF7.3.* KG/S*)
             RETURN
135      C
          C FORMAT STATEMENTS
          C
          900 FORMAT(//.* PREDEAERATION: *.A4.* WATER LOOP*./ .
             ** PARAMETERS:*/ .)
140      901 FORMAT(14X.*INLET WATER TEMP:*.F5.1./ .10X.*MASS FLOW RATE WATER:*.
             *1PE10.2./ .
             *8X.*INTERCOOLER WATER TEMP:*.0PF5.1./ .8X.*INTERCOOLER PRESS DROP:*
             *F6.2./ .11X.*HEAD LOSS PER STAGE:*.F6.2./ .
             *17X.*NO. OF STAGES:*.I3./ .13X.*COMPRESSION RATIO:*.F6.2./ .21X.
145      **MOTOR EFF:*.F6.2./ .11X.*FRAC OF AIR ALLOWED:*.F6.2./ .
             *6X.*FRAC OF AIR LIB(PER STG):*.F6.2./ .3X.*STAGE*.4X.
             **MASS FRAC SUCTION PRESS*.2X.*MF AIR*.4X.*MF VAPOR*.
             *2X.*MF TOTAL*.4X.*COMP EFF*.5X.*STAGE PWR*./ .
             *15X.*PPM*.12X.*N/M2*.8X.*KG/S*.7X.*KG/S*.
150      *6X.*KG/S*.22X.*Mw*./ .)
          902 FORMAT(3X.I2.8X.F6.2.8X.F7.3.6X.F6.2.5X.F6.2.4X.F6.2.7X.
             *F5.2.7X.F6.2)
          903 FORMAT(1H0.72X.*TOTAL POWER=*.F7.2./ .1X.
             ** MF OF AIR RELEASED TO SYSTEM:*.F7.3.* KG/S*./ .
             *11X.*TOTAL HEAD REQUIRED:*.F6.2)
155      999 RETURN
          END
    
```

SYMBOLIC REFERENCE MAP (R=1)

ENTRY POINTS
4 DEAIR

VARIABLES	SN	TYPE	RELOCATION			
663 CHAR		REAL		705	CRS	REAL
667 DELTA		REAL		772	DP	REAL
1066 ETAC		REAL	ARRAY	666	ETAM	REAL
						ARRAY

VARIABLES	SN	TYPE	RELOCATION					
0	FG	REAL	DEAER	1	FL	REAL	DEAER	
2	G	REAL	CONST	0	H	REAL	F.P.	
665	HD	REAL		703	HE	REAL		
2	HLD	REAL	DEAER	676	I	INTEGER		
704	J	INTEGER		0	K	INTEGER	F.P.	
707	MAS	REAL	ARRAY	722	MDOTA	REAL	ARRAY	
734	MDDTAT	REAL	ARRAY	0	MDOTL	REAL	F.P.	
760	MDCOT	REAL	ARRAY	746	MDOTV	REAL	ARRAY	
1	MFCW	REAL	FLOW	2	MFS	REAL	FLOW	
3	MFSO	INTEGER	FLOW	661	MFW	REAL		
0	MFWW	REAL	FLOW	662	MODE	INTEGER		
0	N	INTEGER	F.P.	675	NM1	INTEGER		
674	NP1	INTEGER		677	NSUM	INTEGER		
670	PA	REAL		1054	PAIN	REAL	ARRAY	
1016	PAS	REAL	ARRAY	1030	PCIN	REAL	ARRAY	
1042	PCOUT	REAL	ARRAY	0	PI	REAL	CONST	
706	PPM	REAL		1004	PS	REAL	ARRAY	
0	PT	REAL	F.P.	673	PVC	REAL		
672	PVS	REAL		1100	PWRC	REAL	ARRAY	
1	PO	REAL	CONST	700	RS	REAL		
701	RSTEST	REAL		702	SUM	REAL		
664	T	REAL		671	TC	REAL		
1	TCWI	REAL	TEMP	2	TCWO	REAL	TEMP	
0	TWWI	REAL	TEMP	5	TWVO	REAL	TEMP	
4	TO	REAL	TEMP	3	T1	REAL	TEMP	

FILE NAMES	MODE
TAPE7	FMT

EXTERNALS	TYPE	ARGS			
ALOG	REAL	1 LIBRARY	PSAT	REAL	1

INLINE FUNCTIONS	TYPE	ARGS			
ABS	REAL	1 INTRIN	IABS	INTEGER	1 INTRIN

STATEMENT LABELS

30	1		34	2		0	5	
102	10		0	20		0	30	
0	40		0	50		0	55	
0	60		0	70		0	80	
370	90		516	900	FMT	526	901	FMT
611	902	FMT	620	903	FMT	475	904	FMT
407	999							

LOOPS	LABEL	INDEX	FROM-TO	LENGTH	PROPERTIES
63	5	I	41 42	3B	INSTACK
106	20	* I	52 53	6B	EXT REFS
145	30	I	64 69	10B	OPT
173	40	I	75 77	6B	INSTACK
213	50	I	78 80	5B	INSTACK
227	55	I	81 84	5B	INSTACK
247	60	J	88 91	7B	INSTACK
270	70	* I	97 101	23B	EXT REFS
325	80	I	107 108	3B	INSTACK
340		* I	114 114	20B	EXT REFS

COMMON BLOCKS	LENGTH
CONST	3
TEMP	6
FLOW	4
DEAIR	3

STATISTICS

PROGRAM LENGTH	11258	597
CM LABELED COMMON LENGTH	208	16

```

1      SUBROUTINE FLASH(TH,HZ)
      REAL MFWW,MFCW,MFS,LF,MFPER,LSTAR
      COMMON/CONST/PI,PO,G
      COMMON/FLOW/MFWW,MFCW,MFS
5      COMMON/EVAP/RHOWW
      COMMON/SIZE/DO
      COSTH = 0.9994
      SINTH = 0.0349
      SQSTH = 0.1868
10     ROUGH = 0.014
      WFLOW = 200.0
      LSTAR = 11.83
      DI=DO+4.0
15     DF = (ROUGH*MFWW/RHOWW/WFLOW/SQSTH)**0.6
      XK = SQRT(2.388E*DF**0.1667+.333)
      LF=EPSK(XK,TH)*CF/0.0137
      WFLOW = (DI+2.0*LF*COSTH)*PI
      IF(ABS(LF-LSTAR).LT.0.05) GO TO 20
      LSTAR = LF
20     GO TO 10

C
C     SLUICE GATE PRESSURE LOSS ASSUMED =0.15 M
C
25     HGATE=0.15
      HZ=LF*SINTH+DF*COSTH+HGATE
      MFPER=MFWW/WFLOW
      WRITE (7,701) D,LF,DF,MFPER,TH,HZ
701   FORMAT(//.* FLASH EVAPORATOR: OPEN CHANNEL TOROID*//.
** PARAMETERS:*.//.20X.* INNER DIAM:*.F6.1./ .24X.
** LENGTH:*.F7.2./ .25X.*SLOPE: 2 DEG*./ .17X.*DEPTH OF FLOW:*.
**F8.3./ .6X.*MASS FLOW PER UNIT WIDTH:*.1PE12.3./ .16X.
**THERMAL NON-EQ:*.0PF7.2./ .11X.*TOTAL HEAD REQUIRED:*.F7.2)
      RETURN
      END

```

SYMBOLIC REFERENCE MAP (R=1)

ENTRY POINTS
4 FLASH

VARIABLES	SN	TYPE	RELLOCATION			
156	COSTH	REAL		164	DF	REAL
163	DI	REAL		0	DO	REAL
2	G	REAL	CONST	166	HGATE	REAL
0	HZ	REAL	F.P.	153	LF	REAL
155	LSTAR	REAL		1	MFCW	REAL
154	MFPER	REAL		2	MFS	REAL
0	MFWW	REAL	FLOW	0	PI	REAL
1	PO	REAL	CONST	0	RHOWW	REAL
161	ROUGH	REAL		157	SINTH	REAL
160	SQSTH	REAL		0	TH	REAL
16	IFLOW	REAL		165	XK	REAL


```

1      SUBROUTINE CONDEN1(HZ.HD.HP.PWR)
C
C      THIS ROUTINE MODELS A JET CONDENSER AFTER BAKAY _ JASZAY
C
5      REAL MFWW,MFCW,MFS,MFSO,L,MFGCOND,MFGEVAP,MFA
COMMON/CONST/PI,P0,G
COMMON/TEMP/TWWI,TCWI,TCWO,T1,TO,TWWD
COMMON/FLOW/MFWA,MFCW,MFS,MFSO
COMMON/AIR/MFGEVAP,MFGCOND
10     COMMON/AIR1/SIGMAI,SIGMAO,TEST
COMMON/COND/CKM,RHOCW,D,L,EPS
C
C      COMPUTE INLET _ OUTLET STEAM/AIR RATIOS
C
15     ERROR=0.001
PS=PSAT(T1)
MFA=MFGEVAP+MFGCOND
SIGMAI=MFS/MFA
SIGMAO=MFSO/MFA
C
C      ITERATE EQTN 9. BK. FOR B WHICH GIVES ROOT USING
C      A MODIFIED BISECTION METHOD
C
25     CPT=CPT((TCWI+TCWO)/2.0)
TEST=MFCW+CPT*(1-TCWI)/(HVP(T1)*MFA)
R=1.0E-11
S=1.0E2
ITER=0
RI=XINT(R)
30     Z=10*((ALOG10(R*S)/2.0)
ZI=XINT(Z)
IF (ABS(ZI/TEST).LT.ERROR) GO TO 100
TEST1=RI*ZI
IF (TEST1.LT.0.0) GO TO 20
IF (TEST1.GT.0.0) GO TO 30
35     20 S=Z
GO TO 40
30 R=Z
RI=ZI
40     40 ITER=ITER+1
IF (ITER.GT.100) GO TO 999
GO TO 10
100 B=Z
C
C      COMPUTE HEAD LOSS IN CWP
C
C
50     VCW=(4.0*MFCW)/(RHOCW*PI*D*D)
HF=FRIC(EPS,D,VCW)*L+VCW*VCW/(2.0*G*D)
HR=0.001*L
HP=HR+HF
C
C      COMPUTE HEIGHT(MIN 1 M) NO. NOZZLES REQUIRED. WITH
C      MDOT/NOZZLE=4.5 KG/S.SPACING OF JETS=C.15 M.WIDTH=5 M
C      NOZZLES ARE SPRAYING SYSTEMS CO VEEJET 20502000
C
55     W=5.0
SP=0.15

```

```

MDO TN=4.5
NCH=PI*D/SP
60 AREA=B*MFCW*CPT.
HZ=AREA/(NCH*2.0*W)
IF (HZ.LT.1.0) HZ=1.0
NNOZ=MFCW/MDO TN
65 NZPCH=NNOZ/NCH
SPNOZ=HZ/NZ PCH

C
C COMPUTE HEAD LOSS IN DISTRIBUTION(2.6 M FOR NOZZLES.0.25 FOR PIPES)
C

HNOZ=2.6
70 HDIST=0.25
HD=HNOZ+HDIST
HT=HD+HP+HZ

C
C OUTPUT TO TAPE 7
C

WRITE(7.701) PS.#.SIGMA I.SIGMA O.HZ.NCH.NNOZ.SPNOZ.D.L.HP.HD.HT
701 FORMAT(//.* CONDENSER: JET TYPE(BAKAY AND JASZAY)*.//.
** PARAMETERS:*.//.20X.*COND PRESS:*.F12.4./.20X.
**JET LENGTH:*.F9.1./.9X.*INLET STEAM/AIR RATIO:*.
80 *F9.1./.8X.*OUTLET STEAM/AIR RATIO:*.F9.1./.
*19X.*COND HEIGHT:*.F10.2./.19X.
**NO CHANNELS:*.I7./.20X.*NO NOZZLES:*.I7./.16X.
**NOZZLE SPACING:*.F12.4./.22X.*CWP DIAM:*.F9.1./.20X.
**CWP LENGTH:*.F9.1./.17X.*CWP HEAD LOSS:*.F10.2./.8X.
85 **DISTRIBUTION HEAD LOSS:*.F10.2./.11X.*TOTAL HEAD REQUIRED:*.
*F9.1)
CALL DEAIRC(PWR)
GO TO 900.
999 WRITE(7.700)
90 700 FORMAT(///.*CONVERGENCE PROBLEMS IN JET CONDENSER ROUTINE*)
STOP.
900 RETURN
END
    
```

SYMBOLIC REFERENCE MAP (R=1)

ENTRY POINTS
4 CONDEN1

VARIABLES	SN	TYPE	RELOCATION			
345 AREA		REAL		335 B	REAL	
0 CKM		REAL	COND	325 CPT	REAL	
2 D		REAL	COND	4 EPS	REAL	COND
323 ERROR		REAL		2 G	REAL	CONST
0 HD		REAL	F.P.	352 HDIST	REAL	
337 HF		REAL		351 HNOZ	REAL	
0 HP		REAL	F.P.	340 HR	REAL	
353 HT		REAL		0 HZ	REAL	F.P.
330 ITER		INTEGER		3 L	REAL	COND
343 MDO TN		INTEGER		322 MFA	REAL	

VARIABLES	SN	TYPE	RELOCATION				
1	MFCW	REAL	FLOW	1	MFGCOND	REAL	AIR
0	MFGEVAP	REAL	AIR	2	MFS	REAL	FLW
3	MFSO	REAL	FLOW	0	MFWW	REAL	FILW
344	NCH	INTEGER		346	NNOZ	INTEGER	
347	NZPCH	INTEGER		0	PI	REAL	CONST
324	PS	REAL		0	PWR	REAL	F.P.
1	PO	REAL	CONST	326	R	REAL	
1	RHOCW	REAL	COND	331	RI	REAL	
327	S	REAL		0	SIGMAI	REAL	AIR1
1	SIGMAO	REAL	AIR1	342	SP	REAL	
350	SPNOZ	REAL		1	TCWI	REAL	TEMP
2	TCWO	REAL	TEMP	2	TEST	REAL	AIR1
334	TEST1	REAL		0	TWVI	REAL	TEMP
5	TWVO	REAL	TEMP	4	T0	REAL	TEMP
3	T1	REAL	TEMP	336	VCW	REAL	
341	W	REAL		332	Z	REAL	
333	ZI	REAL					

FILE NAMES MODE
TAPE7 FMT

EXTERNALS	TYPE	ARGS			
ALOG10	REAL	1 LIBRARY	CP	REAL	1
DEAIRC		1	FRIC	REAL	3
HVAP	REAL	1	PSAT	REAL	1
XINT	REAL	1			

INLINE FUNCTIONS TYPE ARGS
ABS REAL 1 INTRIM

STATEMENT LABELS					
41 10		57	20	63	30
66 40		73	100	276	700
217 701	FMT	157	900	153	399

COMMON BLOCKS	LENGTH
CONST	3
TEMP	6
FLOW	4
AIR	2
AIR1	3
COND	5

STATISTICS
PROGRAM LENGTH 3548 236
COMMON LABELED COMMON LENGTH 278 23

```

1      SUBROUTINE DEAIRC(PWR)
      REAL MFSO,MFA,MFGEVAP,MFGCOND,MDOTT
      DIMENSION P(4)
      COMMON/TEMP/TWWI,TCWI,TCWO,T1,TO,TWWD
5      COMMON/FLOW/MFWW,MFCW,MFS,MFSO
      COMMON/CONST/PI,PO,G
      COMMON/AIR/MFGEVAP,MFGCOND
      MFA=MFGEVAP+MFGCOND
      T=(TCWO+TCWI)/2.3
10     TC=6.0
      PVC=PSAT(TC)
      PVS=PSAT(T)
      SIG=MFSO/MFA
      ETAM=0.9
15     DELTA=0.276
      PA=PO*1.01
      N=4
      NM1=N-1
      PS=PVS*(1.0+MFA/MFSO/1.602)
20     C
      C COMPUTE COMPRESSION RATIO
      C
      RS=2.0
10     RST=RS
25     SUM=0.0
      DO 20 I=1,NM1
20     SUM=SUM+RS**I
      RS=((PA+DELTA*SUM)/PS)**(1.0/N)
      IF (ABS(RST-RS)/RS.GT.0.01) GO TO 10
30     C
      C 1ST STAGE, NO INTERCOOLER
      C
      CRS=RS**0.3*ALOG(RS)
      PCIN=PS
35     MDOTT=MFSO+MFA
      ETAC=1.7*(PCIN/PO)**0.4
      IF(ETAC.GT.0.8) ETAC=0.8
      PCOUT=RS*PCIN
      P(1)=293.0*(TC+273.0)*CRS*MDOTT/ETAC/ETAM/1.0E6
40     DO 30 I=2,N
      PS=PCOUT
      PCIN=PS-DELTA
      PAS=PCIN-PVC
      PCOUT=RS*PCIN
45     MDOTT=MFA*(1.0+PVC/PAS/1.602)
      ETAC=1.7*(PCIN/PO)**0.4
      IF(ETAC.GT.0.8) ETAC=0.8
50     P(I)=293.0*(TC+273.0)*CRS*MDOTT/ETAC/ETAM/1.0E6
      PWR=0.0
      DO 40 I=1,4
40     PWR=PWR+P(I)
      C
      C OUTPUT TO TAPE 7
      C
55     WRITE(7,700) N,RS,SIG,(I,P(I),I=1,4),PWR
700  FORMAT(///.* CONDENSER AIR REMOVAL*.,///.* PARAMETERS:*,
      *///.17X.*NO. OF STAGES:*.I5./13X.*COMPRESSION RATIO:*.

```

60

```
*F8.2./9X.=INLET STEAM/AIR RATIO:*.F7.1.//.21X.
**POWER RECD:*.4(4X.*STAGE*.I2.*.F7.2)./.20X.
**TOTAL POWER:*.12X.F7.2)
PWR=PWR+1.0E6
RETURN
END
```

SYMBOLIC REFERENCE MAP (R=t)

ENTRY POINTS
4. DEAIRC

VARIABLES	SN	TYPE	RELOCATION				
303	CRS	REAL		272	DELTA	REAL	
305	ETAC	REAL		271	ETAM	REAL	
2	G	REAL	CONST	302	I	INTEGER	
263	MDDTT	REAL		262	MFA	REAL	
1	MFCW	INTEGER	FLW	1	MFGCOND	REAL	AIR
0	MFGEVAP	REAL	AIR	2	MFS	INTEGER	FLOW
3	MFSO	REAL	FLOW	0	MFWW	INTEGER	FLOW
274	N	INTEGER		275	NM1	INTEGER	
310	P	REAL	ARRAY	273	PA	REAL	
307	PAS	REAL		304	PCIN	REAL	
306	PCDUT	REAL		0	PI	REAL	CONST
1	PD	REAL	CCNST	276	PS	REAL	
266	PVC	REAL		267	PVS	REAL	
0	PWR	REAL	F.P.	277	RS	REAL	
300	RST	REAL		270	SIG	REAL	
301	SUM	REAL		264	T	REAL	
265	TC	REAL		1	TCWI	REAL	TEMP
2	TCWO	REAL	TEMP	0	TWVI	REAL	TEMP
5	TWVO	REAL	TEMP	4	TO	REAL	TEMP
3	T1	REAL	TEMP				

FILE NAMES . MODE
TAPE7 FMT

EXTERNALS TYPE ARGS PSAT REAL 1
ALOG REAL 1 LIBRARY

INLINE FUNCTIONS TYPE ARGS
ABS REAL 1 INTRIM

STATEMENT LABELS

35 10 0 20 0 30
0 40 213 700 FMT

LOOPS	LABEL	INDEX	FROM-TO	LENGTH	PROPERTIES
41	20	* I	26 27	6B	EXT REFS
112	30	* I	40 43	31B	EXT REFS
151	40	I	50 51	3B	INS-ACK
16		* I	55 55	7B	EXT REFS

COMMON BLOCKS	LENGTH
TEMP	6
FLOW	4
CONST	3
AIR	2

STATISTICS

PROGRAM LENGTH	3148	204
CM LABELED COMMON LENGTH	178	15

```

1      SUBROUTINE CONDEN2(HZ,HD,HP,PWR)
      REAL MFWW,MFCW,MFS,KM,L,LMTD
      COMMON/CONST/PI,P0,G
      COMMON/TEMP/TWVI,TCWI,TCWC,T1,TO,TWVO
5      COMMON/FLOW/MFWW,MFCW,MFS,MFSD
      COMMON/COND/CKM,RHOCW,D,L,EPS
      LMTD = (TCWO - TCWI)/(ALOG((T1 - TCWI)/(T1 - TCWO)))
      PS=PSAT(T1)
      KM = CKM * ((PS/P0)**0.2)
10     VCOND = 0.99*MFS/(KM * LMTD)
      ACOND = 940.0
      HZ= VCOND/ACOND

C
C     COMPUTE HEAD LOSS IN COLD WATER PIPE. DISTRIBUTION SYSTEM.
15     C     AND HEAD LOSS DUE TO DENSITY DIFFERENCE
C
      VCW = (4. * MFCW)/(RHOCW * 3.14159 * (D**2.))
      HF = FRIC(EPS,D,VCW)*L*(VCW*VCW)/(2.*G*D)
      HR = 0.001 * L
20     DDIST = 3.E
      LDIST=104.
      HNOZ=2.6
      VDIST=MFCW/(2.*RHOCW*PI*DDIST*DDIST)
      HD=FRIC(EPS,DDIST,VDIST)*LDIST+VDIST*VDIST/(2.*DDIST*G)
25     **HNOZ
      HP=HR+HF
      HNCZ=2.6
      HT=HD+HP+HZ+HNOZ
      WRITE(7,70:) KM,PS,LMTD,ACOND,VCOND,HZ,D,L,HP,HD,HNOZ,HT
30     701 FORMAT(//=' CONDENSER: CASCADE OR SPRAY TYPE',//.
      ** PARAMETERS:*,//.18X,*VOL MT COEFF:*,F6.4,/.20X.
      **COND PRESS:*,F8.4,/.26X,*LMTD:*,F6.3,/.20X.
      **XSECT AREA:*,F6.1,/.18X,*TOTAL VOLUME:*,F8.1,/.19X.
      **COND HEIGHT:*,F6.2,/.22X,*CWP DIAM:*,F5.1,/.20X.
35     **CWP LENGTH:*,F7.1,/.17X,*CWP HEAD LOSS:*,F6.2,/.8X.
      **DISTRIBUTION HEAD LOSS:*,F6.2,/.14X,*NOZZLE HEAD LOSS:*,
      *.F6.1,/.11X,*TOTAL HEAD REQUIRED:*,F6.1)
      CALL DEAIRC(PWR)
      RETURN
40     END
    
```

SYMBOLIC REFERENCE MAP (R=1)

ENTRY POINTS
4 CONDEN2

VARIABLES	SN	TYPE	RELLOCATION			
215	ACOND	REAL		0	CKM	REAL COND
2	D	REAL	COND	221	DDIST	REAL
4	EPS	REAL	COND	2	G	REAL CONST
0	HD	REAL	F.P.	217	HF	REAL
22	HNOZ	REAL		0	HP	REAL F.P.
22	R	REAL		225	HT	REAL

VARIABLES	SN	TYPE	RELOCATION				
0	HZ	REAL	F.P.	211	KM	REAL	
3	L	REAL	COND	222	LDIST	INTEGER	
212	LMTD	REAL		1	MFCW	REAL	FLOW
2	MFS	REAL	FLOW	3	MFSO	INTEGER	FLOW
0	MFWW	REAL	FLOW	0	PI	REAL	CONST
213	PS	REAL		0	PWR	REAL	F.P.
1	PO	REAL	CONST	1	RHOCW	REAL	COND
1	TCWI	REAL	TEMP	2	TCWO	REAL	TEMP
0	TWWI	REAL	TEMP	5	TWVO	REAL	TEMP
4	TO	REAL	TEMP	3	T1	REAL	TEMP
214	VCOND	REAL		216	VCW	REAL	
224	VDIST	REAL					

FILE NAMES MODE
 TAPE7 FMT

EXTERNALS	TYPE	ARGS			
ALOG	REAL	1	LIBRARY	DEAIRC	1
FRIC	REAL	3		PSAT	REAL 1

STATEMENT LABELS
 130 701 FMT

COMMON BLOCKS	LENGTH
CONST	3
TEMP	6
FLOW	4
COND	5

STATISTICS			
PROGRAM LENGTH	2268	150	
COMMON LABELED COMMON LENGTH	228	18	

```

1      SUBROUTINE TURBIN
      REAL MFS
      COMMON/TURB/ETATG,DTTG,DHS
      COMMON/SIZE/DO
5      COMMON/FLOW/MFWW,MFCW,MFS,MFSO
      COMMON/CONST/PI,PO,G
      COMMON/TEMP/TWWI,TCWI,TCWO,T1,TO,TWWO
      RATIO=0.4395
      BLC=0.1
10     BETA=0.412
      SV=SVOL(T1)
      SB=SIN(BETA)
      EPS=(1.0+2.0*BLC)/(2.0/ETATG-1.0)
      GNU=2.0*COS(BETA)/(EPS+1.0)
15     AREA=(MFS*SV)/SB*SQRT(EPS/ETATG/DHS)
      W=MFS*SV/(AREA*SB)
      U=GNU*W
      BLADE=SQRT((AREA/PI)*(1.0-RATIO)/(1.0+RATIO))
      DM=BLADE*(1.0+RATIO)/(1.0-RATIO)
20     DO=BLADE+DM
      DH=DM-BLADE
      SPD=19.099*U/DM
      WRITE(7,700) ETATG,DTTG,DHS,RATIO,DH,DO,SPD
700   FORMAT(///.*TURBINE-VERTICAL AXIS*///.1X.*PARAMETERS:*.
25     *//.23X.*T/G EFF:*.F7.2./23X.*DELTA T:*.F6.1./23X.
      **DELTA H:*.1PE14.5./17X.*HUB/TIP RATIO:*.0PF8.3./22X.
      **HUB DIAM:*.F6.1./20X.*OUTER DIAM:*.F6.1./27X.
      **RPM:*.F6.1)
      RETURN
30     END
    
```

SYMBOLIC REFERENCE MAP (R=1)

ENTRY POINTS
2 TURBIN

VARIABLES	SM	TYPE	RELOCATION			
131 AREA		REAL		124 BETA	REAL	
134 BLADE		REAL		123 BLC	REAL	
136 DH		REAL		2 DHS	REAL	TURB
135 DM		REAL		0 DO	REAL	SIZE
1 DTTG		REAL	TURB	127 EPS	REAL	
0 ETATG		REAL	TURB	2 G	REAL	CONST
130 GNU		REAL		1 MFCW	INTEGER	FLOW
2 MFS		REAL	FLOW	3 MFSO	INTEGER	FLOW
0 MFWW		INTEGER	FLOW	0 PI	REAL	CONST
1 PO		REAL	CONST	122 RATIO	REAL	
126 SB		REAL		137 SPD	REAL	
125 SV		REAL		1 TCWI	REAL	TEMP
2 TCWO		REAL	TEMP	0 TWWI	REAL	TEMP
5 TWWO		REAL	TEMP	4 TO	REAL	TEMP
1		REAL	TEMP	133 U	REAL	
13	1	REAL				

FILE NAMES MODE
TAPE7 FMT

EXTERNALS	TYPE	ARGS			
COS	REAL	1 LIBRARY	SIN	REAL	1 LIBRARY
SORT	REAL	1 LIBRARY	SVOL	REAL	1

STATEMENT LABELS
66 700 FMT

COMMON BLOCKS	LENGTH
TURB	3
SIZE	1
FLDW	4
CONST	3
TEMP	6

STATISTICS
PROGRAM LENGTH 1408 96
COMMON LABELED COMMON LENGTH 218 17


```

1      FUNCTION CP(T)
      DIMENSION A(4)
      DATA A,4.223801E3,-4.32128,1.389518E-1,-1.744959E-3/
      CP=0.0
5      DO 10 I=1,4
      CP=CP+A(I)*T**(I-1)
10     CONTINUE
      RETURN
      END

```

SYMBOLIC REFERENCE MAP (R=1)

ENTRY POINTS
5 CP

VARIABLES	SN	TYPE	RELOCATION			
35 A		REAL	ARRAY	33 CP	REAL	
34 I		INTEGER		0 T	REAL	F.P.

STATEMENT LABELS
0 10

LOOPS	LABEL	INDEX	FROM-TO	LENGTH	PROPERTIES
22	10	* I	5 7	10B	EXT REFS

STATISTICS	PROGRAM LENGTH		
		438	35

```

1      FUNCTION XINT(X)
      REAL K
      DIMENSION FK(100)
5      COMMON/AIR1/SIGMAI,SIGMAO,TEST
      N=25
      NM1=N-1
      DLSI=A LOG10(SIGMAI)
      DLSO=A LOG10(SIGMAO)
      DELTAS=(DLSI-DLSO)/N
10     XL2=A LOG10(2.0)
      C
      C COMPUTE K AS A FUNCTION OF LOG SIGMA
      C
      DO 10 I=1,N
15     DLS=DLSO+(I-1)*DELTAS
      IF (DLS.LT.1.08) K=3.91378E-1-3.416619E-1*DLS+
      *2.57449*DLS*DLS
      IF (DLS.LT.2.0.AND.DLS.GE.1.08) K=-5.646357+1.083838E1*DLS-
      *2.51482*DLS*DLS
20     IF (DLS.LT.4.0.AND.DLS.GE.2.0) K=3.958614+1.322053*DLS-
      *1.608663E-1*DLS*DLS
      IF (DLS.GE.4.0) K=6.672965
      F=(A LOG10(K)/XL2+2.0)*1.0E3
      XX=X*F
25     E=0.0
      IF (XX.LT.675.0) E=EXP(-XX)
      FK(I)=1.0/(1.0-E)
10    CONTINUE
      SUMF=0.0
30    DO 20 I=2,NM1
20    SUMF=SUMF+FK(I)
      XINT=DELTAS/2.0*(FK(1)+2.0*SUMF+FK(N))-TEST
      RETURN
      END

```

SYMBOLIC REFERENCE MAP (R=1)

ENTRY POINTS
5 XINT

VARIABLES	SN	TYPE	RELOCATION			
165 DELTAS		REAL		170 DLS	REAL	
163 DLSI		REAL		164 DLSO	REAL	
173 E		REAL		171 F	REAL	
175 FK		REAL	ARRAY	167 I	INTEGER	
160 K		REAL		161 N	INTEGER	
162 NM1		INTEGER		0 SIGMAI	REAL	AIR1
1 SIGMAO		REAL	AIR1	174 SUMF	REAL	
2 TEST		REAL	AIR1	0 X	REAL	F.P.
157 XINT		REAL		166 XL2	REAL	
172 XX		REAL				

EXTERNALS	TYPE	ARGS	EXP	REAL	LIBRARY
ALOG10	REAL	1 LIBRARY			1 LIBRARY

STATEMENT LABELS

0 10

0 20

LOOPS	LABEL	INDEX	FROM-TO	LENGTH	PROPERTIES	EXT REFS
34	10	I	14 28	60B		
122	20	I	30 31	3B	INSTACK	

COMMON BLOCKS	LENGTH
AIR1	3

STATISTICS

PROGRAM LENGTH	3438	227
COMMON LABELED COMMON LENGTH	38	3


```

1      FUNCTION SG(T)
      DIMENSION A(6)
      DATA A/0.916455E+4,-0.266745E+2,0.10144E+0,0.134376E-2,
5      ?-0.594252E-4,0.712817E-6/
      SG = 0.0
      DO 10 I=1,5,1
      SG = SG + A(I)*T**((I-1))
10     CONTINUE
      RETURN
10     END
    
```

SYMBOLIC REFERENCE MAP (R=1)

ENTRY POINTS
5 SG

VARIABLES	SN	TYPE	RELOCATION			
35 A		REAL	ARRAY	34 I	INTEGER	
33 SG		REAL		0 T	REAL	F.P.

STATEMENT LABELS
0 10

LOOPS	LABEL	INDEX	FROM-TO	LENGTH	PROPERTIES
22	10	+ I	6 8	10B	EXT REFS

STATISTICS
PROGRAM LENGTH 45B 37

```

1      FUNCTION SF(T)
      DIMENSION A(6)
      DATA A/ -0.179799E+0.0.154686E+2. -0.325066E-1. -0.79861E-4.
5      ?0.803928E-5. -0.870136E-7/
      SF = 0.0
      DO 10 I=1,6.1
      SF = SF + A(I)*T**([I-1])
10     CONTINUE
      RETURN
10     END

```

SYMBOLIC REFERENCE MAP (R=1)

ENTRY POINTS

5 SF

VARIABLES

35 A
33 SF

SN. TYPE
REAL
REAL

RELOCATION
ARRAY

34 I
0 T

INTEGER
REAL

F.P.

STATEMENT LABELS

0 10

LOOPS

22 10

INDEX
* I

FROM-TO
6 8

LENGTH
10B

PROPERTIES

EXT REFS

STATISTICS

PROGRAM LENGTH

45B 37

```

1      FUNCTION HG(T)
      DIMENSION A(6)
      DATA A/0.25035E+7,0.17742E+4,0.167545E+2,-0.146192E+1,
5      ?0.50292E-1,-0.6047E-3/
      HG = 0.0
      DO 10 I=1,6,1...
      HG = HG + A(I)*T**I-1)
10     CONTINUE
      RETURN
10     END
    
```

SYMBOLIC REFERENCE MAP (R=1)

ENTRY POINTS

5 HG

VARIABLES

VARIABLES	SN	TYPE	RELOCATION	SN	TYPE	REAL
35 A		REAL	ARRAY	33 HG		REAL
34 I		INTEGER		0 T		REAL

F.P.

STATEMENT LABELS

0 10

LOOPS

LOOPS	LABEL	INDEX	FROM-TO	LENGTH	PROPERTIES
22	10	* I	6 8	10B	EXT REFS

STATISTICS

PROGRAM LENGTH	45B	37
----------------	-----	----

```

1      FUNCTION HF(T)
      DIMENSION A(5)
      DATA A/-0.419093E+2.0.422033E+4.-0.165012E+1.0.328495E-1.
      ?-0.258131E-3/
5      HF = 0.0
      DO 10 I=1.5.1
      HF = HF + A(I)*T**I-1)
10     CONTINUE
      RETURN
10     END

```

SYMBOLIC REFERENCE MAP (R=1)

ENTRY POINTS
5 HF

VARIABLES	SN	TYPE	RELOCATION				
35 A		REAL	ARRAY	33	HF	REAL	
34 I		INTEGER		0	T	REAL	F.P.

STATEMENT LABELS
0 10

LOOPS	LABEL	INDEX	FROM-TO	LENGTH	PROPERTIES	EXT REFS
22	10	* I	6 8	10B		

STATISTICS
PROGRAM LENGTH . 448 36


```

1      FUNCTION HVAP(T)
      DIMENSION A(5)
      DATA A/2503.583615,-2.403948,0.006817,-0.000592,0.000023/
      HVAP = 0.0
5      DO 10 I=1,5,1
      HVAP = HVAP + A(I)*T**(I-1)
10     CONTINUE
      HVAP = HVAP*1.0E3
      RETURN
10     END
    
```

SYMBOLIC REFERENCE MAP (R=1)

ENTRY POINTS
5 HVAP

VARIABLES	SM	TYPE	RELOCATION			
40 A		REAL	ARRAY	36 HVAP	REAL	
37 I		INTEGER		0 T	REAL	F.P.

STATEMENT LABELS
0 10

LOOPS	LABEL	INDEX	FROM-TO	LENGTH	PROPERTIES
22	10	* I	5 7	10B	EXT REFS

STATISTICS
PROGRAM LENGTH 47B 39

```

1      FUNCTION SVOL(T)
      DIMENSION A(5)
      DATA A/2.062302E2,-1.401599E1,.4.863781E-1,-9.330914E-3,
5      *7.567609E-5/
      SVOL=0.0
      DO 10 I=1,5
      SVOL=SVOL+A(I)*T**(I-1)
10     CONTINUE
      RETURN
10     END

```

SYMBOLIC REFERENCE MAP (R=1)

ENTRY POINTS

5 SVOL

VARIABLES

SN	TYPE
35 A	REAL
33 SVOL	REAL

RELOCATION
ARRAY

34 I
0 T

INTEGER
REAL

F.P.

STATEMENT LABELS

0 10

LOOPS

LABEL	INDEX
22 10	* I

FROM-TO
6 8

LENGTH
108

PROPERTIES

EXT REFS

STATISTICS

PROGRAM LENGTH

448 36

```

1      FUNCTION PSAT(T)
      DIMENSION A(6)
      DATA A/.610802E0.,.443917E-1.,.14202E-2.,.273291E-4.,
5      *.2E2311E-6.,.2E9737E-8/
      PSAT = 0.0
      DO 10 I=1,6,1
      PSAT = PSAT + A(I)+T**(I-1)
10     CONTINUE
      RETURN
10     END

```

SYMBOLIC REFERENCE MAP (R=1)

ENTRY POINTS
5 PSAT

VARIABLES	SN	TYPE	RELOCATION			
35 A		REAL	ARRAY	34	I	INTEGER
33 PSAT		REAL		0	T	REAL

F.P.

STATEMENT LABELS
0 10

LOOPS	LABEL	INDEX	FROM-TO	LENGTH	PROPERTIES
22	10	= I	6 8	108	EXT REFS

STATISTICS
PROGRAM LENGTH 145E 37

```
1      FUNCTION FRIC(EPS,D,V)
      RE=V*D/1.3E-6
      FRIC=0.0055*(1.+(2.E4*EPS/D+1.E6/RE)**0.33)
      RETURN
5      END
```

SYMBOLIC REFERENCE MAP (R=1)

ENTRY POINTS
5 FRIC

VARIABLES	SN	TYPE	RELOCATION				
0 D		REAL	F.P.	0	EPS	REAL	F.P.
31 FRIC		REAL		32	RE	REAL	
0 V		REAL	F.P.				

STATISTICS
PROGRAM LENGTH

338 27

Document Control Page	1. SERI Report No. TR-631-692	2. NTIS Accession No.	3. Recipient's Accession No.
4. Title and Subtitle Open-Cycle OTEC System Performance Analysis		5. Publication Date October 1980	6.
7. Author(s) A. A. Lewandowski, D. A. Olson, and D. H. Johnson		8. Performing Organization Rept. No.	
9. Performing Organization Name and Address Solar Energy Research Institute 1617 Cole Boulevard Golden, Colorado 80401		10. Project/Task/Work Unit No. 3451.10	11. Contract (C) or Grant (G) No. (C) (G)
12. Sponsoring Organization Name and Address		13. Type of Report & Period Covered	
		14.	
15. Supplementary Notes			
16. Abstract (Limit: 200 words) <p>This report describes an algorithm developed to calculate the performance of Claude-Cycle ocean thermal energy conversion (OTEC) systems. The algorithm treats each component of the system separately and then interfaces them to form a complete system, allowing a component to be changed without changing the rest of the algorithm. Two components that are subject to change are the evaporator and condenser. For this study we developed mathematical models of a channel-flow evaporator and both a horizontal jet and spray director contact condenser. The algorithm was then programmed to run on SERI's CDC 7600 computer and used to calculate the effect on performance of deaerating the warm and cold water streams before entering the evaporator and condenser, respectively. This study indicates that there is no advantage to removing air from these streams compared with removing the air from the condenser.</p>			
17. Document Analysis a. Descriptors Ocean Thermal Energy Conversion; Open Cycle; Mathematical Models; Turbines; Performance; Evaporators; Condensers; Deaerators b. Identifiers/Open-Ended Terms c. UC Categories 64			
18. Availability Statement National Technical Information Service U.S. Department of Commerce 5285 Port Royal Road Springfield, Virginia 22161		19. No. of Pages 105	20. Price \$6.50